

# Uncertainty Quantification of PDEs with Random Parameters on Random Domains

**Elias Reutelsterz**

Thesis for the attainment of the academic degree

**Master of Science**

at the TUM School of Computation, Information and Technology of the Technical University of Munich

**Supervisor:**

Prof. Dr. Elisabeth Ullmann

**Advisor:**

Prof. Dr. Elisabeth Ullmann

**Submitted:**

Bahía Blanca, 4. June 2025



I hereby declare that this thesis is entirely the result of my own work except where otherwise indicated. I have only used the resources given in the list of references.

*E.Reutelsterz*

Bahía Blanca, 4. June 2025

Elias Reutelsterz



## Zusammenfassung

Diese Masterarbeit befasst sich mit Methoden der Unsicherheitsquantifizierung (UQ), einem wichtigen Teilgebiet der angewandten Mathematik. Im Fokus steht die Analyse von Differentialgleichungen mit zufälligen Parametern, die auf geometrisch zufälligen Gebieten definiert sind.

Ein zentraler methodischer Ansatz ist die Domain Mapping Methode. Hierbei werden die Samples des stochastischen Gebiets durch eine bijektive Abbildung mit einem Referenzgebiet verbunden. Dies ermöglicht die Formulierung einer äquivalenten Differentialgleichung mit zufälligen Parametern auf dem deterministischen Referenzgebiet, welche dann mit Standardverfahren wie der Finite-Elemente-Methode (FEM) numerisch gelöst werden kann. Die Unsicherheit in den Eingangsdaten wird durch Zufallsvariablen und Zufallsfelder modelliert, deren statistische Eigenschaften mit Hilfe von Monte-Carlo-Methoden und der Karhunen-Loève-Entwicklung (KLE) beschrieben werden.

Die Domain Mapping Methode wird zunächst anhand verschiedener Variationen der Poisson-Gleichung eingeführt, um ihre grundlegenden Eigenschaften und Anwendungsmöglichkeiten zu demonstrieren. Anschließend wird die Methode auf das anspruchsvollere Problem einer Elastizitätsgleichung angewandt, welche auf einer Stahlplatte mit einem zufällig positionierten und dimensionierten Loch definiert ist. Die Arbeit untersucht, wie sich die Unsicherheit in der Geometrie des Lochs auf die Lösung der Elastizitätsgleichung auswirkt. Ein besonderer Schwerpunkt liegt auf der Quantifizierung der Sensitivität der Ausgabegrößen bezüglich der Eingangsparameter. Hierzu wird die Theorie der Sobol-Indizes herangezogen, welche auf vektorwertige Funktionen erweitert wird.

Die numerische Implementierung der Methoden erfolgt in der Open-Source-Software FEniCS. Die Ergebnisse der Arbeit liefern Einblicke in die Anwendung von UQ-Methoden auf ingenieurwissenschaftliche Probleme mit geometrischer Unsicherheit.

## Abstract

This master's thesis deals with methods of Uncertainty Quantification (UQ), an important subfield of applied mathematics. The focus is on the analysis of differential equations with random parameters, which are defined on geometrically random domains.

A central methodological approach is the Domain Mapping Method. Here, the samples of the stochastic domain are connected to a fixed reference domain by a bijective mapping. This enables the formulation of an equivalent differential equation with random parameters on the deterministic reference domain, which can then be solved numerically using standard methods such as the Finite Element Method (FEM). The uncertainty in the input data is modelled by random variables and random fields, whose statistical properties are described with the aid of Monte Carlo methods and the Karhunen-Loève expansion (KLE).

The Domain Mapping Method is first introduced using various variations of the Poisson equation in order to demonstrate its basic properties and possible applications. Subsequently, the method is applied to the more demanding problem of an elasticity equation, which is defined on a steel plate with a randomly positioned and dimensioned hole. The work investigates how the uncertainty in the geometry of the hole affects the solution of the elasticity equation. A special focus is on quantifying the sensitivity of the output quantities with respect to the input parameters. For this purpose, the theory of Sobol' indices is used, which is extended to vector-valued functions.

The numerical implementation of the methods is carried out in the open-source software FEniCS. The results of the work provide insights into the application of UQ methods to engineering problems with geometric uncertainty.

# Contents

<b>1</b>	<b>Introduction</b>	<b>1</b>
1.1	Research Landscape . . . . .	1
1.2	Problem Statement and Significance . . . . .	1
1.3	Thesis Structure and Methodology . . . . .	2
<b>2</b>	<b>Theoretical Foundations</b>	<b>5</b>
2.1	General Theory . . . . .	5
2.2	Random Fields . . . . .	5
2.2.1	Karhunen-Loève Expansion . . . . .	7
2.2.2	Domain Independence of the Karhunen-Loève Expansion . . . . .	10
2.3	Sobolev Spaces . . . . .	12
<b>3</b>	<b>Sensitivity Analysis</b>	<b>14</b>
3.1	Single-valued Model Output . . . . .	14
3.2	Vector-valued Model Output . . . . .	15
3.3	Functional-valued Model Output . . . . .	17
3.4	Estimation of Sobol' Indices . . . . .	20
<b>4</b>	<b>Domain Mapping Method for the Poisson Equation</b>	<b>24</b>
4.1	Introduction to the Domain Mapping Method . . . . .	24
4.2	The Connection of the two Problems . . . . .	26
4.3	Implementation and Numerical Results . . . . .	29
4.3.1	Two-dimensional Karhunen-Loève Expansion . . . . .	29
4.3.2	Jacobian of the truncated Karhunen-Loève Expansion . . . . .	31
4.3.3	Numerical Results . . . . .	33
<b>5</b>	<b>Domain Mapping Method for Variants of the Poisson Equation</b>	<b>36</b>
5.1	Random right-hand Side . . . . .	36
5.2	Diffusion Model . . . . .	39
<b>6</b>	<b>Steel Plate Problem</b>	<b>44</b>
6.1	Model Problem . . . . .	44
6.1.1	Model on a deterministic Domain . . . . .	44
6.1.2	Perturbation Function and Model on stochastic Domain . . . . .	45
6.2	Variational Formulation . . . . .	46
6.2.1	Pathwise Unique Existence . . . . .	52
6.3	Computational Experiments and Results . . . . .	54
6.4	Model Extension: Random Field Perturbation for the Circle . . . . .	58
<b>7</b>	<b>Conclusion</b>	<b>62</b>
<b>A</b>	<b>Appendix</b>	<b>64</b>
A.1	Theory . . . . .	64
A.2	Code . . . . .	66
	<b>Bibliography</b>	<b>69</b>

# 1 Introduction

Like Richard Feynman wrote in "The Character of Physical Law" in 1965 [FW17]:

*"If you thought before that science was certain – well, that is just an error on your part."*

uncertainty plays an inevitable role in every relevant scientific experiment. Especially with the ever-increasing influence of information and data on our daily lives and the role of AI, the calibration of models and the estimation of erroneous predictions are becoming increasingly important. In this master's thesis, I try to make a small contribution to understanding the possibilities of statistical methods and their influence.

## 1.1 Research Landscape

Uncertainty Quantification (UQ) is a flourishing topic in the broad field of mathematical numerical methods and has applications in all quantitative topics in science. Wherever random variables and probabilities occur, the question comes to mind to quantify and reduce the model's uncertainty.

In recent years, many different methods have been developed for the problem of all sorts of stochastic domains in differential equations. One can divide them into the Remeshing Method [BHP19], the Domain Mapping Method [XT06], [HPS16], [Zhe+23], [CDE19], the Fictitious Method [CK07], [NCS11] and the Extended Stochastic Finite Element Method [LDM13], [NC10] etc.. Still, this work focuses on the parametrized Domain Mapping Method, where each sample of the random domain is mapped bijectively onto a deterministic domain. The Domain Mapping Method transforms the differential equation with deterministic or random parameters on a stochastic domain to a differential equation with stochastic parameters on a unique, deterministic reference domain. Methods like Monte Carlo FEM or the Stochastic Galerkin Method can solve the variational formulation of the resulting differential equation. The mapping depends on the Jacobian of the bijective function and, therefore, the whole stochastic form of the domain. The influence of the boundary roughness was first analyzed through different approaches for deterministic parameterization like sinusoidal corrugation [FP01] or fractal representation [BP03]. Then stochastic methods, including random fields, were analyzed, i.e., random fractal representations [SM93] and random nominal geometries [XT06], [MNK11].

Building upon those foundations recently, many problems from fluid mechanics or mechanical engineering are analyzed similarly. The Poisson problem was investigated in [Hak+23], a linear elasticity model in [HKS24], and the two-dimensional Helmholtz transmission problem in [Hip+18].

## 1.2 Problem Statement and Significance

The work addresses various topics in Uncertainty Quantification of partial differential equations with random parameters and their numerical analysis. The main focus is on the application of the Domain Mapping Method to diverse equations and different geometries, and the difficulties encountered in applying the method. Consequently, the method was applied to variations of the well-known Poisson equation, leading to interesting results and comparisons. Furthermore, in addition to the easily handled Dirichlet boundary conditions, Neumann boundary conditions were also analyzed later.

A second focus was on the Karhunen-Loëve expansion (KLE) for modeling random fields. This involved the search for the most efficient representation and computation of the random fields within the limited numerical constraints regarding existing packages and limited computational capacity. For this purpose, many approximation solutions were used, and the most efficient algorithms were utilized and implemented.

In general, the thesis has a strong application focus and, by providing the implementation of the numerical problems in Python, offers an overview of the possibilities of using the open-source package FEniCS. Constant attention was paid to ensuring that the code can be directly followed in tandem with the theoretical problems, maintaining a balance between mathematical correctness and numerical approximations.

To quantify the uncertainties of the various models, Sobol' indices from the subfield of Sensitivity Analysis were introduced. To cover all cases, the theory of Sobol' indices had to be extended to models with functional output and a multi-dimensional range.

Finally, a model from the field of mechanical engineering is analyzed. Specifically, an elasticity equation on a two-dimensional steel plate is considered. The model has three different sources of uncertainty. Firstly, the geometry is uncertain: more precisely, there is a hole in the center of the steel plate, which is described by a random radius and a random position. Secondly, the tensile force on the right edge of the plate is normally distributed. And thirdly, a material-specific parameter (specifically, the so-called Young's Modulus) is defined as a random field over the steel plate. The main and final research question is now the application of the Domain Mapping Method to this model and its numerical analysis using the (among other things, newly introduced) Sobol' indices from the chapter on Sensitivity Analysis.

As a model extension, a description of the random geometry of the cut-out central circle was used as a random field, as in the previous models. The numerical analysis of both models and their comparison was very exciting and reveals the influence of the geometry modeling on the various quantities of interest of an elasticity equation.

### 1.3 Thesis Structure and Methodology

The structure of this thesis follows the problem statement outlined in the last section. First, we introduce the necessary fundamental theory for random fields  $V(x, \omega)$  and their Karhunen-Loève Expansion (KLE)

$$V(x, \omega) = \mu(x) + \sum_{m=1}^{\infty} \sqrt{\gamma_m} \cdot g_m(x) \cdot \xi_m(\omega)$$

in chapter 2. We highlight an important property that will be used later for defining random fields on random domains: the so-called domain independence of the KLE [PG15]. The theory section is then supplemented with definitions and theorems on Sensitivity Analysis (especially Sobol' indices) in chapter 3. Since models with multidimensional function-valued output  $u : D_{ref} \times \Omega \rightarrow \mathbb{R}^k$  are analyzed later in the thesis, we introduce new Sobol' indices based on the Hoeffding decomposition that are consistent with the general theory from [Gam+14]. An efficient algorithm for computing multiple single and total effect indices based on [Sal02] is then introduced. This is extended to the model form of the Sobol' indices defined in the previous section.

In chapter 4, the Domain Mapping Method is introduced using the Poisson equation with a constant right-hand side  $f \equiv 1$ .

$$\begin{aligned} -\Delta u(x, \omega) &= 1 & | & \quad x \in D(\omega) \\ u(x, \omega) &= 0 & | & \quad x \in \delta D(\omega) \end{aligned}$$

Here, the model from [HPS16] with the unit circle as the reference domain  $D_{ref} \subset \mathbb{R}^2$  is used along with a random field  $V : \overline{D_{ref}} \times \Omega \rightarrow \mathbb{R}^2$  with a matrix-valued covariance function. The random field describes a bijective mapping between the reference domain and a sample of the random domain. More precisely, the perturbation of a finite element grid on the two domains looks as follows.

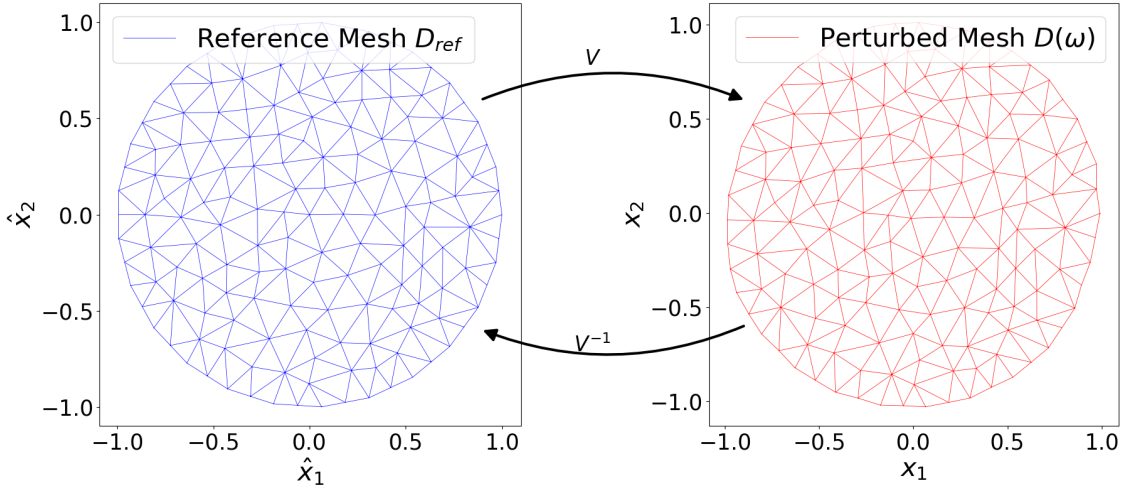


**Figure 1.1** Poisson Problem Random Field and Grid Perturbation

The Domain Mapping Method is applied to the weak formulation of the Poisson equation

$$\int_{D(\omega)} \langle \nabla u(x, \omega), \nabla v(x, \omega) \rangle dx = \int_{D(\omega)} v(x, \omega) dx \quad \forall v \in H_0^1(D(\omega)).$$

We obtain the following problem

$$\begin{aligned} & \int_{D_{ref}} \left\langle \det(J(\hat{x}, \omega)) \cdot \left( J(\hat{x}, \omega)^T \cdot J(\hat{x}, \omega) \right)^{-1} \cdot \nabla \hat{u}(\hat{x}, \omega), \nabla \hat{v}(\hat{x}) \right\rangle d\hat{x} \\ &= \int_{D_{ref}} \det(J(\hat{x}, \omega)) \cdot \hat{v}(\hat{x}) d\hat{x} \quad \forall \hat{v} \in H_0^1(D_{ref}) \end{aligned}$$

where  $J$  denotes the Jacobian of the random field  $V$ . The two solutions are linked as follows

$$\hat{u}(\hat{x}, \omega) = u(V(\hat{x}, \omega), \omega).$$

For these two variational formulations of PDEs, we obtain an equivalence via an endomorphism of the two function spaces used. Furthermore, the unique existence of the solution is shown using the Lax-Milgram lemma. At this point, challenges encountered during the implementation are addressed. For example, the efficient computation of the eigenpairs for the two-dimensional KLE for a matrix-valued covariance function by applying the Galerkin method, which leads to a generalized eigenvalue problem [BEU11]. In addition, the problem arose that the FEM toolbox FEniCS does not contain differentiable basis functions for two-dimensional domains. Therefore, an approximation for the Jacobian is introduced, which can be handled with constant basis functions. At the end of the chapter, the model is analyzed using Monte Carlo methods and Sensitivity Analysis.

In the following chapter 5, two variations of the Poisson equation are treated. The first variation changes the constant right-hand side of the equation to a random function

$$f : D(\omega_2) \times \Omega_1 \rightarrow \mathbb{R},$$

$$f(x, \omega_1) = \begin{cases} \omega_1^{(1)}, & x_1 \leq 0, x \in D_{ref} \cap D(\omega_2) \\ \omega_1^{(2)}, & x_1 > 0, x \in D_{ref} \cap D(\omega_2) \\ 0 & \text{otherwise} \end{cases}$$

where  $\omega_1^{(1)}, \omega_1^{(2)} \sim U([0, 1])$ , which leads to the following Poisson equation.

$$\begin{aligned} -\Delta u(x, \omega) &= f(x, \omega_1) & | & x \in D(\omega_2) \\ u(x, \omega) &= 0 & | & x \in \delta D(\omega_2) \end{aligned}$$

## 1 Introduction

The perturbation function stays the same as in the first model, but the random variable is denoted by  $\omega_2$ . The second variation introduces a diffusion coefficient  $A$  in the form of a log-normal random field

$$\begin{aligned} -\nabla \cdot (A(x, \omega_1) \cdot \nabla u(x, \omega)) &= 1 & | & x \in D(\omega_2) \\ u(x, \omega) &= 0 & | & x \in \delta D(\omega_2) \end{aligned}$$

Both models are again analyzed with Monte Carlo methods and Sensitivity Analysis.

The last substantive chapter 6 deals with the Steel Plate problem from [UC20]. Here, an elasticity equation from mechanics is analyzed

$$\begin{aligned} \frac{E(x, \omega_1)}{2(1+\nu)} \cdot \nabla^2 u(x, \omega) + \frac{E(x, \omega_1)}{2(1-\nu)} \cdot \nabla(\nabla \cdot u(x, \omega)) + b &= 0 & | x \in D(\omega_2) \\ u(x, \omega) &= 0 & | x \in \Gamma_1 \\ \sigma(u, x) \cdot n(x) &= g & | x \in \Gamma_2 \end{aligned}$$

This is defined on a square steel plate with a randomly located and dimensioned hole. The perturbation function applied to an FEM grid looks as follows.

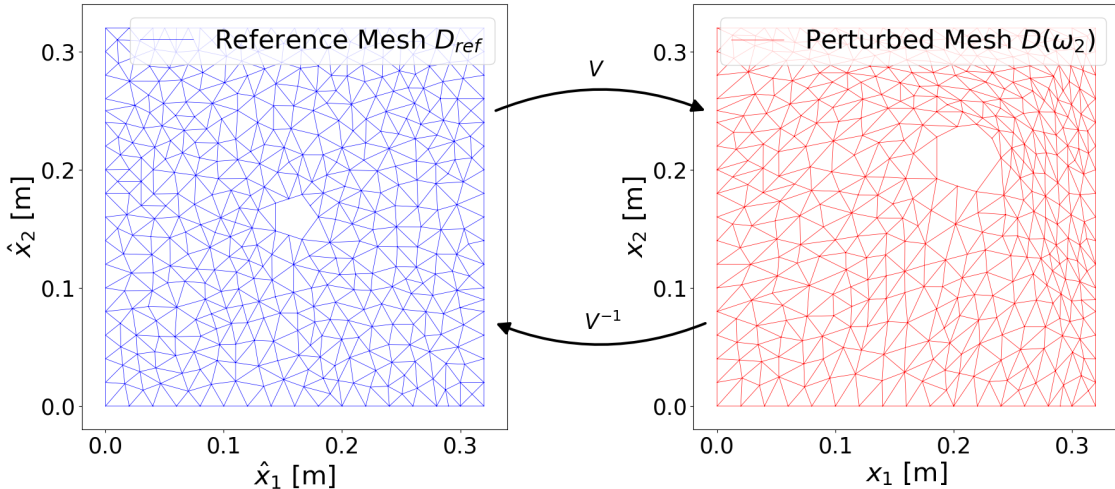


**Figure 1.2** Steel Plate Problem Random Field and Grid Perturbation

During the application, the novel treatment of the Neumann boundary condition on  $\Gamma_2$  was an exciting challenge. After the pathwise existence of a unique solution was proven for this model too, a Monte Carlo and a Sensitivity Analysis were carried out here as well. In the Monte Carlo analysis, the convergence to a self-calculated reference solution of the displacement function was calculated using the  $L^2$ - and  $H^1$ -errors and the components of the covariance function of the reference solution were visualized. The Sensitivity Analysis refers to three different sources of uncertainty: the geometric perturbation of the circle, the tensile force on the right edge, and the Young's modulus  $E$ , which is modeled as a log-normal random field. The quantities of interest are, on the one hand, the stress tensor  $\sigma$  at the upper middle point adjacent to the reference circle and, on the other hand, the total displacement output of the equation. The latter is analyzed over the entire domain using the newly introduced Sobol' indices. The geometric perturbation of the circle was modeled in two different ways. First, the radius and the position of the circle in both coordinates were introduced randomly. Then the circle was perturbed with a random field similar to the Poisson equation model. The Sobol' analysis was performed for both different methods. The individual and total influences of the random variables from the various random sources could be calculated and quantified using the single and total Sobol' indices. It became clear that the way of modeling the geometric uncertainty of the circle and the quantity of interest significantly influence the indices.

## 2 Theoretical Foundations

### 2.1 General Theory

**Definition 2.1.1** (Gamma function  $\Gamma(x)$ ). *The gamma function is defined for  $x \in \mathbb{C}$  with positive real part as*

$$\Gamma(x) := \int_0^\infty t^{x-1} \exp(-t) dt, \quad \operatorname{Re}(x) > 0$$

**Definition 2.1.2** (Modified Bessel function  $K_q(r)$ ). *For all  $r, q > 0$  the modified Bessel function is defined by (compare [LPS14] p.485)*

$$K_q(r) = \frac{c_q}{r^q} \int_0^\infty \left(\frac{2}{\pi}\right)^{1/2} \cos(\gamma r) \frac{1}{(1+\gamma^2)^{q+1/2}} d\gamma$$

$$c_q := 2^{q-1/2} \Gamma(q+1/2)$$

For  $q = 1/2$ , the integral takes the form

$$K_{1/2}(r) = \left(\frac{\pi}{2r}\right)^{1/2} \exp(-r), \quad r \geq 0$$

**Definition 2.1.3** (Galerkin approximation). *Compare with [JL01].*

Let  $H$  be a Hilbert space. Consider the problem: find  $u \in H$  s.t.

$$a(u, v) = l(v) \quad \forall v \in H$$

where  $a$  is a bilinear form and  $l$  is a linear functional.

Choose a finite-dimensional subspace  $V_h \subset H$ . The Galerkin approximation  $u_h \in V_h$  is defined by:

$$a(u_h, v_h) = l(v_h) \quad \forall v_h \in V_h$$

with the following orthogonality condition

$$a(u - u_h, v_h) = 0 \quad \forall v_h \in V_h$$

**Lemma 2.1.4.** *Let  $\varphi : \overline{D_{ref}} \rightarrow \overline{D(\omega_2)}$  be injective so that the matrix  $\nabla \varphi$  is invertible at all points. Then it holds*

$$\det(\nabla \varphi(\hat{x})) \cdot \|\nabla \varphi(\hat{x})^{-T} \cdot n\|_2 d\hat{s} = ds$$

for the boundary  $\hat{x} \in \delta D_{ref}$  with  $n$  being the outer unit normal vector for  $D_{ref}$ .

*Proof.* The proof can be found on p.39 of [Cia94] with the application to the elasticity problem on p.74.  $\square$

### 2.2 Random Fields

**Definition 2.2.1** (Random field). *Given a set  $D \subset \mathbb{R}^d$ ,  $d \in \mathbb{N}$ , and a probability space  $(\Omega, \mathcal{E}, \mathbb{P})$ , a real-valued random field  $Z$  is a mapping  $Z : D \times \Omega \rightarrow \mathbb{R}$  such that each function  $Z(x, \cdot) : \Omega \rightarrow \mathbb{R}$  is a random variable.*

For  $d = 1$  we call  $Z$  a stochastic process.

For each fixed  $\omega \in \Omega$  the function  $Z(\cdot, \omega) : D \rightarrow \mathbb{R}$  is called a realisation of the random field.

For  $d = 1$ , we call  $Z(\cdot, \omega)$  a sample path.

**Definition 2.2.2** (Second order random field). A random field  $Z$  on  $D \subset \mathbb{R}^d$  is said to be of second order if for all  $x \in D$  there holds  $Z(x) \equiv Z(x, \cdot) \in L^2(\Omega; \mathbb{P})$ , that is

$$\mathbb{E}[Z(x, \cdot)^2] = \int_{\Omega} Z(x, \omega)^2 d\mathbb{P}(\omega) < \infty \quad \forall x \in D.$$

For second order random fields the mean function is given by

$$\mu : D \rightarrow \mathbb{R}, \quad \mu(x) := \mathbb{E}[Z(x, \cdot)]$$

and the covariance function by

$$c : D \times D \rightarrow \mathbb{R}, \quad c(x, y) = \text{Cov}(Z(x, \cdot), Z(y, \cdot)).$$

The associated covariance operator  $C : L^2(D) \rightarrow L^2(D)$  is defined as

$$C[u](x) = \int_D c(x, y) u(y) dy,$$

where  $u \in L^2(D)$ .

**Example 2.2.3** (Exponential covariance). The exponential covariance function

$$c : D \times D \rightarrow \mathbb{R}, \quad c(x, y) = \text{Cov}(Z(x, \cdot), Z(y, \cdot))$$

is given by

$$c(x, y) := \sigma^2 \cdot \exp\left(-\frac{\|x - y\|_2}{l}\right), \quad l, \sigma > 0.$$

**Definition 2.2.4** (Gaussian random field). A real-valued random field  $Z$  on  $D \subset \mathbb{R}^d$  is called Gaussian random field if the random vector

$$Z := [Z(x_1), \dots, Z(x_n)]^T : \Omega \rightarrow \mathbb{R}^n$$

follows the  $n$ -variate normal distribution for any  $x_1, \dots, x_n \in D$  and any  $n \in \mathbb{N}$ . In this case we write  $Z \sim \mathcal{N}(\mu, C)$  where  $\mu_i := \mu(x_i)$  and  $c_{ij} := c(x_i, x_j)$ ,  $i, j = 1, \dots, n$ .

Gaussian random fields are second order random fields.

**Definition 2.2.5** (Log-normal random field). Let  $\{Z(x) : x \in D\}$  be a Gaussian random field on a domain  $D \subset \mathbb{R}^d$ . The random field  $\{\exp(Z(x)) : x \in D\}$  is called log-normal random field.

**Definition 2.2.6** (Whittle-Matérn kernel). The so called Whittle-Matérn covariance (compare [LPS14] Example 7.17) is defined as

$$c_q(t) := \frac{\sigma^2}{2^{q-1}\Gamma(q)} \left(\frac{t}{l}\right)^q K_q\left(\frac{t}{l}\right)$$

where  $t = \|x - y\|_2$  is the euclidean distance for two points  $x, y \in D$ ;  $q, l, \sigma > 0$ ,  $\Gamma(q)$  is the Gamma function 2.1.1 and  $K_q(t)$  is the modified Bessel function 2.1.2.

For  $q = 1/2$  the function simplifies to

$$c_{1/2}(t) = \sigma^2 \exp\left(-\frac{t}{l}\right)$$

**Assumption 2.2.7** (Pathwise ellipticity and boundedness). *Realisations of the random field  $a(\cdot, \omega) \in C(\overline{D})$  satisfy  $\mathbb{P}$ -a.s.*

$$0 < a_{\min}(\omega) \leq a(x, \omega) \leq a_{\max}(\omega) < \infty, \quad \text{a.e. in } D,$$

for some real-valued random variables  $a_{\min}$  and  $a_{\max}$ .

**Assumption 2.2.8** (Log-normal diffusion coefficient). *Let  $a(x) := \exp(Z(x))$  where  $\{Z(x) : x \in D\}$  is a mean-zero Gaussian random field on a bounded domain  $D \subset \mathbb{R}^d$ . Let  $c$  be the covariance function of  $Z$  and assume that  $c(x, y) = \tilde{c}(x - y)$  where  $\tilde{c}$  is Lipschitz continuous on  $\overline{D}$ .*

**Definition 2.2.9** (Hölder continuity). *Assume  $D \subset \mathbb{R}^d$  is open and  $0 < \gamma \leq 1$ . A function  $u : D \rightarrow \mathbb{R}$  is called Hölder continuous with exponent  $\gamma$  if there is a constant  $C \in \mathbb{R}$  for which it holds*

$$|u(x) - u(y)| \leq C \cdot \|x - y\|_2^\gamma \quad \forall x, y \in D.$$

**Lemma 2.2.10.** *Let  $a(x) = \exp(Z(x))$  be a log-normal random field which satisfies assumption 2.2.8. Then,  $a(x)$  satisfies assumption 2.2.7 as well.*

*Proof.* By lemma A.1.3 realisations of  $Z(x)$  are a.s. Hölder continuous on  $\overline{D}$  for any exponent  $\gamma < 1/2$ . Hence we can define a.s.

$$a_{\min}(\omega) := \min_{x \in \overline{D}} a(x, \omega), \quad a_{\max}(\omega) := \max_{x \in \overline{D}} a(x, \omega).$$

□

## 2.2.1 Karhunen-Loève Expansion

**Definition 2.2.11** (Integral operator). *For a domain  $D$  and a function  $G \in L^2(D \times D)$  the integral operator  $L : L^2(D) \rightarrow L^2(D)$  with kernel  $G$  is defined by*

$$(Lu)(x) := \int_D G(x, y)u(y)dy, \quad x \in D, \quad u \in L^2(D).$$

**Definition 2.2.12** (Eigenvalue). *If  $L : H \rightarrow H$ , then  $\gamma$  is an eigenvalue of  $L$  if there exists a non-zero function  $g \in H$  such that  $Lg = \gamma g$ . Here,  $g$  is called eigenfunction.*

**Theorem 2.2.13** (Hilbert-Schmidt spectral). *Let  $H$  be a separable Hilbert space and let  $L : H \rightarrow H$  be a linear, compact and symmetric operator on  $H$ . Let  $N \in [0, +\infty]$  denote the rank of  $L$ . Denote the eigenvalues of  $L$  by  $\gamma_m$ ,  $m = 1, \dots, N$ , ordered s.t.  $|\gamma_m| \geq |\gamma_{m+1}|$  and denote the corresponding eigenfunctions by  $g_m$ . Then,*

(I) *all eigenvalues  $\gamma_m$  are real and, if  $N = +\infty$ ,  $\gamma_m \rightarrow 0$  as  $m \rightarrow \infty$*

(II)  *$\{g_m\}$  can be chosen to form an orthonormal basis for the range of  $L$*

(III) *for any  $u \in H$  it holds  $Lu = \sum_{m=1}^N \gamma_m \langle u, g_m \rangle_H g_m$*

*Proof.* The proof can be found at [Zei12] corresponding to theorem 4.A. □

**Definition 2.2.14** (Trace-class operator). *For a separable Hilbert space  $H$ , a positive semi-definite bounded, linear operator  $L$  is a trace-class operator if  $\text{Tr } L < \infty$  where the trace is defined by*

$$\text{Tr } L := \sum_{m=1}^{\infty} \langle Lg_m, g_m \rangle_H$$

for an orthonormal basis  $\{g_m, m \in \mathbb{N}\}$  of  $H$ .

**Definition 2.2.15** (Hilbert-Schmidt kernel). Let  $D \subset \mathbb{R}^d$  be a bounded domain and let  $k : D \times D \rightarrow \mathbb{R}$ . If  $\int_D \int_D |k(x, y)|^2 dx dy < \infty$  then  $k$  is referred to as Hilbert-Schmidt kernel.

**Definition 2.2.16** (Hilbert-Schmidt operator). Let  $k$  be a Hilbert-Schmidt kernel and  $u(y) \in L^2(D)$ . An integral operator  $K : L^2(D) \rightarrow L^2(D)$  defined as

$$(Ku)(x) = \int_D k(x, y)u(y)dy$$

is called Hilbert-Schmidt operator.

**Lemma 2.2.17.** For  $G \in L^2(D \times D)$ , the integral operator  $L$  of  $G$  is compact.

*Proof.* For a proof, see [RS78].  $\square$

**Definition 2.2.18.** Let  $H$  be a Hilbert space with inner product  $\langle \cdot, \cdot \rangle_H$ . A bounded linear operator  $L : H \rightarrow H$  is called symmetric if  $\langle Lu, v \rangle_H = \langle u, Lv \rangle_H$  for any  $u, v \in H$ .

**Theorem 2.2.19** (Mercer). For a bounded domain  $D$ , let  $G \in C(\overline{D} \times \overline{D})$  be a positive semi-definite function. Let  $L$  be the integral operator with kernel  $G$ . Assume that  $L$  is an infinite-rank operator. Then there exist eigenfunctions  $g_m$  of  $L$  with eigenvalue  $\gamma_m > 0$  s.t.  $g_m \in C(\overline{D})$  and

$$G(x, y) = \sum_{m=1}^{\infty} \gamma_m g_m(x)g_m(y), \quad x, y \in \overline{D},$$

where the sum converges in  $C(\overline{D}, \overline{D})$ . Furthermore,

$$\sup_{x, y \in \overline{D}} \left| G(x, y) - \sum_{m=1}^M \gamma_m g_m(x)g_m(y) \right| \leq \sup_{x \in \overline{D}} \sum_{m=M+1}^{\infty} \gamma_m |g_m(x)|^2$$

Finally, the operator  $L$  is a trace-class operator and

$$\text{Tr } L = \int_D G(x, x)dx$$

*Proof.* The proof can be found at [LPS14].  $\square$

**Definition 2.2.20** (Bochner space). Let  $(\Omega, \mathcal{E}, \mathbb{P})$  be a probability space and  $W$  a Banach space with norm  $\|\cdot\|$ . Then  $L^p(\Omega; W)$ ,  $1 \leq p < \infty$ , is the space of all  $W$ -valued, strongly  $\mathcal{E} - \mathcal{B}(W)$ -measurable random variables  $X : \Omega \rightarrow W$  with  $\mathbb{E}[\|X\|^p] < \infty$ .  $L^p(\Omega; W)$  is a Banach space equipped with the norm

$$\|X\|_{L^p(\Omega; W)} := \left( \int_{\Omega} \|X(\omega)\|^p d\mathbb{P}(\omega) \right)^{1/p} = \mathbb{E}[\|X\|^p]^{1/p}.$$

$L^\infty(\Omega; W)$  is the Banach space of  $W$ -valued random variables with

$$\|X\|_{L^\infty(\Omega; W)} := \text{ess sup}_{\omega \in \Omega} \|X(\omega)\| < \infty.$$

$L^p(\Omega; W)$  is also called Bochner space.

**Theorem 2.2.21** ( $L^2$  convergence of the KLE (compare [LPS14])). Consider a random field  $\{Z(x) : x \in D\}$  and suppose that  $Z \in L^2(\Omega; L^2(D))$ . Then it holds

$$Z(x, \omega) = \mu(x) + \sum_{m=1}^{\infty} \sqrt{\gamma_m} g_m(x) \xi_m(\omega)$$

where the sum converges in  $L^2(\Omega; L^2(D))$ , with the random variables

$$\xi_m(\omega) := \frac{1}{\sqrt{\gamma_m}} \langle Z(x, \omega) - \mu(x), g_m(x) \rangle_{L^2(D)},$$

and  $(\gamma_m, g_m)$  denote the eigenvalues and eigenfunctions of the covariance integral operator  $C$ . The random variables  $\xi_m$  have mean zero, unit variance and are pairwise uncorrelated. If the random field is Gaussian, then  $\xi_m \sim \mathcal{N}(0, 1)$  iid.

*Proof.* The integral operator  $C$  is symmetric and compact and the Hilbert-Schmidt spectral theorem 2.2.13 gives an orthonormal basis  $\{g_m\}$  of eigenfunctions for the range of  $C$  which can be enlarged to a basis of  $L^2(D)$ . We obtain a representation of the form

$$Z(x, \omega) - \mu(x) = \sum_{m=1}^{\infty} g_m(x) \lambda_m(\omega)$$

where  $g_m$  are the eigenfunctions of  $C$  and  $\lambda_m(\omega) := \langle Z(x, \omega) - \mu(x), g_m(x) \rangle_{L^2(D)}$  are random variables. We define the truncated expansion

$$Z_M(x, \omega) := \mu(x) + \sum_{m=1}^M \sqrt{\gamma_m} g_m(x) \xi_m(\omega).$$

Since  $\{g_m : m \in \mathbb{N}\}$  is a basis for  $L^2(D)$ ,  $Z_M(x, \omega) \rightarrow Z(x, \omega)$  as  $M \rightarrow \infty$  in  $L^2(D)$  almost surely. Observe further that

$$\|Z - \mu\|_{L^2(D)}^2 = \sum_{m=1}^{\infty} |\langle g_m, Z - \mu \rangle_{L^2(D)}|^2$$

and

$$\|Z_M - \mu\|_{L^2(D)}^2 = \sum_{m=1}^M |\langle g_m, Z - \mu \rangle_{L^2(D)}|^2$$

hence  $\|Z_M - \mu\|_{L^2(D)}^2 \leq \|Z - \mu\|_{L^2(D)}^2$ . Using the Dominated Convergence Theorem this implies  $(Z_M - \mu) \rightarrow (Z - \mu)$  in  $L^2(\Omega, L^2(D))$ . Hence  $Z_M \rightarrow Z$  in  $L^2(\Omega, L^2(D))$  as  $M \rightarrow \infty$ .

Finally, recall that the random variables  $\lambda_m = \langle Z(x, \omega) - \mu(x), g_m(x) \rangle_{L^2(D)}$ . Hence  $\mathbb{E}[\lambda_m] = 0$  and thus  $\mathbb{E}[\xi_m] = \mathbb{E}[\lambda_m]/\sqrt{\gamma} = 0$ . Fubini's Theorem gives

$$\begin{aligned} \text{Cov}(\lambda_m, \lambda_k) &= \mathbb{E} \left[ \int_{D \times D} (Z(x) - \mu(x)) g_m(x) (Z(y) - \mu(y)) g_k(y) dx dy \right] \\ &= \int_{D \times D} c(x, y) g_m(x) g_k(y) dx dy = \langle g_m, C g_k \rangle_{L^2(D)}. \end{aligned}$$

The eigenfunctions are orthonormal,

$$\text{Var}[\lambda_m] = \text{Cov}(\lambda_m, \lambda_m) = \langle g_m, C g_m \rangle = \gamma_m.$$

This also shows that  $\gamma_m = \text{Var}[\lambda_m] \geq 0$ . Since  $\xi_m = \lambda_m/\sqrt{\gamma_m}$  we see that  $\{\xi_m\}$  are pairwise uncorrelated, have mean zero and that  $\text{Var}[\xi_m] = \text{Var}[\lambda_m]/\gamma_m = 1$ .  $\square$

**Theorem 2.2.22** (Uniform convergence of the KLE (compare [LPS14])). Consider a real-valued random field  $Z \in L^2(\Omega; L^2(D))$  and let  $Z_M(x, \omega) = \mu(x) + \sum_{m=1}^M \sqrt{\gamma_m} g_m(x) \xi_m(\omega)$  denote the KLE truncated after  $M$

## 2 Theoretical Foundations

terms. If  $D$  is a bounded domain and the covariance function  $c \in C(\overline{D} \times \overline{D})$ , then  $g_m \in C(\overline{D})$  and the series expansion

$$c(x, y) = \sum_{m=1}^{\infty} \gamma_m g_m(x) g_m(y)$$

converges uniformly for  $x, y \in \overline{D}$ . In particular

$$\sup_{x, y \in \overline{D}} |c(x, y) - c_M(x, y)| \leq \sup_{x \in \overline{D}} \sum_{m=M+1}^{\infty} \gamma_m g_m^2(x)$$

where  $c_M(x, y) := \sum_{m=1}^M \gamma_m g_m(x) g_m(y)$ . Moreover,

$$\sup_{x \in D} \mathbb{E} [|Z(x) - Z_M(x)|^2] \rightarrow 0 \text{ as } M \rightarrow \infty$$

*Proof.* By Mercer's theorem 2.2.19 we know that  $g_m \in C(\overline{D})$ , the series  $c(x, y) = \sum_{m=1}^{\infty} \gamma_m g_m(x) g_m(y)$  converges in  $C(\overline{D} \times \overline{D})$  and that

$$\sup_{x, y \in \overline{D}} |c(x, y) - c_M(x, y)| \leq \sup_{x \in \overline{D}} \sum_{m=M+1}^{\infty} \gamma_m g_m^2(x) \rightarrow 0 \text{ as } M \rightarrow \infty.$$

Moreover,

$$\sup_{x \in \overline{D}} \mathbb{E} [|Z(x) - Z_M(x)|^2] = \sup_{x \in \overline{D}} \sum_{m=M+1}^{\infty} \gamma_m g_m^2(x) \rightarrow 0 \text{ as } M \rightarrow \infty.$$

□

### 2.2.2 Domain Independence of the Karhunen-Loève Expansion

The source for this subsection is [PG15].

**Lemma 2.2.23.** Let  $V(x, \omega) \in L^2(D \times \Omega)$  be a mean-square continuous random field defined on  $D \subset \mathbb{R}^d$ , specified up to second order moments with  $\mu(x)$  as the mean and  $c(x, y)$  as the covariance function. Consider another domain  $D' \subset \mathbb{R}^d$  such that  $D \cap D' \neq \emptyset$  and define another mean-square continuous random field  $V'(x, \omega) \in L^2(D' \times \Omega)$  with the same mean  $\mu(x)$  and covariance function  $c(x, y)$ . Let  $(\gamma_i, g_i)$  be the  $i$ -th eigenpair of the integral operator of  $c$  on  $D$  and  $(\gamma'_i, g'_i)$  be the  $i$ -th eigenpair on  $D'$ . Let  $Z(x, \omega)$  and  $Z'(x, \omega)$  denote the complete (that is, without truncation) KL expansions of  $V(x, \omega)$  and  $V'(x, \omega)$ , respectively. Then for any  $x \in D \cap D'$  it holds:

- (I)  $\mathbb{E}[Z(x, \omega)] = \mathbb{E}[Z'(x, \omega)]$
- (II)  $\mathbb{E}[Z^2(x, \omega)] = \mathbb{E}[Z'^2(x, \omega)]$
- (III)  $\mathbb{E}[Z(x, \omega)Z(y, \omega)] = \mathbb{E}[Z'(x, \omega)Z'(y, \omega)]$

*Proof.* Since the covariance  $c(x, y)$  between any two points  $x, y \in D \cap D'$  is the same for both the domains, by Mercer's theorem, we can conclude that

$$c(x, y) = \sum_{i=1}^{\infty} \gamma_i g_i(x) g_i(y) = \sum_{i=1}^{\infty} \gamma'_i g'_i(x) g'_i(y) \quad \forall x, y \in D \cap D'$$

The KL expansions  $Z(x, \omega)$  and  $Z'(x, \omega)$  of random fields  $V(x, \omega)$  and  $V'(x, \omega)$ , respectively, are given by

$$\begin{aligned} Z(x, \omega) &= \mu(x) + \sum_{i=1}^{\infty} \sqrt{\gamma_i} g_i(x) \xi_i(\omega) \\ Z'(x, \omega) &= \mu(x) + \sum_{i=1}^{\infty} \sqrt{\gamma'_i} g'_i(x) \xi'_i(\omega) \end{aligned}$$

Each of the conclusions will be shown separately

(I)

$$\begin{aligned} \mathbb{E}[Z(x, \omega)] &= \mathbb{E}\left[\mu(x) + \sum_{i=1}^{\infty} \sqrt{\gamma_i} g_i(x) \xi_i(\omega)\right] \\ &= \mu(x) + \sum_{i=1}^{\infty} \sqrt{\gamma_i} g_i(x) \cdot \mathbb{E}[\xi_i(\omega)] \\ &= \mu(x) \end{aligned}$$

Similarly  $\mathbb{E}[Z'(x, \omega)] = \mu(x)$ . Hence  $\mathbb{E}[Z(x, \omega)] = \mathbb{E}[Z'(x, \omega)]$ .

(II)

$$\begin{aligned} \mathbb{E}[Z^2(x, \omega)] &= \mathbb{E}\left[\sum_{i=1}^{\infty} \sum_{j=1}^{\infty} \sqrt{\gamma_i} \sqrt{\gamma_j} g_i(x) g_j(x) \xi_i(\omega) \xi_j(\omega)\right] \\ &= \sum_{i=1}^{\infty} \sum_{j=1}^{\infty} \sqrt{\gamma_i} \sqrt{\gamma_j} g_i(x) g_j(x) \mathbb{E}[\xi_i(\omega) \xi_j(\omega)] \\ &= \sum_{i=1}^{\infty} \gamma_i g_i^2(x) \end{aligned}$$

Similarly  $\mathbb{E}[Z'^2(x, \omega)] = \sum_{i=1}^{\infty} \gamma'_i g'^2_i(x)$ .

(III)

$$\begin{aligned} \mathbb{E}[Z(x, \omega)Z(y, \omega)] &= \mathbb{E}\left[\sum_{i=1}^{\infty} \sum_{j=1}^{\infty} \sqrt{\gamma_i} \sqrt{\gamma_j} g_i(x) g_j(y) \xi_i(\omega) \xi_j(\omega)\right] \\ &= \sum_{i=1}^{\infty} \sum_{j=1}^{\infty} \sqrt{\gamma_i} \sqrt{\gamma_j} g_i(x) g_j(y) \mathbb{E}[\xi_i(\omega) \xi_j(\omega)] \\ &= \sum_{i=1}^{\infty} \gamma_i g_i(x) g_i(y) \end{aligned}$$

Similarly  $\mathbb{E}[Z'(x, \omega)Z'(y, \omega)] = \sum_{i=1}^{\infty} \gamma'_i g'_i(x) g'_i(y)$  which leads to

$$\mathbb{E}[Z(x, \omega)Z(y, \omega)] = \mathbb{E}[Z'(x, \omega)Z'(y, \omega)]$$

□

**Remark 2.2.24.** If the random field is Gaussian, the mean and second order moments completely specify the random field. 2.2.23 implies that a Gaussian random field is invariant to the change of the physical domain provided the functional form of the covariance kernel is retained the same.

However, the coefficients of the two KL-expansions  $Z$  and  $Z'$  do not retain the same, which leads to a difference in the truncated KL-expansion.

**Lemma 2.2.25.** Let  $\hat{Z}, \hat{Z}'$  denote the truncated versions of  $Z$  and  $Z'$ , respectively. Let

$$\begin{aligned} Z(x, \omega) - \hat{Z}(x, \omega) &= \epsilon(x, \omega) \\ Z'(x, \omega) - \hat{Z}'(x, \omega) &= \epsilon'(x, \omega) \end{aligned}$$

Then

$$\|\hat{Z}(x, \omega) - \hat{Z}'(x, \omega)\|_{L^2(\Omega)} \leq \|\epsilon'(x, \omega)\|_{L^2(\Omega)} + \|\epsilon(x, \omega)\|_{L^2(\Omega)}$$

where  $\|\cdot\|_{L^2(\Omega)}$  denotes the  $L^2(\Omega)$  norm.

## 2.3 Sobolev Spaces

The following definitions follow [Eva10]. By  $D^\alpha$  we denote the differential operator defined as  $D^\alpha u = \frac{\partial^{\alpha_1}}{\partial x_1^{\alpha_1}} \dots \frac{\partial^{\alpha_n}}{\partial x_n^{\alpha_n}} u$  for a multiindex  $\alpha \in \mathbb{N}^n$ .

**Definition 2.3.1** (Sobolev space). *The Sobolev space*

$$W^{k,p}(D) \tag{2.1}$$

consists of all locally summable functions  $u : D \rightarrow \mathbb{R}$  such that for each multi-index  $\alpha$  with  $|\alpha| \leq k$ ,  $D^\alpha u$  exists in the weak sense and belongs to  $L^p(D)$ .

If  $p = 2$ , we usually write

$$H^k(D) = W^{k,2}(D).$$

**Definition 2.3.2.** If  $u \in W^{k,p}(D)$ , we define its norm to be

$$\|u\|_{W^{k,p}(D)} := \begin{cases} \left( \sum_{|\alpha| \leq k} \int_D |D^\alpha u|^p dx \right)^{1/p} & (1 \leq p < \infty) \\ \sum_{|\alpha| \leq k} \text{ess sup}_D |D^\alpha u| & (p = \infty). \end{cases}$$

**Definition 2.3.3.** We denote by  $W_0^{k,p}(D)$  the closure of  $C_c^\infty(D)$  in  $W^{k,p}(D)$ .

Thus  $u \in W_0^{k,p}(D)$  if and only if there exist functions  $u_m \in C_c^\infty(D)$  such that  $u_m \rightarrow u$  in  $W^{k,p}(D)$ . We interpret  $W_0^{k,p}(D)$  as comprising those functions  $u \in W^{k,p}(D)$  such that

$$D^\alpha u = 0 \text{ on } \partial D \quad \forall |\alpha| \leq k-1$$

It is customary to write  $H_0^k(D) = W_0^{k,2}(D)$ .

**Definition 2.3.4** (Coercive). Let  $H$  be a Hilbert space. A bilinear form  $a : H \times H \rightarrow \mathbb{R}$  is called coercive if there exists a constant  $c > 0$  such that

$$a(u, u) \geq c\|u\|^2 \quad \forall u \in H.$$

**Theorem 2.3.5** (Lax-Milgram). Let  $H$  be a real Hilbert space with norm  $\|\cdot\|$  and let  $l$  be a bounded linear form on  $H$ . Let  $a : H \times H \rightarrow \mathbb{R}$  be a bilinear form that is bounded and coercive. Then there exists a unique  $u_l \in H$  such that  $a(u_l, v) = l(v)$  for all  $v \in H$ .

*Proof.* The proof can be found in [Eva10]. □

**Lemma 2.3.6** (Poincaré's inequality). *Let  $p$  be given such that  $1 \leq p < \infty$  and  $D \subset \mathbb{R}^d$  be bounded. Then there exists a constant  $C$  depending only on  $D$  and  $p$ , so that every function  $u$  of the Sobolev space  $W_0^{1,p}(D)$  satisfies:*

$$\|u\|_{L^p(D)} \leq C \cdot \|\nabla u\|_{L^p(D)}$$

*Especially there is a constant  $C$  for which  $\forall u \in H_0^1(D)$  it holds*

$$\|u\|_{L^2(D)} \leq C \cdot \|u\|_{H_0^1(D)}$$

*Proof.* The proof can be found in [Eva10]. □

**Theorem 2.3.7** (Trace theorem). *Assume  $D$  is bounded and  $\delta D$  is  $C^1$ . Then, there exists a bounded linear operator*

$$T : W^{1,p}(D) \rightarrow L^p(\delta D)$$

*such that*

(I)

$$Tu = u|_{\delta D} \quad \text{if } u \in W^{1,p}(D) \cap C(\overline{D})$$

(II)

$$\|Tu\|_{L^p(\delta D)} \leq C \cdot \|u\|_{W^{1,p}(D)},$$

*for each  $u \in W^{1,p}(D)$ , with the constant  $C$  depending only on  $p$  and  $D$ .*

*Proof.* The proof can be found in [Eva10]. □

# 3 Sensitivity Analysis

## 3.1 Single-valued Model Output

The notation and most of the general concepts of this chapter are based on [DV+21]. Throughout the whole section, we assume property 3.1.1 and use the following notation.

**Assumption 3.1.1.** *Each component  $X_i$ ,  $i = 1, \dots, l$ , of the random input vector  $X$  takes values in a complete, separable, metric space  $\Omega_i$ . All components are mutually statistically independent.*

**Remark 3.1.2** (Notation). *Let  $\mathcal{E}_i := \mathcal{B}(\Omega_i)$  denote the Borel  $\sigma$ -algebra associated with  $\Omega_i$ ,  $i = 1, \dots, l$ . Let  $\mathbb{P}_{X_i}$  denote the probability distribution of  $X_i$ ,  $i = 1, \dots, l$ . For any non-empty subset of indices  $A \in \mathcal{P}_l$ , where  $\mathcal{P}_l$  is the power set of  $\{1, \dots, l\}$ , let*

$$(\Omega_A, \mathcal{E}_A, \mathbb{P}_A) := \left( \bigotimes_{i \in A} \Omega_i, \bigotimes_{i \in A} \mathcal{E}_i, \prod_{i \in A} \mathbb{P}_{X_i} \right),$$

$$\Omega := \Omega_{1:l}, \mathcal{E} := \mathcal{E}_{1:l} \text{ and } \mathbb{P}_X = \prod_{i=1}^l \mathbb{P}_{X_i}.$$

For any subset of indices  $A \in \mathcal{P}_l$  we define the  $\sigma$ -algebra

$$\mathcal{F}_A := \left( \bigotimes_{i \in A} \mathcal{E}_i \right) \otimes \left( \bigotimes_{i \in A^c} \{\emptyset, \Omega_i\} \right)$$

We denote by  $L^2(\mathbb{P}_X) := L^2(\Omega, \mathcal{E}, \mathbb{P}_X)$  the following set:

$$L^2(\mathbb{P}_X) := \{f : \Omega \rightarrow \mathbb{R}, f \text{ is } \mathcal{E} - \mathcal{B}(\mathbb{R})\text{-measurable}, \mathbb{E}[f(X)^2] < \infty\}.$$

For any  $A \in \mathcal{P}_l$  let  $L_A^2$  denote the subspace of functions in  $L^2(\mathbb{P}_X)$  that are  $\mathcal{F}_A - \mathcal{B}(\mathbb{R})$ -measurable

$$L_A^2 := \{f \in L^2(\mathbb{P}_X), f \text{ is } \mathcal{F}_A - \mathcal{B}(\mathbb{R})\text{-measurable}\}.$$

**Theorem 3.1.3** (Hoeffding decomposition). *Let  $G \in L^2(\mathbb{P}_X)$ . Under assumption 3.1.1 there exists a unique decomposition of  $G$  in  $L^2(\mathbb{P}_X)$  of the form*

$$G(X) = \sum_{A \in \mathcal{P}_l} G_A(X_A), \quad \mathbb{P}_X - a.s.,$$

such that the following properties hold:

- (I)  $G_\emptyset$  is constant  $\mathbb{P}_X - a.s.$ .
- (II) For all  $A \in \mathcal{P}_l$ ,  $A \neq \emptyset$  it holds  $\int_{\Omega_i} G_A(x_A) d\mathbb{P}_{X_i}(x_i) = 0 \quad \forall i \in A$ .

The functions  $G_A$ ,  $A \in \mathcal{P}_l$  are given by

$$G_A(X_A) = \sum_{B \subseteq A} (-1)^{|A|-|B|} \mathbb{E}[G(X)|X_B] \quad \mathbb{P}_X - a.s..$$

*Proof.* Can be found at [DV+21]. □

**Lemma 3.1.4** (Functional ANOVA). *Let  $G \in L^2(\mathbb{P}_X)$ . For any  $A \in \mathcal{P}_l$ ,  $A \neq \emptyset$ , let  $V_A := \text{Var}G_A(X_A)$ . Then under assumption 3.1.1 it holds*

$$\text{Var}G(X) = \sum_{A \in \mathcal{P}_l, A \neq \emptyset} V_A$$

Moreover, for any  $A \in \mathcal{P}_l$ ,  $A \neq \emptyset$  it holds

$$V_A = \sum_{B \subseteq A} (-1)^{|A|-|B|} \text{Var} \mathbb{E}[G(X)|X_B] \quad (3.1)$$

*Proof.* Can be found at [DV+21].  $\square$

**Definition 3.1.5** (Sobol' sensitivity index). *Let  $G \in L^2(\mathbb{P}_X)$ . Let  $A \in \mathcal{P}_l$ . Let assumption 3.1.1 be satisfied.*

- *The Sobol' sensitivity index (in short, the Sobol' index) associated with  $A$  is defined as*

$$S_A = \frac{V_A}{V}$$

where  $V = \text{Var}G(X)$ ,  $A \neq \emptyset$  and  $V_A = \text{Var}G_A(X_A)$  is given in (3.1). For  $A = \emptyset$  we define  $S_0 = 0$ .

- *The index  $S_j := S_{\{j\}}$  associated with the singleton  $\{j\}$  is called Sobol' single effect sensitivity index for the input  $X_j$ .*
- *Let  $p := |A|$ , then  $S_A$  is called  $p$ -th order Sobol' index for the input  $X_A$ .*
- *The closed Sobol' index associated with  $A$  is defined as*

$$S_A^{clos} = \sum_{A' \subseteq A} S_{A'}$$

- *The Sobol' total effect sensitivity index associated with  $A$  is defined as*

$$S_A^t = \sum_{A' \in \mathcal{P}_l, A' \cap A \neq \emptyset} S_{A'}$$

## 3.2 Vector-valued Model Output

This section's theory and notation is based on [DV+21]. Consider a model of the form  $Y = G(X)$  where  $G : \Omega \rightarrow \mathbb{R}^k$  with  $\Omega \subset \mathbb{R}^l$ ,  $l, k \in \mathbb{N}$ ,  $k > 1$ . As before assume that the input components  $X_1, \dots, X_l$  are mutually statistically independent.

We introduce the corresponding Hilbert space:

$$\begin{aligned} L^2(\mathbb{P}_X)^k &:= \{f : \Omega \rightarrow \mathbb{R}^k, f \text{ is } \mathcal{E} - \mathcal{B}(\mathbb{R}^k) \text{ measurable, } \mathbb{E}[\|f\|^2] < \infty\} \\ \langle f, g \rangle &:= \mathbb{E}[g(X)^T f(X)] \quad \forall f, g \in L^2(\mathbb{P}_X)^k \\ \|f\|_{L^2} &:= \sqrt{\langle f, f \rangle}, \quad \forall f \in L^2(\mathbb{P}_X)^k. \end{aligned}$$

**Definition 3.2.1.** *For random vectors  $U, V$  taking values in  $\mathbb{R}^k$  we define the covariance matrix  $C_{U,V} := \mathbb{E}[(U - \mathbb{E}[U])(V - \mathbb{E}[V])^T]$ .*

**Lemma 3.2.2.** *Let  $U, V \in L^2(\mathbb{P}_X)^k$ , then it holds*

$$\langle U - \mathbb{E}[U], V - \mathbb{E}[V] \rangle = \text{Tr}(C_{U,V})$$

where  $\text{Tr}(\cdot)$  denotes the trace (sum of diagonal elements) of a matrix.

### 3 Sensitivity Analysis

*Proof.* Using the cyclic invariance of the trace of the product of two matrices, that is,  $\text{Tr}(AB) = \text{Tr}(BA)$  for matrices  $A \in \mathbb{R}^{n \times m}, B \in \mathbb{R}^{m \times n}$ , together with the linearity of both the trace and the expectation operator, we obtain

$$\begin{aligned}\langle U - \mathbb{E}[U], V - \mathbb{E}[V] \rangle &= \mathbb{E}[(V - \mathbb{E}[V])^T(U - \mathbb{E}[U])] \\ &= \mathbb{E}\left[\text{Tr}\left((V - \mathbb{E}[V])^T(U - \mathbb{E}[U])\right)\right] \\ &= \mathbb{E}\left[\text{Tr}\left((U - \mathbb{E}[U])(V - \mathbb{E}[V])^T\right)\right] \\ &= \text{Tr}\left(\mathbb{E}\left[(U - \mathbb{E}[U])(V - \mathbb{E}[V])^T\right]\right) = \text{Tr}(C_{U,V})\end{aligned}$$

□

**Definition 3.2.3** (Hoeffding-like decomposition for vector-valued model). *We introduce a decomposition in the manner of theorem 3.1.3 for vector-valued models.*

$$\begin{aligned}G(X) &= G_0 + G_A(X_A) + G_{A^c}(X_{A^c}) + G_{A,A^c}(X_A, X_{A^c}) \\ Y &= Y_0 + Y_A + Y_{A^c} + Y_{A,A^c} \\ Y_0 &:= \mathbb{E}[G(X)] \\ Y_A &:= \mathbb{E}[Y|X_A] - Y_0 \\ Y_{A^c} &:= \mathbb{E}[Y|X_{A^c}] - Y_0 \\ Y_{A,A^c} &:= Y - Y_A - Y_{A^c} - Y_0\end{aligned}$$

**Lemma 3.2.4** (Trace decomposition). *It holds*

$$\text{Tr}(C_{Y,Y}) = \text{Tr}(C_{Y_A,Y_A}) + \text{Tr}(C_{Y_{A^c},Y_{A^c}}) + \text{Tr}(C_{Y_{A,A^c},Y_{A,A^c}})$$

*Proof.* We use that the four components are mutually orthogonal in the  $L^2$ -inner product. For example, it holds

$$\langle Y_A, Y_{A,A^c} \rangle = \mathbb{E}[Y_{A,A^c}^T Y_A] = \mathbb{E}[(Y - Y_A - Y_{A^c} - Y_0)^T Y_A] = \mathbb{E}[(Y - Y_A)^T Y_A] = 0.$$

$$\begin{aligned}\|Y - Y_0\|_{L^2}^2 &= \langle Y - Y_0, Y - Y_0 \rangle \\ &= \langle Y_A + Y_{A^c} + Y_{A,A^c}, Y_A + Y_{A^c} + Y_{A,A^c} \rangle \\ &\stackrel{\text{orthog.}}{=} \langle Y_A, Y_A \rangle + \langle Y_{A^c}, Y_{A^c} \rangle + \langle Y_{A,A^c}, Y_{A,A^c} \rangle \\ &= \|Y_A\|_{L^2}^2 + \|Y_{A^c}\|_{L^2}^2 + \|Y_{A,A^c}\|_{L^2}^2\end{aligned}\tag{3.2}$$

$$\begin{aligned}\text{Tr}(C_{Y,Y}) &\stackrel{3.2.2}{=} \|Y - Y_0\|_{L^2}^2 \stackrel{(3.2)}{=} \|Y_A\|_{L^2}^2 + \|Y_{A^c}\|_{L^2}^2 + \|Y_{A,A^c}\|_{L^2}^2 \\ &\stackrel{3.2.2}{=} \text{Tr}(C_{Y_A,Y_A}) + \text{Tr}(C_{Y_{A^c},Y_{A^c}}) + \text{Tr}(C_{Y_{A,A^c},Y_{A,A^c}})\end{aligned}$$

□

**Definition 3.2.5.** Let  $G \in L^2(\mathbb{P}_X)^k$  and  $\text{Tr}(C_{Y,Y}) \neq 0$ . Let  $A \in \mathcal{P}_l$ . Let assumption 3.1.1 be satisfied. The aggregated closed Sobol' sensitivity index associated with  $A$  is defined as

$$S_A^{\text{clos},Y} = \frac{\text{Tr}(C_{Y_A,Y_A})}{\text{Tr}(C_{Y,Y})}.$$

The aggregated total Sobol' sensitivity index associated with  $A$  is defined as

$$S_A^{t,Y} = 1 - \frac{\text{Tr}(C_{Y_{A^c},Y_{A^c}})}{\text{Tr}(C_{Y,Y})}.$$

### 3.3 Functional-valued Model Output

For the following Sensitivity Analysis, given the probability space  $(\Omega, \mathcal{E}, \mathbb{P}_X)$ , consider a model  $G : D \times \Omega \rightarrow \mathbb{R}$  of the following form:

$$Y = G(y, X), \quad y \in D \quad (3.3)$$

where  $D \subset \mathbb{R}^d$  and  $X$  is a random vector with independent components, taking values in  $\Omega$ . The general concept of Sensitivity Analysis for Hilbert-space-valued models is explained in [Gam+14]. For  $D = [t_0, t_1] \subset \mathbb{R}$  time-dependent Sobol' indices are introduced in [AGS19].

**Assumption 3.3.1.** Consider a model of the form (3.3) then assume

(I)  $X$  is a random vector with independent components taking values in  $\Omega \subset \mathbb{R}^l$ .

(II)  $G \in L^2(D; \mathbb{P}_X)$ , that is

$$\int_D \int_{\Omega} G(y, x)^2 d\mathbb{P}_X(x) dy < \infty \quad (3.4)$$

(III)  $G$  is mean-square continuous, that is

$$\lim_{\|h\|_2 \rightarrow 0} \int_{\Omega} (G(y + h, x) - G(y, x))^2 d\mathbb{P}_X(x) = 0 \quad \forall y \in D \quad (3.5)$$

**Definition 3.3.2** (Hoeffding-like decomposition for functional-valued model). Consider a model  $G(y, X)$  of the form (3.3) and  $A \in \mathcal{P}_l$ . Then we can find a similar decomposition as in theorem 3.1.3 (compare [AGS19])

$$\begin{aligned} G(y, X) &= G_0(y) + G_A(y, X_A) + G_{A^c}(y, X_{A^c}) + G_{A,A^c}(y, X) \\ G_0(y) &:= \mathbb{E}[G(y, X)] \\ G_A(y, X_A) &:= \mathbb{E}[G(y, X)|X_A] - G_0(y) \\ G_{A^c}(y, X_{A^c}) &:= \mathbb{E}[G(y, X)|X_{A^c}] - G_0(y) \\ G_{A,A^c}(y, X) &:= G(y, X) - G_A(y, X_A) - G_{A^c}(y, X_{A^c}) - G_0(y) \end{aligned}$$

**Lemma 3.3.3.** The components of the decomposition in definition 3.3.2 satisfy the following properties

(I) For the expected values it holds

$$\mathbb{E}[G_A] = \mathbb{E}[G_{A^c}] = \mathbb{E}[G_{A,A^c}] = 0$$

(II) Mutual orthogonality

$$\mathbb{E}[G_A G_{A^c}] = \mathbb{E}[G_A G_{A,A^c}] = \mathbb{E}[G_{A^c} G_{A,A^c}] = 0$$

*Proof.* The expected values immediately follow by the definition.

The proof of  $\mathbb{E}[G_{A^c} G_{A,A^c}] = 0$  works equivalently to  $\mathbb{E}[G_A G_{A,A^c}] = 0$ .

$$\begin{aligned} \mathbb{E}[G_A G_{A^c}] &\stackrel{\text{indep.}}{=} \mathbb{E}[G_A] \cdot \mathbb{E}[G_{A^c}] = 0 \\ \mathbb{E}[G_A G_{A,A^c}] &= \mathbb{E}[G_A \cdot (G - G_0 - G_A - G_{A^c})] \\ &= \mathbb{E}[G_A G] - \underbrace{\mathbb{E}[G_A G_0]}_{=0} - \underbrace{\mathbb{E}[G_A G_A]}_{=0} - \underbrace{\mathbb{E}[G_A G_{A^c}]}_{=0} \\ &= \mathbb{E}[G_A \cdot (G - G_A)] \\ &\stackrel{\text{indep.}}{=} \mathbb{E}[G_A] \mathbb{E}[G - G_A] = 0 \end{aligned}$$

□

**Lemma 3.3.4.** Under assumption 3.3.1 the mean-function  $\mu(y) = \mathbb{E}[G(y, x)]$  and the covariance function  $c(y_1, y_2) = \mathbb{E}[(G(y_1, x) - \mu(y_1)) \cdot (G(y_2, x) - \mu(y_2))]$  are well-defined and continuous on  $D$ , resp.  $D \times D$ .

*Proof.* The mean-function and the covariance function are immediately well-defined by assumption 3.4. The continuity of the mean-function follows by

$$\begin{aligned} |\mu(y + h) - \mu(y)| &= |\mathbb{E}[G(y + h, x) - G(y, x)]| \\ &\leq \mathbb{E}[|G(y + h, x) - G(y, x)|] \\ &\leq \sqrt{\mathbb{E}[(G(y + h, x) - G(y, x))^2]} \xrightarrow{\|h\|_2 \rightarrow 0} 0 \end{aligned}$$

The continuity of the covariance function is derived as follows (with the notation  $G(y) := G(y, x)$ ):

$$\begin{aligned} &|c(y_1 + h_1, y_2 + h_2) - c(y_1, y_2)| \\ &= |\mathbb{E}[(G(y_1 + h_1) - \mu(y_1 + h_1)) \cdot (G(y_2 + h_2) - \mu(y_2 + h_2))] - \mathbb{E}[(G(y_1) - \mu(y_1)) \cdot (G(y_2) - \mu(y_2))]| \\ &= |\mathbb{E}[G(y_1 + h_1) \cdot G(y_2 + h_2)] - \underbrace{\mathbb{E}[G(y_1) \cdot G(y_2)] + \mu(y_1) \cdot \mu(y_2) - \mu(y_1 + h_1) \cdot \mu(y_2 + h_2)}_{\|h_1\|_2, \|h_2\|_2 \rightarrow 0} | \\ &\leq \mathbb{E}[|(G(y_1 + h_1) - G(y_1)) \cdot G(y_2 + h_2)|] + \mathbb{E}[|G(y_1) \cdot (G(y_2 + h_2) - G(y_2))|] \\ &\leq \sqrt{\mathbb{E}[(G(y_1 + h_1) - G(y_1))^2] \cdot \mathbb{E}[(G(y_2 + h_2))^2]} + \sqrt{\mathbb{E}[(G(y_1))^2] \cdot \mathbb{E}[(G(y_2 + h_2) - G(y_2))^2]} \\ &\xrightarrow{\|h_1\|_2, \|h_2\|_2 \rightarrow 0} 0 \end{aligned}$$

□

**Lemma 3.3.5.** Let  $H$  be the separable Hilbert-space  $L^2(D)$  and  $\{\phi_m, m \in \mathbb{N}\}$  be an orthonormal basis of  $H$ . Then under assumption 3.3.1 we can define traces for the covariance operator  $C$  of the model  $G(y, X)$  (3.3) and the covariance operator  $C_A$  of  $G_A(y, X)$  for  $A \in \mathcal{P}_l$  with the covariance functions  $c$  and  $c_A$  respectively. It holds

$$\begin{aligned} Tr(C) &= \sum_{m=1}^{\infty} \langle C\phi_m, \phi_m \rangle_H = \int_D c(y, y) dy = \int_D Var G(y, X) dy \\ Tr(C_A) &= \sum_{m=1}^{\infty} \langle C_A\phi_m, \phi_m \rangle_H = \int_D c_A(y, y) dy = \int_D Var G_A(y, X_A) dy. \end{aligned}$$

*Proof.* We use the previous lemma 3.3.4 for the continuity of  $c$ , and the continuity of  $c_A$  follows. Then we apply Mercer's theorem 2.2.19. □

**Definition 3.3.6** (Sobol' indices for functional-valued model output). This definition follows the general Hilbert-spaced model outputs from [Gam+14].

Let assumption 3.3.1 be satisfied. Let  $A \in \mathcal{P}_l$ . Let  $c_A$  and  $C_A$  denote the covariance function and the associated covariance operator of the field  $G_A$  in the pointwise Hoeffding decomposition. The generalized Sobol' sensitivity index associated with  $A$  is defined as

$$S_A^{clos}(G) = \frac{Tr(C_A)}{Tr(C)} = \frac{\int_D Var G_A(y, X_A) dy}{\int_D Var G(y, X) dy}.$$

The total generalized Sobol' sensitivity index associated with  $A$  is defined as

$$S_A^t(G) = 1 - \frac{Tr(C_{A^c})}{Tr(C)} = 1 - \frac{\int_D Var G_{A^c}(y, X_{A^c}) dy}{\int_D Var G(y, X) dy}$$

**Definition 3.3.7** (Sobol' indices for functional-valued multidimensional model output). Consider a model of the form  $Y = G(y, X)$  where  $G : D \times \Omega \rightarrow \mathbb{R}^k$  and assume 3.1.1. We use the same pointwise Hoeffding-like decomposition as in definition 3.3.2 to define the components denoted by

$$G(y, X) := \begin{pmatrix} G^{(1)}(y, X) \\ \vdots \\ G^{(k)}(y, X) \end{pmatrix} \in \mathbb{R}^k, \quad G_0(y) := \begin{pmatrix} G_0^{(1)}(y) \\ \vdots \\ G_0^{(k)}(y) \end{pmatrix} \in \mathbb{R}^k, \quad G_A(y, X_A) := \begin{pmatrix} G_A^{(1)}(y, X_A) \\ \vdots \\ G_A^{(k)}(y, X_A) \end{pmatrix} \in \mathbb{R}^k,$$

$$G_{A^c}(y, X_{A^c}) := \begin{pmatrix} G_{A^c}^{(1)}(y, X_{A^c}) \\ \vdots \\ G_{A^c}^{(k)}(y, X_{A^c}) \end{pmatrix} \in \mathbb{R}^k, \quad G_{A,A^c}(y, X) := \begin{pmatrix} G_{A,A^c}^{(1)}(y, X) \\ \vdots \\ G_{A,A^c}^{(k)}(y, X) \end{pmatrix} \in \mathbb{R}^k$$

with  $G(y, X) = G_0(y) + G_A(y, X_A) + G_{A^c}(y, X_{A^c}) + G_{A,A^c}(y, X)$ .

For  $A \in \mathcal{P}_l$  we define the following Sobol' indices:

$$S_A^{\text{clos}}(G) = \frac{\int_D \left( \sum_{j=1}^k \text{Var } G_A^{(j)}(y, X_A) \right) dy}{\int_D \left( \sum_{j=1}^k \text{Var } G^{(j)}(y, X) \right) dy}, \quad (3.6)$$

$$S_A^t(G) = 1 - \frac{\int_D \left( \sum_{j=1}^k \text{Var } G_{A^c}^{(j)}(y, X_{A^c}) \right) dy}{\int_D \left( \sum_{j=1}^k \text{Var } G^{(j)}(y, X) \right) dy} \quad (3.7)$$

**Lemma 3.3.8.** The defined Sobol' indices in (3.6) and (3.7) align with the general formulation of Gamboa [Gam+14].

*Proof.* As for a sample  $x$  the model output  $G(y, x)$  is in the Hilbert-space  $H = L^2(D)^k$  we consider  $\langle u, v \rangle := \langle u, v \rangle_{L^2(D)^k}$  and  $\|u\| := \sqrt{\langle u, u \rangle}_{L^2(D)^k}$ .

The general approach in [Gam+14] introduces the Sobol' indices as

$$\begin{aligned} S_A^{\text{clos}}(G) &= \frac{\text{Tr}(\Gamma_A)}{\text{Tr}(\Gamma)} \\ \Gamma(h) &:= \mathbb{E}[\langle Y, h \rangle Y] \quad \forall h \in H \\ \Gamma_A(h) &:= \mathbb{E}[\langle Y^{\sim A}, h \rangle Y] \quad \forall h \in H \\ \text{Tr}(\Gamma) &= \mathbb{E}[\|Y\|^2] - \|\mathbb{E}[Y]\|^2 \\ \text{Tr}(\Gamma_A) &= \frac{1}{4} \left( \mathbb{E}[\|Y + Y^{\sim A}\|^2] - \mathbb{E}[\|Y - Y^{\sim A}\|^2] - 4 \cdot \|\mathbb{E}[Y]\|^2 \right) \end{aligned}$$

where  $Y = G(y, X)$  and  $Y^{\sim A} = G(y, X^{\sim A})$ ,  $X^{\sim A} = (X_A, X'_{A^c})^T$  and  $X'_{A^c}$  is an independent copy of  $X_{A^c}$ .

Therefore, we have to show that

$$\begin{aligned} \frac{\text{Tr}(\Gamma_A)}{\text{Tr}(\Gamma)} &= \frac{\int_D \left( \sum_{j=1}^k \text{Var } G_A^{(j)}(y, X_A) \right) dy}{\int_D \left( \sum_{j=1}^k \text{Var } G^{(j)}(y, X) \right) dy} \\ \text{Tr}(\Gamma) &= \int_{\Omega} \|G\|^2 d\mathbb{P}_X(x) - \int_D \mathbb{E}[G]^T \mathbb{E}[G] dy \\ &= \int_{\Omega} \int_D G^T G dy d\mathbb{P}_X(x) - \int_D \left( \int_{\Omega} G d\mathbb{P}_X(x) \right)^T \left( \int_{\Omega} G d\mathbb{P}_X(x) \right) dy \\ &= \int_D \left( \sum_{j=1}^k \int_{\Omega} \left( G^{(j)} \right)^2 d\mathbb{P}_X(x) - \sum_{j=1}^k \left( \int_{\Omega} G^{(j)} d\mathbb{P}_X(x) \right)^2 \right) dy \\ &= \int_D \left( \sum_{j=1}^k \text{Var}[G^{(j)}(y, X)] \right) dy \end{aligned}$$

### 3 Sensitivity Analysis

For the denominator, we need the following auxiliary statement

$$\begin{aligned}\mathbb{E}[Y^{(j)} \cdot Y^{\sim A, (j)}] &= \mathbb{E}[\mathbb{E}[Y^{(j)} \cdot Y^{\sim A, (j)} | X_A]] = \mathbb{E}[\mathbb{E}[Y^{(j)} | X_A] \cdot \mathbb{E}[Y^{\sim A, (j)} | X_A]] \\ &= \mathbb{E}[\mathbb{E}[Y^{(j)} | X_A]^2] = \mathbb{E}[\mathbb{E}[G_0^{(j)} + G_A^{(j)} + G_{A^c}^{(j)} + G_{A,A^c}^{(j)} | X_A]^2] \\ &= \mathbb{E}[(G_0^{(j)} + G_A^{(j)})^2] = (G_0^{(j)})^2 + \mathbb{E}[(G_A^{(j)})^2]\end{aligned}\tag{3.8}$$

where we used the properties derived in lemma 3.3.3.

$$\begin{aligned}\text{Tr}(\Gamma_A) &= \frac{1}{4} \left( \mathbb{E}[\|Y + Y^{\sim A}\|^2] - \mathbb{E}[\|Y - Y^{\sim A}\|^2] - 4\|\mathbb{E}[Y]\|^2 \right) \\ &= \frac{1}{4} \left( \int_{\Omega} \int_D (Y + Y^{\sim A})^T (Y + Y^{\sim A}) dy d\mathbb{P}_X(x) \right. \\ &\quad \left. - \int_{\Omega} \int_D (Y - Y^{\sim A})^T (Y - Y^{\sim A}) dy d\mathbb{P}_X(x) \right. \\ &\quad \left. - 4 \int_D (G_0(y))^T G_0(y) dy \right) \\ &= \int_D \left( \int_{\Omega} Y^T Y^{\sim A} d\mathbb{P}_X(x) - (G_0(y))^T G_0(y) \right) dy \\ &= \int_D \left( \sum_{j=1}^k \int_{\Omega} Y^{(j)} Y^{\sim A, (j)} d\mathbb{P}_X(x) - (G_0^{(j)}(y))^2 \right) dy \\ &= \int_D \left( \sum_{j=1}^k \mathbb{E}[Y^{(j)} Y^{\sim A, (j)}] - (G_0^{(j)}(y))^2 \right) dy \\ &\stackrel{(3.8)}{=} \int_D \left( \sum_{j=1}^k \text{Var}[G_A^{(j)}] \right) dy\end{aligned}$$

By definition, it holds  $S_A^t(G) = 1 - S_{A^c}^{\text{clos}}(G)$ , so the derivation for the total index follows immediately from the derivation for the closed index.  $\square$

### 3.4 Estimation of Sobol' Indices

The following algorithm in the notation of [Smi13] was invented by Saltelli in [Sal02]. It is based on the general approach of Sobol [Sob01]. In comparison to other algorithms it reduces the model evaluation for calculating multiple Sobol' indices at the same time.

**Algorithm 3.4.1** (Sobol' index estimation for single-valued model output). *Let  $(\Omega, \mathcal{E}, \mathbb{P}_X)$  be a probability space and let  $X_i \sim \mathbb{P}_{X_i}$  for  $i = 1, \dots, l$  with corresponding densities  $p_i(X_i)$ , taking values in  $\Omega_i$ , be independent random variables. Furthermore let  $Y = f(X)$  be a one-dimensional model.*

1. Create two  $M \times l$  sample matrices

$$A = \begin{pmatrix} x_1^1 & \dots & x_i^1 & \dots & x_l^1 \\ \vdots & & & & \vdots \\ x_1^M & \dots & x_i^M & \dots & x_l^M \end{pmatrix}, \quad B = \begin{pmatrix} \hat{x}_1^1 & \dots & \hat{x}_i^1 & \dots & \hat{x}_l^1 \\ \vdots & & & & \vdots \\ \hat{x}_1^M & \dots & \hat{x}_i^M & \dots & \hat{x}_l^M \end{pmatrix}$$

where  $x_i^j$  and  $\hat{x}_i^j$  are samples drawn from the respective densities of  $X_i$ .

2. Create  $M \times l$  matrices for  $i = 1, \dots, l$

$$C_i = \begin{pmatrix} \hat{x}_1^1 & \dots & x_i^1 & \dots & \hat{x}_l^1 \\ \vdots & & & & \vdots \\ \hat{x}_1^M & \dots & x_i^M & \dots & \hat{x}_l^M \end{pmatrix}$$

which are identical to  $B$  with the exception that the  $i$ -th column is taken from  $A$ .

3. Compute  $M \times 1$  vectors of model outputs

$$\tilde{y}_A = f(A), \quad \tilde{y}_B = f(B), \quad \tilde{y}_{C_i} = f(C_i)$$

by evaluating the model at the input values in  $A$ ,  $B$ , and  $C_i$  row by row. The evaluation of  $\tilde{y}_A$  and  $\tilde{y}_B$  requires  $2M$  model evaluations, whereas the evaluation of  $\tilde{y}_{C_i}, i = 1, \dots, l$ , requires  $l \cdot M$  evaluations. Hence the total number of model evaluations is  $M \cdot (l + 2)$ .

4. The estimates for the first order sensitivity indices are

$$S_i = \frac{\text{Var } \mathbb{E}[Y|x_i]}{\text{Var } Y} = \frac{\frac{1}{M} \tilde{y}_A^T \tilde{y}_{C_i} - f_0^2}{\frac{1}{M} \tilde{y}_A^T \tilde{y}_A - f_0^2} = \frac{\frac{1}{M} \sum_{j=1}^M \tilde{y}_A^j \tilde{y}_{C_i}^j - f_0^2}{\frac{1}{M} \sum_{j=1}^M (\tilde{y}_A^j)^2 - f_0^2}$$

where the mean is approximated by

$$f_0^2 = \left( \frac{1}{M} \sum_{j=1}^M \tilde{y}_A^j \right) \cdot \left( \frac{1}{M} \sum_{j=1}^M \tilde{y}_B^j \right)$$

The estimates for the total effect indices are

$$S_i^t = 1 - \frac{\text{Var } \mathbb{E}[Y|x_{\sim i}]}{\text{Var } Y} = 1 - \frac{\frac{1}{M} \tilde{y}_B^T \tilde{y}_{C_i} - f_0^2}{\frac{1}{M} \tilde{y}_A^T \tilde{y}_A - f_0^2} = 1 - \frac{\frac{1}{M} \sum_{j=1}^M \tilde{y}_B^j \tilde{y}_{C_i}^j - f_0^2}{\frac{1}{M} \sum_{j=1}^M (\tilde{y}_A^j)^2 - f_0^2}.$$

Here  $x_{\sim i}$  denotes all components of  $x$  but the  $i$ -th.

*Proof.* As the estimators don't seem intuitive at first sight, the following computation should explain the convergence. It follows the explanation in [Sal02] with a reference to [Sob01] and [IH90].

For reasons of notation, the set  $\Omega_{\sim i} = \bigotimes_{j \in \{1, \dots, i-1, i+1, \dots, l\}} \Omega_j$  is introduced. First, we emphasize the estimation of the first order sensitivity index  $S_i$ :

$$\begin{aligned} \text{Var}[Y|x_i = \tilde{x}_i] &= \int_{\Omega_{\sim i}} (f(x_1, \dots, x_{i-1}, \tilde{x}_i, x_{i+1}, \dots, x_l) - \mathbb{E}[Y|x_i = \tilde{x}_i])^2 \prod_{\substack{j=1 \\ j \neq i}}^l p_j(x_j) dx_j \\ &= \int_{\Omega_{\sim i}} f^2(x_1, \dots, x_{i-1}, \tilde{x}_i, x_{i+1}, \dots, x_l) \prod_{\substack{j=1 \\ j \neq i}}^l p_j(x_j) dx_j - \int_{\Omega_i} \mathbb{E}^2[Y|x_i = \tilde{x}_i] p_i(\tilde{x}_i) d\tilde{x}_i \\ \mathbb{E}[\text{Var}[Y|x_i]] &= \int_{\Omega_1} \dots \int_{\Omega_l} f^2(x_1, \dots, x_{i-1}, x_i, x_{i+1}, \dots, x_l) \prod_{j=1}^l p_j(x_j) dx_j - \int_{\Omega_i} \mathbb{E}^2[Y|x_i = \tilde{x}_i] p_i(\tilde{x}_i) d\tilde{x}_i \\ \text{Var}[\mathbb{E}[Y|x_i]] &= \text{Var}[Y] - \mathbb{E}[\text{Var}[Y|x_i]] \\ &= \int_{\Omega_i} \mathbb{E}^2[Y|x_i = \tilde{x}_i] p_i(\tilde{x}_i) d\tilde{x}_i - \mathbb{E}^2[Y] \end{aligned}$$

### 3 Sensitivity Analysis

This hints at a double-loop Monte Carlo estimation, which is computationally disastrous. Ishigami and Homma [IH90] rewrote the integral as follows:

$$\begin{aligned}
& \int_{\Omega_i} \mathbb{E}^2[Y|x_i = \tilde{x}_i] p_i(\tilde{x}_i) d\tilde{x}_i \\
&= \int_{\Omega_i} \left( \int_{\Omega_{\sim i}} f(x_1, \dots, \tilde{x}_i, \dots, x_l) \prod_{\substack{j=1 \\ j \neq i}}^l p_j(x_j) dx_j \right)^2 p_i(\tilde{x}_i) d\tilde{x}_i \\
&= \int_{\Omega_{\sim i}} \int_{\Omega_1} \dots \int_{\Omega_l} f(x_1, \dots, x_i, \dots, x_l) \cdot f(x'_1, \dots, x_j, \dots, x'_l) \prod_{j=1}^l (p_j(x_j) dx_j) \prod_{\substack{j=1 \\ j \neq i}}^l (p_j(x'_j) dx'_j)
\end{aligned}$$

which is the expected value of a function  $F$  depending on  $(2l - 1)$  factors.

$$F(x_1, \dots, x_i, \dots, x_l, x'_1, \dots, x'_{i-1}, x'_{i+1}, \dots, x'_l) = f(x_1, \dots, x_l) \cdot f(x'_1, \dots, x'_{i-1}, x_i, x'_{i+1}, \dots, x'_l)$$

This is the term we are estimating with a single Monte-Carlo loop in the algorithm above with  $\frac{1}{M} \sum_{j=1}^M \tilde{y}_A^j \tilde{y}_{C_i}^j$ .

A similar computation follows for the total index  $S_i^t$ :

$$\begin{aligned}
S_i^t &= 1 - \frac{\text{Var } \mathbb{E}[Y|x_{\sim i}]}{\text{Var } Y} = 1 - \frac{\text{Var } Y - \mathbb{E}[\text{Var}[Y|x_{\sim i}]]}{\text{Var } Y} \\
&= 1 - \left( \int_{\Omega_{\sim i}} \mathbb{E}^2[Y|x_j = \tilde{x}_j \text{ for } j = 1, \dots, l, j \neq i] \prod_{\substack{j=1 \\ j \neq i}}^l p_j(\tilde{x}_j) d\tilde{x}_j - \mathbb{E}[Y^2] \right) / \text{Var } Y
\end{aligned}$$

For the crucial part, it holds

$$\begin{aligned}
& \int_{\Omega_{\sim i}} \mathbb{E}^2[Y|x_j = \tilde{x}_j \text{ for } j = 1, \dots, l, j \neq i] \prod_{\substack{j=1 \\ j \neq i}}^l p_j(\tilde{x}_j) d\tilde{x}_j \\
&= \int_{\Omega_{\sim i}} \left( \int_{\Omega_i} f(\tilde{x}_i, \dots, x_i, \dots, \tilde{x}_l) p_i(x_i) \right)^2 \prod_{\substack{j=1 \\ j \neq i}}^l p_j(\tilde{x}_j) d\tilde{x}_j \\
&= \int_{\Omega_{\sim i}} \left( \int_{\Omega_i} f(\tilde{x}_i, \dots, x'_i, \dots, \tilde{x}_l) p_i(x'_i) \right) \cdot \left( \int_{\Omega_i} f(\tilde{x}_i, \dots, x_i, \dots, \tilde{x}_l) p_i(x_i) \right) \prod_{\substack{j=1 \\ j \neq i}}^l p_j(\tilde{x}_j) d\tilde{x}_j \\
&= \int_{\Omega_1} \dots \int_{\Omega_l} f(x_1, \dots, x'_i, \dots, x_l) \cdot f(x_i, \dots, x_i, \dots, x_l) p_i(x'_i) \prod_{j=1}^l p_j(x_j) dx'_i \prod_{j=1}^l p_j(x_j) dx_j
\end{aligned}$$

We can reformulate the integrand as a function depending on  $(l + 1)$  factors

$$F(x_1, \dots, x_l, x'_i) = f(x_1, \dots, x_{i-1}, x'_i, x_{i+1}, \dots, x_l) \cdot f(x_1, \dots, x_l)$$

which is estimated in the algorithm above by  $\frac{1}{M} \sum_{j=1}^M \tilde{y}_B^j \tilde{y}_{C_i}^j$ . □

**Algorithm 3.4.2** (Sobol' index estimation for functional-valued model output). *Consider a model of the form  $Y = G(y, X)$  (3.3) again. The Sobol' indices derived in definition 3.3.6*

$$S_A^{clos}(G) = \frac{\int_D \text{Var}[G_A(y, X_A)] dy}{\int_D \text{Var}[G(y, X)] dy}, \quad S_A^t(G) = 1 - \frac{\int_D \text{Var}[G_{A^c}(y, X_{A^c})] dy}{\int_D \text{Var}[G(y, X)] dy}$$

can be computed via quadrature. For instance, we show the estimation of the denominator of  $S_A^{clos}(G)$ ; for the other integrals, it follows similarly.

For the quadrature weights and nodes  $(w_i, y_i)_{i=1}^N$  of the domain  $D$  we derive

$$\int_D \text{Var}[G(y, X)] dy \approx \sum_{i=1}^N w_i \cdot \text{Var}[G(y_i, X)].$$

The point evaluations  $G(y_i, X)$  are single-valued. Now algorithm 3.4.1 can be used for each point. In most cases, the computationally expensive part is obtaining  $G(y, x)$  for a sample  $x$  and not evaluating the function at  $N$  points afterwards. This is why for each sample in the algorithm  $G(y, x)$  is evaluated at each point  $y_i \in D, i = 1, \dots, N$  and stored.

Unlike algorithm 3.4.1, for this case we consider  $f(X) = \begin{pmatrix} G(y_1, X) \\ \vdots \\ G(y_N, X) \end{pmatrix} \in \mathbb{R}^N$  and the resulting dimensions of

the auxiliary variables are now  $\tilde{y}_A, \tilde{y}_B, \tilde{y}_{C_i} \in \mathbb{R}^{M \times N}$ . Now the Sobol' indices can be calculated pointwise at  $y_i$  and assembled together by the quadrature formula.

This leads just like the algorithm for single-valued model outputs to  $M \cdot (l + 2)$  model calculations and an additional  $N$  function evaluations per model calculation.

**Algorithm 3.4.3** (Sobol' index estimation for multidimensional functional-valued model output). Consider a model  $Y = G(y, X)$  where  $G : D \times \Omega \rightarrow \mathbb{R}^2$  and assume 3.1.1.

The Sobol' indices defined in 3.3.7 are

$$S_A^{clos}(G) = \frac{\int_D \left( \sum_{j=1}^k \text{Var} G_A^{(j)}(y, X_A) \right) dy}{\int_D \left( \sum_{j=1}^k \text{Var} G^{(j)}(y, X) \right) dy}, \quad S_A^t(G) = 1 - \frac{\int_D \left( \sum_{j=1}^k \text{Var} G_{A^c}^{(j)}(y, X_{A^c}) \right) dy}{\int_D \left( \sum_{j=1}^k \text{Var} G^{(j)}(y, X) \right) dy}.$$

Just like in algorithm 3.4.2, for instance, we show the estimation of the denominator of  $S_A^{clos}(G)$ ; for the other integrals, it follows similarly.

For the quadrature weights and nodes  $(w_i, y_i)_{i=1}^N$  of the domain  $D$  we derive

$$\int_D \sum_{j=1}^k \text{Var} G^{(j)}(y, X) dy \approx \sum_{j=1}^k \sum_{i=1}^N w_i \text{Var} G^{(j)}(y_i, X)$$

which is single-valued again and can be calculated in the same manner as in algorithm 3.4.2 for each  $j = 1, \dots, k$ .

This results in  $k \cdot M \cdot (l + 2)$  model evaluations and an additional  $N$  function evaluations for each model output.

# 4 Domain Mapping Method for the Poisson Equation

## 4.1 Introduction to the Domain Mapping Method

The main source for this chapter is [HPS16]. As a note on the notation used, it should be mentioned that an attempt is made throughout to point out the difference between the domains  $D_{ref}$  and  $D(\omega)$  by using  $\hat{x} \in D_{ref}$  and  $x \in D(\omega)$  to avoid confusion.

The initial problem is the following: we want to solve a partial differential equation on a certain domain. This domain is not deterministic but parameterized stochastically. For each sample of the stochastic domain, the solution of the differential equation is, therefore, different and is defined on a different domain in each case. The Domain Mapping Method solves this problem by selecting a reference domain and introducing a random field defined as follows for each sample

$$V : \overline{D_{ref}} \times \Omega \rightarrow \mathbb{R}^d. \quad (4.1)$$

$V$  is called a mapping function and is invertible for all fixed  $\omega \in \Omega$ .

To show how this method is applied to a variational formulation of a partial differential equation, we take a look at the strong Poisson equation with  $u(\cdot, \omega) \in C^2(D(\omega), \mathbb{R}^2)$ .

$$\begin{aligned} -\Delta u(x, \omega) &= f(x) & | & x \in D(\omega) \\ u(x, \omega) &= 0 & | & x \in \partial D(\omega) \end{aligned}$$

We can reformulate the variational formulation of the Poisson equation as derived later in lemma 4.2.3:  
Find  $u(\cdot, \omega) \in H_0^1(D(\omega))$  s.t.

$$\int_{D(\omega)} \langle \nabla u(x, \omega), \nabla v(x, \omega) \rangle dx = \int_{D(\omega)} f(x) v(x, \omega) dx \quad \forall v \in H_0^1(D(\omega))$$

as:

Find  $\hat{u}(\cdot, \omega) \in H_0^1(D_{ref})$  s.t.

$$\begin{aligned} \hat{a}(\hat{u}, \hat{v}) &= \hat{l}(\hat{v}) \quad \forall \hat{v} \in H_0^1(D_{ref}) \\ \hat{a}(\hat{u}, \hat{v}) &:= \int_{D_{ref}} \left\langle \det(J(\hat{x}, \omega)) \cdot \left( J(\hat{x}, \omega)^T \cdot J(\hat{x}, \omega) \right)^{-1} \cdot \nabla \hat{u}(\hat{x}, \omega), \nabla \hat{v}(\hat{x}) \right\rangle d\hat{x} \\ \hat{l}(\hat{v}) &:= \int_{D_{ref}} \det(J(\hat{x}, \omega)) \cdot (f \circ V)(\hat{x}, \omega) \cdot \hat{v}(\hat{x}) d\hat{x} \end{aligned} \quad (4.2)$$

where  $J(\hat{x}, \omega)$  denotes the Jacobian of  $V(\hat{x}, \omega)$ . This formulation is a PDE with random coefficients on a deterministic reference domain. The two solutions are related via:

$$\hat{u}(\hat{x}, \omega) = u(V(\hat{x}, \omega), \omega)$$

Explicitly Example 7.2 in [HPS16] uses the unit disc as reference domain  $D_{ref} = \{x \in \mathbb{R}^2 | \|x\|_2 < 1\}$ . The right-hand-side is fixed as  $f \equiv 1$  and the following random field  $V(x, \omega)$  is considered:

$$\mathbb{E}[V](\hat{x}) = \mu(\hat{x}) = \hat{x} \quad (4.3)$$

$$\text{Cov}[V](\hat{x}, \hat{y}) = \frac{1}{100} \begin{pmatrix} 5 \cdot \exp(-4\|\hat{x} - \hat{y}\|_2^2) & \exp(-0.1\|2\hat{x} - \hat{y}\|_2^2) \\ \exp(-0.1\|\hat{x} - 2\hat{y}\|_2^2) & 5 \cdot \exp(-\|\hat{x} - \hat{y}\|_2^2) \end{pmatrix} \quad (4.4)$$

as shown in figure 4.1b for a discretized grid on the reference domain  $D_{ref}$ .

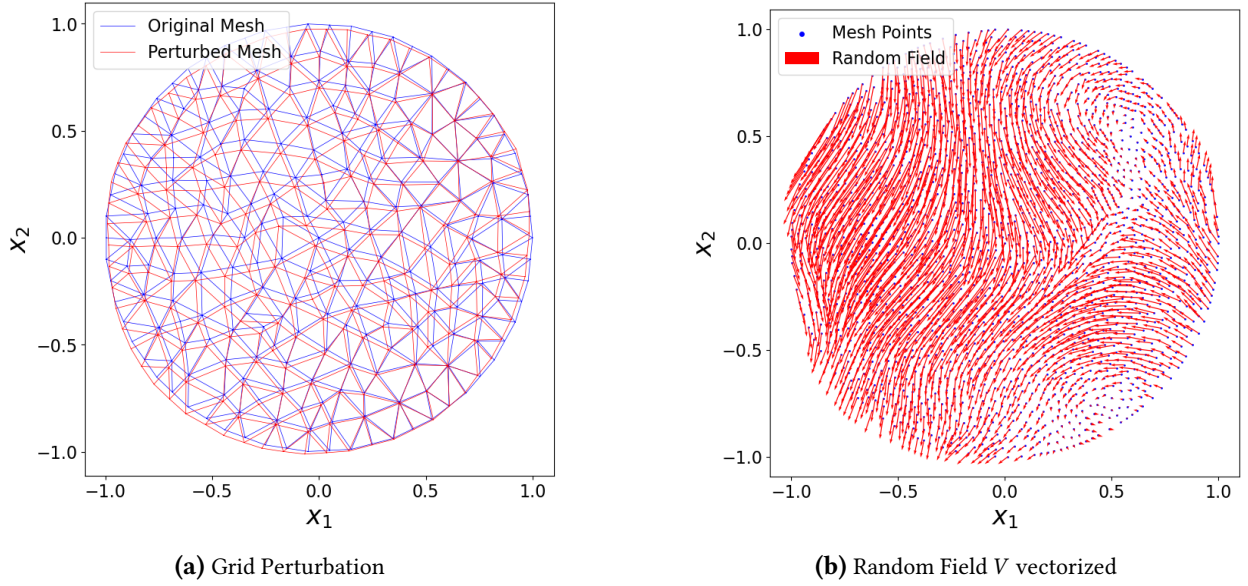


**Figure 4.1** Random Field  $V$

For the calculation of the random field, the following representation, called the truncated Karhunen-Loëve expansion, is used:

$$V(\hat{x}, \omega) = \mu(\hat{x}) + \sum_{m=1}^M \sqrt{\gamma_m} \cdot g_m(\hat{x}) \cdot \xi_m(\omega) \quad \text{with } \xi_m(\omega) \sim U(-\sqrt{3}, \sqrt{3})$$

where the sum converges in  $L^2$  as shown in theorem 2.2.21 and uniformly as shown in theorem 2.2.22. This representation consists of the eigenpairs  $(\gamma_m, g_m(\hat{x}))$  of the covariance kernel defined in 2.2.11 where  $g_m(\hat{x}) \in L^2(D_{ref}, \mathbb{R}^2)$ . To calculate the eigenfunctions, we use the Galerkin method for the resulting two-dimensional KL-eigenproblem described in subsection 4.3.1. Because of the domain-independence property (shown in lemma 2.2.23) of the KLE, we can calculate the eigenpairs on  $D_{ref}$  and apply the KLE for the perturbed domains  $D(\omega)$  as well.

The solutions  $u(x, \omega)$  and  $\hat{u}(\hat{x}, \omega)$  for a sample  $\omega$  look as follows

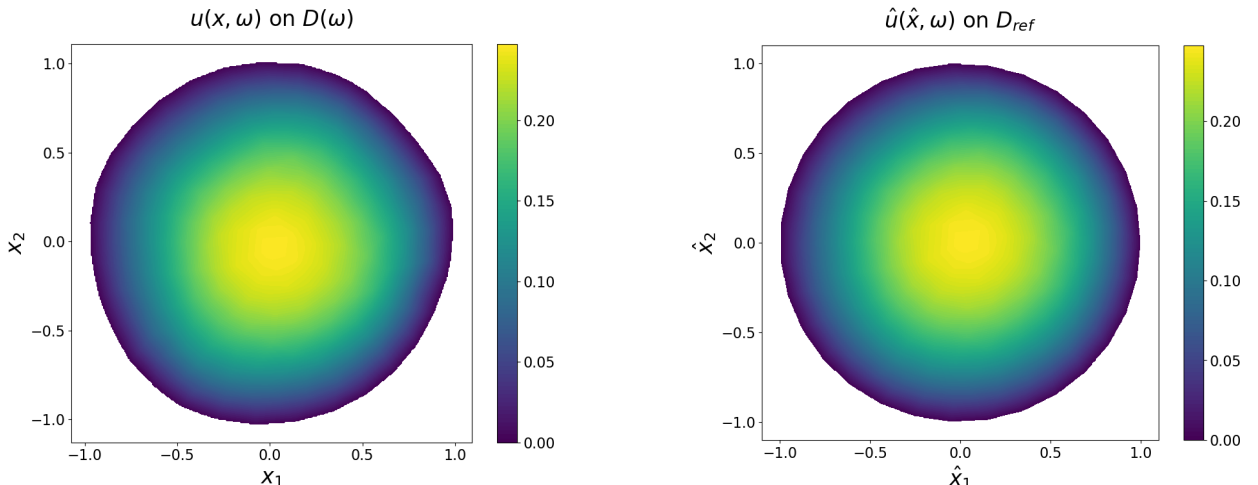


**Figure 4.2** Solution Sample of Poisson Equation

## 4.2 The Connection of the two Problems

**Assumption 4.2.1.** Let  $D_{ref} \subset \mathbb{R}^d$  for  $d \in \mathbb{N}$  denote a domain with Lipschitz continuous boundary  $\partial D_{ref}$  and let  $(\Omega, \mathcal{F}, \mathbb{P})$  be a complete probability space with  $\sigma$ -algebra  $\mathcal{F} \subset 2^\Omega$  and probability measure  $\mathbb{P}$ . Let  $\Omega$  be a separable set.

Let  $V : \overline{D_{ref}} \times \Omega \rightarrow \mathbb{R}^d$  be an invertible vector field of class  $C^2$ . We impose the following uniformity condition

$$\exists C \in \mathbb{R} : \|V(\omega)\|_{C^2(\overline{D_{ref}}; \mathbb{R}^d)} + \|V^{-1}(\omega)\|_{C^2(\overline{D(\omega)}; \mathbb{R}^d)} \leq C$$

for almost every  $\omega \in \Omega$ .

From this condition we infer for almost every  $\omega \in \Omega$  and every  $x \in D_{ref}$  that the singular-values of the vector field  $V$ 's Jacobian  $J(x, \omega)$  satisfy

$$0 < \sigma_{min} \leq \min\{\sigma(J(x, \omega))\} \leq \max\{\sigma(J(x, \omega))\} \leq \sigma_{max} < \infty \quad \text{for some } \sigma_{min}, \sigma_{max} \in \mathbb{R}$$

Since  $V$  is assumed to be a  $C^2$ -diffeomorphism, we have for almost every  $\omega \in \Omega$  that

$$V^{-1} \circ V = Id \Rightarrow J^{-1}J = I \Rightarrow \det(J^{-1})\det(J) = 1 \quad \forall \hat{x} \in D_{ref}.$$

Herein,  $I \in \mathbb{R}^{d \times d}$  denotes the identity matrix. Especially, we infer  $\det(J^{-1}), \det(J) \neq 0$ . The continuity of  $J, J^{-1}$  and of the determinant function imply now that either  $\det(J^{-1}), \det(J) > 0$  or  $\det(J^{-1}), \det(J) < 0 \quad \forall \hat{x} \in D_{ref}$ . Therefore, without loss of generality, we will assume the positiveness of the determinants.

**Lemma 4.2.2.** Under assumption 4.2.1, we have the following result. The spaces  $H_0^1(D_{ref})$  and  $H_0^1(D(\omega))$  are isomorphic by the isomorphism

$$\mathcal{E} : H_0^1(D_{ref}) \rightarrow H_0^1(D(\omega)), \quad v \mapsto v \circ V(\omega)^{-1}$$

The inverse mapping is given by

$$\mathcal{E}^{-1} : H_0^1(D(\omega)) \rightarrow H_0^1(D_{ref}), \quad v \mapsto v \circ V(\omega)$$

It should also be mentioned at this point that the dependency of  $\hat{v}(\hat{x}) = v(V(\hat{x}, \omega), \omega)$  on the sample  $\omega$  is deliberately omitted, as the entire set of test functions is always considered. The isomorphism leads to a redundancy of the dependency, since in the variational formulation all test functions  $\hat{v} \in H_0^1(D_{ref})$  are considered. This should be clarified by omitting the dependency.

*Proof.* The mapping  $\mathcal{E}$  is well-defined because of the following chain rule property

$$\nabla \mathcal{E}(v) = (\nabla v) \circ V(\omega)^{-1} \cdot \nabla (V(\omega)^{-1})$$

leading to:

$$\begin{aligned} \|\mathcal{E}(v)\|_{H_0^1(D(\omega))} &= \|v(V(\omega)^{-1})\|_{H_0^1(D(\omega))} \\ &= \|\nabla(v(V(\omega)^{-1}))\|_{L^2(D(\omega))} \\ &= \|(\nabla v) \circ V(\omega)^{-1} \cdot \nabla(V(\omega)^{-1})\|_{L^2(D(\omega))} \\ &\leq C \cdot \|v\|_{H_0^1(D_{ref})} \cdot \|V(\omega)^{-1}\|_{C^2(D(\omega); \mathbb{R}^d)} < \infty \end{aligned}$$

The bijectivity follows from the assumption that  $V(\omega)$  is bijective. The linearity follows immediately from the definition of  $\mathcal{E}$ .  $\square$

**Lemma 4.2.3.** Let's assume 4.2.1 for the random field  $V$ . For a fixed  $\omega \in \Omega$  the two variational problems:  
Find  $u(\cdot, \omega) \in H_0^1(D(\omega))$  s.t.

$$\begin{aligned} a(u, v) &= l(v) \quad \forall v \in H_0^1(D(\omega)) \\ a(u, v) &:= \int_{D(\omega)} \langle \nabla u(x, \omega), \nabla v(x, \omega) \rangle dx \\ l(v) &:= \int_{D(\omega)} f(x) v(x, \omega) dx \end{aligned} \tag{4.5}$$

and:

Find  $\hat{u}(\cdot, \omega) \in H_0^1(D_{ref})$  s.t.

$$\begin{aligned} \hat{a}(\hat{u}, \hat{v}) &= \hat{l}(\hat{v}) \quad \forall \hat{v} \in H_0^1(D_{ref}) \\ \hat{a}(\hat{u}, \hat{v}) &:= \int_{D_{ref}} \left\langle \det(J(\hat{x}, \omega)) \cdot \left( J(\hat{x}, \omega)^T \cdot J(\hat{x}, \omega) \right)^{-1} \cdot \nabla \hat{u}(\hat{x}, \omega), \nabla \hat{v}(\hat{x}) \right\rangle d\hat{x} \\ \hat{l}(\hat{v}) &:= \int_{D_{ref}} \det(J(\hat{x}, \omega)) \cdot (f \circ V)(\hat{x}, \omega) \cdot \hat{v}(\hat{x}) d\hat{x} \end{aligned} \tag{4.6}$$

are connected via

$$\hat{u}(\hat{x}, \omega) = u(V(\hat{x}, \omega), \omega).$$

*Proof.*

$$\begin{aligned} &\int_{D_{ref}} \det(J(\hat{x}, \omega)) \cdot (f \circ V)(\hat{x}, \omega) \cdot (v \circ V)(\hat{x}, \omega) d\hat{x} \\ &= \int_{D(\omega)} f(x) \cdot v(x, \omega) dx \\ &= \int_{D(\omega)} \langle \nabla_x u(x, \omega), \nabla_x v(x, \omega) \rangle dx \\ &= \int_{D_{ref}} \langle J^{-T}(\hat{x}, \omega) \cdot \nabla_{\hat{x}} \hat{u}(\hat{x}, \omega), J^{-T}(\hat{x}, \omega) \cdot \nabla_{\hat{x}} \hat{v}(\hat{x}) \rangle \cdot \det(J(\hat{x}, \omega)) d\hat{x} \\ &= \int_{D_{ref}} \left( J^{-T}(\hat{x}, \omega) \cdot \nabla \hat{u}(\hat{x}, \omega) \right)^T J^{-T}(\hat{x}, \omega) \cdot \nabla \hat{v}(\hat{x}) \cdot \det(J(\hat{x}, \omega)) d\hat{x} \\ &= \int_{D_{ref}} \left( \left( J^{-1}(\hat{x}, \omega) \cdot J^{-T}(\hat{x}, \omega) \right)^T \cdot \nabla \hat{u}(\hat{x}, \omega) \right)^T \cdot \nabla \hat{v}(\hat{x}) \cdot \det(J(\hat{x}, \omega)) d\hat{x} \\ &= \int_{D_{ref}} \langle J^{-1}(\hat{x}, \omega) \cdot J^{-T}(\hat{x}, \omega) \cdot \nabla \hat{u}(\hat{x}, \omega), \nabla \hat{v}(\hat{x}) \rangle \cdot \det(J(\hat{x}, \omega)) d\hat{x} \\ &= \int_{D_{ref}} \langle \det(J(\hat{x}, \omega)) \cdot J^{-1}(\hat{x}, \omega) \cdot J^{-T}(\hat{x}, \omega) \cdot \nabla \hat{u}(\hat{x}, \omega), \nabla \hat{v}(\hat{x}) \rangle d\hat{x} \end{aligned}$$

Where the connections  $\hat{u}(\hat{x}, \omega) = u \circ V(\hat{x}, \omega)$  and  $\hat{v}(\hat{x}) = v \circ V(\hat{x}, \omega)$  follow from lemma 4.2.2 as we have  $H_0^1(D(\omega)) = \{\mathcal{E}(v) : v \in H_0^1(D_{ref})\}$  and for an arbitrary function  $\mathcal{E}(v) \in H_0^1(D(\omega))$  it holds  $\hat{\mathcal{E}}(v) = \mathcal{E}(v) \circ V = v \circ V^{-1} \circ V = v \in H_0^1(D_{ref})$  which is independent of  $\omega \in \Omega$ .

□

**Lemma 4.2.4.** Under assumption 4.2.1 and the choice  $f \equiv 1$ ,  $D_{ref} = \{x \in \mathbb{R}^2 | \|x\|_2 < 1\}$  for the variational problem in lemma 4.2.3, there exists a unique solution  $\hat{u} \in H_0^1(D_{ref})$ .

*Proof.* The proof uses the Lax-Milgram lemma 2.3.5. To apply the lemma for the Hilbert-space  $H_0^1(D_{ref})$ , we have to verify the three conditions

## 4 Domain Mapping Method for the Poisson Equation

(I)  $\hat{l}$  is bounded

(II)  $\hat{a}$  is bounded

(III)  $\hat{a}$  is coercive

Throughout the proof, the dependence of  $J$ ,  $\hat{u}$ , and  $\hat{v}$  on  $\hat{x}$  and  $\omega$  is not mentioned explicitly.

First, some auxiliary statements are shown.

Use the singular value decomposition  $J = U \cdot \Sigma \cdot V^T$  for the orthogonal matrices  $U, V$  and the diagonal matrix  $\Sigma = \begin{pmatrix} \sigma_1 & 0 \\ 0 & \sigma_2 \end{pmatrix} \in \mathbb{R}^{2 \times 2}$ .

$$(J^T \cdot J)^{-1} = (V \cdot \Sigma^T \cdot U^T \cdot U \cdot \Sigma \cdot V^T)^{-1} = (V \cdot \Sigma^2 \cdot V^T)^{-1} = V \cdot \Sigma^{-2} \cdot V^T \quad (4.7)$$

Let  $w = V^T \cdot \nabla \hat{u}$ , then

$$\begin{aligned} \nabla \hat{u}^T \cdot V \cdot \Sigma^{-k} \cdot V^T \cdot \nabla \hat{u} &= w^T \cdot \Sigma^{-k} \cdot w = \frac{w_1^2}{\sigma_1^k} + \frac{w_2^2}{\sigma_2^k} \\ &\leq \left( \frac{1}{\sigma_{min}} \right)^k \cdot w^T \cdot w = \left( \frac{1}{\sigma_{min}} \right)^k \cdot (V^T \nabla \hat{u})^T (V^T \nabla \hat{u}) = \left( \frac{1}{\sigma_{min}} \right)^k \cdot \|\nabla \hat{u}\|_2^2 \end{aligned} \quad (4.8)$$

and for the other direction, it follows equally.

$$\left( \frac{1}{\sigma_{max}} \right)^k \cdot \|\nabla \hat{u}\|_2^2 \leq \nabla \hat{u}^T \cdot V \cdot \Sigma^{-k} \cdot V^T \cdot \nabla \hat{u} \quad (4.9)$$

For  $\det(J)$  it holds

$$\sigma_{min}^2 \leq |\det(J)| = |\det(U) \det(\Sigma) \det(V^T)| = |\det(\Sigma)| \leq \sigma_{max}^2 \quad (4.10)$$

where we used that  $|\det(U)| = |\det(V^T)| = 1$  which follows from orthogonality because

$$1 = \det(I) = \det(U^T \cdot U) = \det(U^T) \cdot \det(U) = \det(U)^2 \Rightarrow |\det(U)| = 1.$$

Now we are ready to show the conditions.

(I)

$$\begin{aligned} |\hat{l}(\hat{v})| &= \left| \int_{D_{ref}} \det(J) \cdot \hat{v} \, d\hat{x} \right| \stackrel{(4.10)}{\leq} \sigma_{max}^2 \cdot \int_{D_{ref}} |\hat{v}| \, d\hat{x} \leq C_1 \cdot \sigma_{max}^2 \cdot \|\hat{v}\|_{L^2(D_{ref})} \\ &\stackrel{2.3.6}{\leq} C_2 \cdot \sigma_{max}^2 \cdot \|\hat{v}\|_{H_0^1(D_{ref})} \end{aligned}$$

(II)

$$\begin{aligned}
|\hat{a}(\hat{u}, \hat{v})| &= \left| \int_{D_{ref}} \det(J) \left\langle \left( J^T \cdot J \right)^{-1} \cdot \nabla \hat{u}, \nabla \hat{v} \right\rangle d\hat{x} \right| \\
&\stackrel{(4.10)}{\leq} \sigma_{max}^2 \int_{D_{ref}} \left| \left( \left( J^T \cdot J \right)^{-1} \cdot \nabla \hat{u} \right)^T \cdot \nabla \hat{v} \right| d\hat{x} \\
&\stackrel{(4.7)}{=} \sigma_{max}^2 \int_{D_{ref}} |\nabla \hat{u}^T \cdot V \cdot \Sigma^{-2} \cdot V^T \cdot \nabla \hat{v}| d\hat{x} \\
&\leq \sigma_{max}^2 \cdot \left( \int_{D_{ref}} \|\nabla \hat{u}^T \cdot V \cdot \Sigma^{-2} \cdot V^T\|_2^2 d\hat{x} \right)^{1/2} \cdot \left( \int_{D_{ref}} \|\nabla \hat{v}\|_2^2 d\hat{x} \right)^{1/2} \\
&\leq C \cdot \sigma_{max}^2 \cdot \left( \int_{D_{ref}} \nabla \hat{u}^T \cdot V \cdot \Sigma^{-2} \cdot V^T \cdot V \cdot \Sigma^{-2} \cdot V^T \cdot \nabla \hat{u} d\hat{x} \right)^{1/2} \cdot \|\hat{v}\|_{H_0^1(D_{ref})} \\
&= C \cdot \sigma_{max}^2 \cdot \left( \int_{D_{ref}} \nabla \hat{u}^T \cdot V \cdot \Sigma^{-4} \cdot V^T \cdot \nabla \hat{u} d\hat{x} \right)^{1/2} \cdot \|\hat{v}\|_{H_0^1(D_{ref})} \\
&\stackrel{(4.8)}{\leq} C \cdot \frac{\sigma_{max}^2}{\sigma_{min}^4} \cdot \|\hat{u}\|_{H_0^1(D_{ref})} \cdot \|\hat{v}\|_{H_0^1(D_{ref})}
\end{aligned}$$

(III)

$$\begin{aligned}
\hat{a}(\hat{u}, \hat{u}) &= \int_{D_{ref}} \det(J) \left\langle \left( J^T \cdot J \right)^{-1} \cdot \nabla \hat{u}, \nabla \hat{u} \right\rangle d\hat{x} \stackrel{(4.10)}{\geq} \sigma_{min}^2 \cdot \int_{D_{ref}} \nabla \hat{u}^T \cdot \left( J^T \cdot J \right)^{-1} \cdot \nabla \hat{u} d\hat{x} \\
&\stackrel{(4.7)}{=} \sigma_{min}^2 \cdot \int_{D_{ref}} \nabla \hat{u}^T \cdot V \cdot \Sigma^{-2} \cdot V^T \cdot \nabla \hat{u} d\hat{x} \stackrel{(4.9)}{\geq} \left( \frac{\sigma_{min}}{\sigma_{max}} \right)^2 \cdot \|\hat{u}\|_{H_0^1(D_{ref})}^2
\end{aligned}$$

□

## 4.3 Implementation and Numerical Results

The Domain Mapping Method leads to the need for differentiable eigenfunctions, which presuppose differentiable basis functions in the Galerkin representation. Sadly, there is no implementation of differentiable basis functions in two dimensions in the Python package FEniCS [Bar+23], which is used for the numerical experiments. This is the main reason for taking constant basis functions because, as long as we cannot obtain differentiability, this choice leads to minimal computational effort.

### 4.3.1 Two-dimensional Karhunen-Loève Expansion

This chapter is based on the source [BEU11]. To use the Galerkin method for approximating the eigenfunctions, the set of piecewise constant basis functions  $\{\phi_1, \dots, \phi_N\}$  on a discretized grid of  $D_{ref}$  is used. We define  $d = 2$ ,  $N = \dim(Z_h)$ ,  $Z_h = \text{span}\{\phi_1(\hat{x}), \dots, \phi_N(\hat{x})\}$  where  $\phi_j : D_{ref} \rightarrow \mathbb{R}$  and reformulate the resulting truncated vector KL-eigenproblem with  $\hat{x}, \hat{y} \in D_{ref} \subset \mathbb{R}^2$  and truncation level  $M$ .

Let  $(\gamma_m, g_m(\hat{x}))$  denote the eigenpairs with  $g_m(\hat{x}) = \begin{pmatrix} g_m^{(1)}(\hat{x}) \\ g_m^{(2)}(\hat{x}) \end{pmatrix} = \begin{pmatrix} \sum_{j=1}^N a_{j,m}^{(1)} \cdot \phi_j(\hat{x}) \\ \sum_{j=1}^N a_{j,m}^{(2)} \cdot \phi_j(\hat{x}) \end{pmatrix}$

and  $\text{Cov}(\hat{x}, \hat{y}) = c(\hat{x}, \hat{y}) = \begin{pmatrix} c_{1,1}(\hat{x}, \hat{y}) & c_{1,2}(\hat{x}, \hat{y}) \\ c_{2,1}(\hat{x}, \hat{y}) & c_{2,2}(\hat{x}, \hat{y}) \end{pmatrix}$  the covariance function of the random field  $V(\hat{x}, \omega)$ .

For  $m = 1, \dots, M$  we derive the following:

$$\begin{aligned}
& \int_{D_{ref}} \underbrace{c(\hat{x}, \hat{y})}_{2x2} \cdot \underbrace{g_m(\hat{y})}_{2x1} d\hat{y} = \underbrace{\gamma_m}_{1x1} \cdot \underbrace{g_m(\hat{x})}_{2x1} \\
\Leftrightarrow & \left( \int_{D_{ref}} \left( c_{1,1}(\hat{x}, \hat{y}) \cdot \sum_{j=1}^N a_{j,m}^{(1)} \cdot \phi_j(\hat{y}) + c_{1,2}(\hat{x}, \hat{y}) \cdot \sum_{j=1}^N a_{j,m}^{(2)} \cdot \phi_j(\hat{y}) \right) d\hat{y} \right) = \left( \gamma_m \cdot \sum_{j=1}^N a_{j,m}^{(1)} \cdot \phi_j(\hat{x}) \right) \\
\Leftrightarrow & \left( \int_{D_{ref}} \left( c_{2,1}(\hat{x}, \hat{y}) \cdot \sum_{j=1}^N a_{j,m}^{(1)} \cdot \phi_j(\hat{y}) + c_{2,2}(\hat{x}, \hat{y}) \cdot \sum_{j=1}^N a_{j,m}^{(2)} \cdot \phi_j(\hat{y}) \right) d\hat{y} \right) = \left( \gamma_m \cdot \sum_{j=1}^N a_{j,m}^{(2)} \cdot \phi_j(\hat{x}) \right) \\
\Leftrightarrow & \left( \sum_{j=1}^N a_{j,m}^{(1)} \cdot \int_{D_{ref} \times D_{ref}} c_{1,1}(\hat{x}, \hat{y}) \phi_j(\hat{y}) \phi_i(\hat{x}) d\hat{y} d\hat{x} + \sum_{j=1}^N a_{j,m}^{(2)} \cdot \int_{D_{ref} \times D_{ref}} c_{1,2}(\hat{x}, \hat{y}) \phi_j(\hat{y}) \phi_i(\hat{x}) d\hat{y} d\hat{x} \right. \\
& \left. + \sum_{j=1}^N a_{j,m}^{(1)} \cdot \int_{D_{ref} \times D_{ref}} c_{2,1}(\hat{x}, \hat{y}) \phi_j(\hat{y}) \phi_i(\hat{x}) d\hat{y} d\hat{x} + \sum_{j=1}^N a_{j,m}^{(2)} \cdot \int_{D_{ref} \times D_{ref}} c_{2,2}(\hat{x}, \hat{y}) \phi_j(\hat{y}) \phi_i(\hat{x}) d\hat{y} d\hat{x} \right) \\
= & \begin{pmatrix} \gamma_m \sum_{j=1}^N a_{j,m}^{(1)} \cdot \int_{D_{ref}} \phi_j(\hat{x}) \phi_i(\hat{x}) d\hat{x} \\ \gamma_m \sum_{j=1}^N a_{j,m}^{(2)} \cdot \int_{D_{ref}} \phi_j(\hat{x}) \phi_i(\hat{x}) d\hat{x} \end{pmatrix} \quad \forall \phi_i(\hat{x}) \in \{\phi_1(\hat{x}), \dots, \phi_N(\hat{x})\} \\
\Leftrightarrow & C \cdot \hat{a}^{(m)} = \gamma_m \cdot M \cdot \hat{a}^{(m)}
\end{aligned}$$

with the following definitions:

$$\begin{aligned}
\hat{a}^{(m)} &:= \begin{pmatrix} a_m^{(1)} \\ a_m^{(2)} \end{pmatrix} \in \mathbb{R}^{2N} \\
C &:= \begin{pmatrix} \hat{C}_{1,1} & \hat{C}_{1,2} \\ \hat{C}_{2,1} & \hat{C}_{2,2} \end{pmatrix} \in \mathbb{R}^{2N \times 2N} \\
\hat{C}_{i,j} &:= \begin{pmatrix} \int_{D_{ref}} \int_{D_{ref}} c_{i,j}(\hat{x}, \hat{y}) \cdot \phi_1(\hat{y}) \cdot \phi_1(\hat{x}) d\hat{y} d\hat{x} & \dots & \int_{D_{ref}} \int_{D_{ref}} c_{i,j}(\hat{x}, \hat{y}) \cdot \phi_n(\hat{y}) \cdot \phi_1(\hat{x}) d\hat{y} d\hat{x} \\ \vdots & \ddots & \vdots \\ \int_{D_{ref}} \int_{D_{ref}} c_{i,j}(\hat{x}, \hat{y}) \cdot \phi_1(\hat{y}) \cdot \phi_n(\hat{x}) d\hat{y} d\hat{x} & \dots & \int_{D_{ref}} \int_{D_{ref}} c_{i,j}(\hat{x}, \hat{y}) \cdot \phi_n(\hat{y}) \cdot \phi_n(\hat{x}) d\hat{y} d\hat{x} \end{pmatrix} \in \mathbb{R}^{N \times N} \\
M &:= \begin{pmatrix} \hat{M} & 0 \\ 0 & \hat{M} \end{pmatrix} \in \mathbb{R}^{2N \times 2N} \\
\hat{M} &:= \begin{pmatrix} \int_{D_{ref}} \phi_1(\hat{x}) \cdot \phi_1(\hat{x}) d\hat{x} & \dots & \int_{D_{ref}} \phi_n(\hat{x}) \cdot \phi_1(\hat{x}) d\hat{x} \\ \vdots & \ddots & \vdots \\ \int_{D_{ref}} \phi_1(\hat{x}) \cdot \phi_n(\hat{x}) d\hat{x} & \dots & \int_{D_{ref}} \phi_n(\hat{x}) \cdot \phi_n(\hat{x}) d\hat{x} \end{pmatrix} \in \mathbb{R}^{N \times N}
\end{aligned}$$

which is a generalized matrix eigenvalue problem.

The resulting representation of the random field looks as follows

$$\begin{aligned}
V(\hat{x}, \omega) &= \mu(\hat{x}) + \sum_{m=1}^M \sqrt{\gamma_m} \cdot g_m(\hat{x}) \cdot \xi_m(\omega) \\
&= \mu(\hat{x}) + \sum_{m=1}^M \sqrt{\gamma_m} \cdot \left( \frac{\sum_{j=1}^N a_{j,m}^{(1)} \cdot \phi_j(\hat{x})}{\sum_{j=1}^N a_{j,m}^{(2)} \cdot \phi_j(\hat{x})} \right) \cdot \xi_m(\omega) \quad \text{with } \xi_m(\omega) \sim U(-\sqrt{3}, \sqrt{3}).
\end{aligned}$$

Figures 4.3 and 4.4 show the eigenvalues and the first four eigenfunctions for the FEniCS mesh resolution 8 leading to  $h = 1/12$ ,  $N = 258$ .

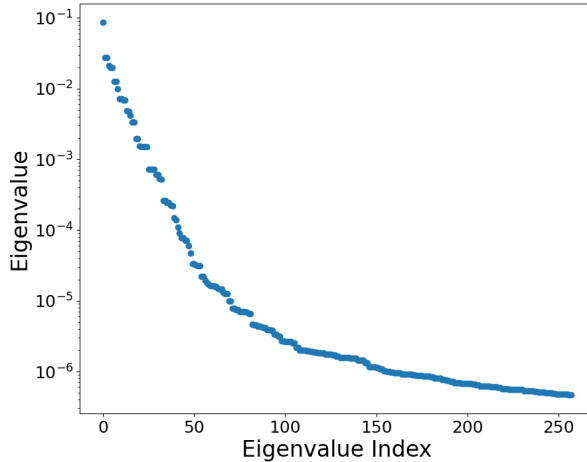


**Figure 4.3** First  $N$  Eigenvalues  $\gamma_m$  of KLE of the Random Field  $V$

Random Variable of KLE of $V$	Eigenvalue $\gamma_m$
$\xi_1$	0.087
$\xi_2$	0.02741
$\xi_3$	0.02739
$\xi_4$	0.021

**Table 4.1** Eigenvalues of KLE of the Random Field  $V$

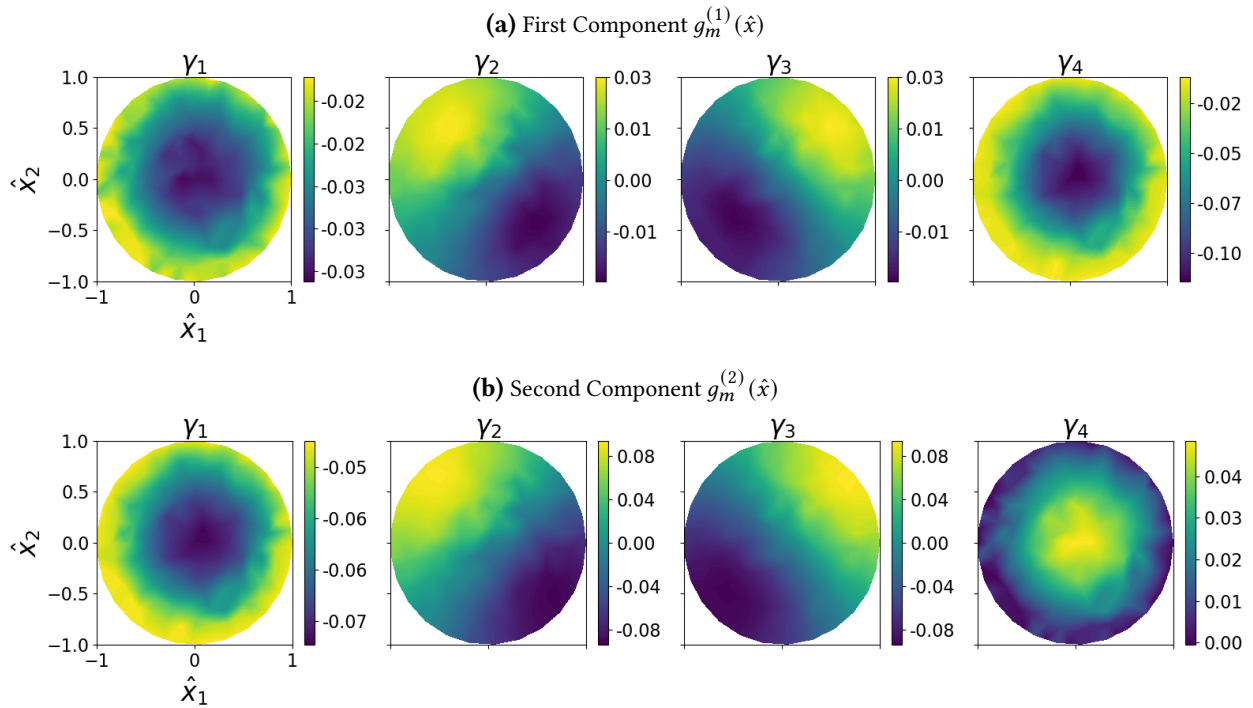


**Figure 4.4** First four Eigenfunctions  $g_m(\hat{x})$  of KLE of the Random Field  $V$

### 4.3.2 Jacobian of the truncated Karhunen-Loève Expansion

As in the implementation, non-differentiable basis functions are used, but the Jacobian of the random field  $V$  is needed; we need to approximate it. To solve this problem, we use the ansatz from chapter 2 of [BEU11] for the truncated KLE.

$$J(\hat{x}, \omega) = \frac{\partial V(\hat{x}, \omega)}{\partial \hat{x}} = \frac{\partial \mu(\hat{x})}{\partial \hat{x}} + \sum_{m=1}^M \sqrt{\gamma_m} \cdot \frac{\partial g_m(\hat{x})}{\partial \hat{x}} \cdot \xi_m(\omega)$$

#### 4 Domain Mapping Method for the Poisson Equation

We use the eigen-property for approximating  $\partial_{\hat{x}} g_m(\hat{x})$ , with  $g_m(\hat{x}) = \begin{pmatrix} \sum_{j=1}^N a_{j,m}^{(1)} \cdot \phi_j(\hat{x}) \\ \sum_{j=1}^N a_{j,m}^{(2)} \cdot \phi_j(\hat{x}) \end{pmatrix}$ .

$$\begin{aligned} \int_{D_{ref}} c(\hat{x}, \hat{y}) \cdot g_m(\hat{y}) d\hat{y} &= \gamma_m \cdot g_m(\hat{x}) \\ \int_{D_{ref}} \frac{\partial c(\hat{x}, \hat{y})}{\partial \hat{x}_i} \cdot g_m(\hat{y}) d\hat{y} &= \gamma_m \cdot \frac{\partial g_m(\hat{x})}{\partial \hat{x}_i} \end{aligned}$$

$$\begin{aligned} \frac{\partial g_m(\hat{x})}{\partial \hat{x}_i} &= \gamma_m^{-1} \cdot \int_{D_{ref}} \frac{\partial c(\hat{x}, \hat{y})}{\partial \hat{x}_i} \cdot g_m(\hat{y}) d\hat{y} \\ &= \gamma_m^{-1} \left( \sum_{j=1}^N a_{j,m}^{(1)} \int_{D_{ref}} \frac{\partial c_{1,1}(\hat{x}, \hat{y})}{\partial \hat{x}_i} \cdot \phi_j(\hat{y}) d\hat{y} + \sum_{j=1}^N a_{j,m}^{(2)} \int_{D_{ref}} \frac{\partial c_{1,2}(\hat{x}, \hat{y})}{\partial \hat{x}_i} \cdot \phi_j(\hat{y}) d\hat{y} \right) \\ &\quad \left( \sum_{j=1}^N a_{j,m}^{(1)} \int_{D_{ref}} \frac{\partial c_{2,1}(\hat{x}, \hat{y})}{\partial \hat{x}_i} \cdot \phi_j(\hat{y}) d\hat{y} + \sum_{j=1}^N a_{j,m}^{(2)} \int_{D_{ref}} \frac{\partial c_{2,2}(\hat{x}, \hat{y})}{\partial \hat{x}_i} \cdot \phi_j(\hat{y}) d\hat{y} \right) \end{aligned}$$

with  $\frac{\partial g_m(\hat{x})}{\partial \hat{x}} = \left( \frac{\partial g_m(\hat{x})}{\partial \hat{x}_1}, \frac{\partial g_m(\hat{x})}{\partial \hat{x}_2} \right)$ .

To reduce computational costs in the evaluation in  $\hat{x}$ , we use the following approximation of the derivatives:

$$\frac{\partial c_{r,s}(\hat{x}, \hat{y})}{\partial \hat{x}_t} = \sum_{k,l=1}^N c_{l,k}^{(r,s,t)} \cdot \phi_l(\hat{x}) \cdot \phi_k(\hat{y})$$

where  $c_{l,k}^{(r,s,t)} := \int_{D_{ref} \times D_{ref}} \frac{\partial c_{r,s}(\hat{x}, \hat{y})}{\partial x_t} \cdot \phi_l(\hat{x}) \cdot \phi_k(\hat{y}) d\hat{x} d\hat{y} \cdot (\text{area}(D_l) \cdot \text{area}(D_k))^{-1}$  and  $r, s, t \in \{1, 2\}$  which can be calculated via quadrature as described in A.1.1. This is the  $L^2$ -projection with the Galerkin-orthogonality condition 2.1.3, which is simplified using the orthogonality of the piecewise constant basis functions.

The simplification is shown in the upper left entry of the Jacobian (for the other entries, it follows similarly):

$$\begin{aligned} J_{1,1}(\hat{x}, \omega) - \frac{\partial \mu_1(\hat{x})}{\partial \hat{x}_1} &= \sum_{m=1}^M (\gamma_m)^{-\frac{1}{2}} \cdot \xi_m(\omega) \cdot \left( \sum_{j=1}^N a_{j,m}^{(1)} \cdot \int_{D_{ref}} \frac{\partial c_{1,1}(\hat{x}, \hat{y})}{\partial \hat{x}_1} \cdot \phi_j(\hat{y}) d\hat{y} + \sum_{j=1}^N a_{j,m}^{(2)} \cdot \int_{D_{ref}} \frac{\partial c_{1,2}(\hat{x}, \hat{y})}{\partial \hat{x}_1} \cdot \phi_j(\hat{y}) d\hat{y} \right) \\ &\stackrel{\text{approx.}}{=} \sum_{m=1}^M (\gamma_m)^{-\frac{1}{2}} \cdot \xi_m(\omega) \\ &\cdot \left( \sum_{j=1}^N a_{j,m}^{(1)} \cdot \int_{D_{ref}} \left( \sum_{k,l=1}^N c_{l,k}^{(1,1,1)} \cdot \phi_k(\hat{x}) \cdot \phi_l(\hat{y}) \cdot \phi_j(y) \right) d\hat{y} + \sum_{j=1}^N a_{j,m}^{(2)} \cdot \int_{D_{ref}} \left( \sum_{k,l=1}^N c_{l,k}^{(1,2,1)} \cdot \phi_k(\hat{x}) \cdot \phi_l(\hat{y}) \cdot \phi_j(y) \right) d\hat{y} \right) \\ &\stackrel{(*)}{=} \sum_{m=1}^M (\gamma_m)^{-\frac{1}{2}} \cdot \xi_m(\omega) \cdot \left( \sum_{j=1}^N a_{j,m}^{(1)} \cdot \text{area}(D_j) \cdot c_{j,\hat{k}}^{(1,1,1)} + \sum_{j=1}^N a_{j,m}^{(2)} \cdot \text{area}(D_j) \cdot c_{j,\hat{k}}^{(1,2,1)} \right) \\ &= \sum_{m=1}^M (\gamma_m)^{-\frac{1}{2}} \cdot \xi_m(\omega) \cdot \begin{pmatrix} a_m^{(1)} \\ a_m^{(2)} \end{pmatrix}^T \cdot \begin{pmatrix} c_{\hat{k}}^{(1,1,1)} \\ c_{\hat{k}}^{(1,2,1)} \end{pmatrix} \\ &= \bar{a}^T \cdot \begin{pmatrix} c_{\hat{k}}^{(1,1,1)} \\ c_{\hat{k}}^{(1,2,1)} \end{pmatrix} \quad \text{where} \quad \bar{a} = \sum_{m=1}^M (\gamma_m)^{-\frac{1}{2}} \cdot \xi_m(\omega) \cdot \begin{pmatrix} a_m^{(1)} \\ a_m^{(2)} \end{pmatrix} \in \mathbb{R}^{2N} \end{aligned}$$

(\*) for a fixed  $\hat{x}$  only one  $\phi_k(\hat{x})$  is supported, let  $\hat{k}$  denote this index; let  $D_j$  be the supported triangle of  $\phi_j(\hat{y})$ .

Applying this approximation for each entry results in the following representation:

$$J(\hat{x}, \omega) = \frac{\partial \mu(\hat{x})}{\partial \hat{x}} + \begin{pmatrix} \bar{a} & 0 \\ 0 & \bar{a} \end{pmatrix}^T \cdot \begin{pmatrix} c_{\hat{k}}^{(1,1,1)} & c_{\hat{k}}^{(1,1,2)} \\ c_{\hat{k}}^{(1,2,1)} & c_{\hat{k}}^{(1,2,2)} \\ c_{\hat{k}}^{(2,1,1)} & c_{\hat{k}}^{(2,1,2)} \\ c_{\hat{k}}^{(2,2,1)} & c_{\hat{k}}^{(2,2,2)} \end{pmatrix}$$

where 0 is the  $2N$ -dimensional 0-vector.

The computation reduces to finding the supported basis function index  $\hat{k}$  for the given  $x$ , which gives  $O(N)$  function evaluations. The rest can be precomputed, which saves a lot of computation power in solving the PDE numerically.

### 4.3.3 Numerical Results

The code for the numerical evaluations was written in Python and can be viewed at <https://github.com/EliasReutelsterz/Masterthesis>. The numerical solution of the differential equations was carried out using the package FEniCS [Bar+23].

During the implementation, attention was paid to calculating the samples as efficiently as possible.

For example, the KLE of the random field, as shown in subsection 4.3.1, is only calculated once before an arbitrary number of samples of  $\xi_m$  are taken. The rank of the truncated KLE is limited by the number of eigenvalues calculated in the Galerkin discretization. Since only  $2N$  of these eigenvalues are calculated, it has to hold  $M \leq 2N$ . Additionally, the Jacobian is calculated and approximated as described in subsection 4.3.2.

All of the following numerical experiments used  $M = N$ . A distinction must be made between two different mesh resolutions. The mesh resolution KLE describes the FEniCS mesh resolution used for the KLE mesh. The mesh resolution FEM describes the FEniCS mesh resolution, which was used for the function space in the numerical calculation of the differential equation solution. When talking about these mesh resolutions, the number  $M = N$  of the KLE truncation level is passed for information and the approximate cell size  $h$ , whereby it is specified relative to the domain size, i.e. in two-dimensional space as if the domain had a height and width of 1. The following Monte Carlo estimation of the mean and variance of the solution works with 20000 samples with mesh resolution KLE 14 ( $h = 1/24$ ,  $M = 769$ ); mesh resolution FEM 10 ( $h = 1/16$ ). More precisely, 20000 samples were taken for  $\omega$ , then the solution  $\hat{u}$  was calculated and then the mean and the variance of these solution samples were estimated point by point on  $D_{ref}$ .

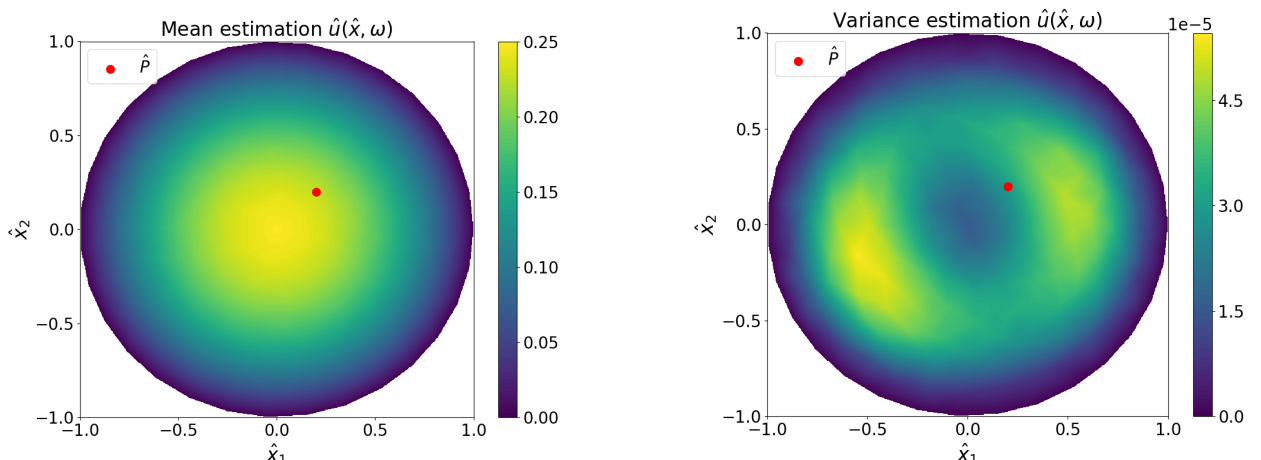


**Figure 4.5** Poisson Model Monte Carlo Estimation

The Monte Carlo convergence analysis works with the comparison of two different KLE grid discretizations. The fine samples use mesh resolution KLE 14 and mesh resolution FEM 10. The coarse samples use mesh resolution KLE 10 (leading to  $M = 386$ ) and mesh resolution FEM 10. For the fine solution (i.e. reference solution), 20000 sample solutions were calculated. The coarse solutions consist of  $[2^i \text{ for } i = 5, \dots, 13]$  samples. The model was evaluated at the point  $\hat{P} = (0.2, 0.2)^T$  to compare the mean and the variance.

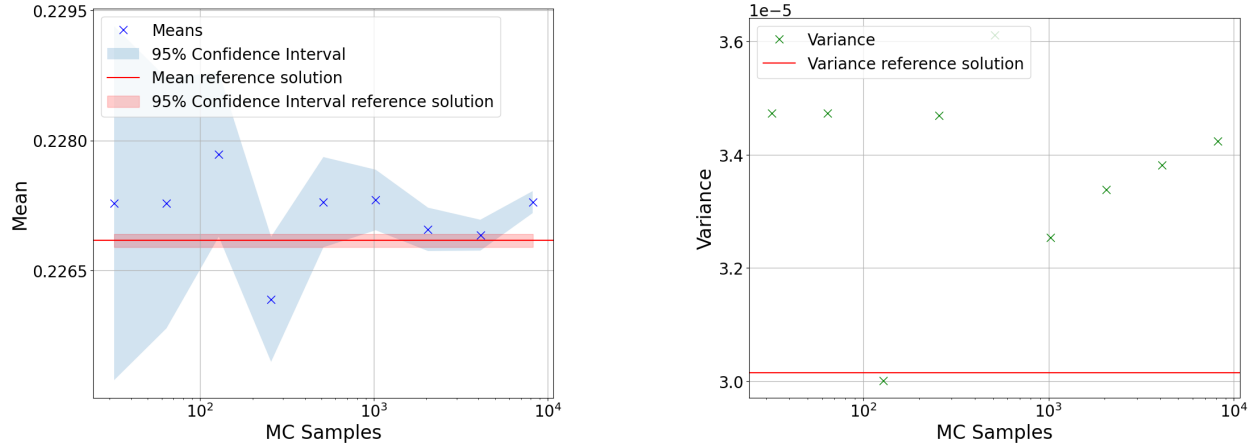


**Figure 4.6** Poisson Model Monte Carlo Convergence Analysis

We see that the approximation of the mean and the variance of the reference solution does not necessarily improve with an exponential increase in the Monte Carlo sample size. This may be partly due to the geometry of the KLE and the influence of the larger  $M$  in the reference solution. Comparing the means of the sparse solutions to the mean of the reference solution, we can also calculate the  $L^2$ - and  $H^1$ -errors on the whole domain  $D_{ref}$  instead of only comparing the evaluation in one point.

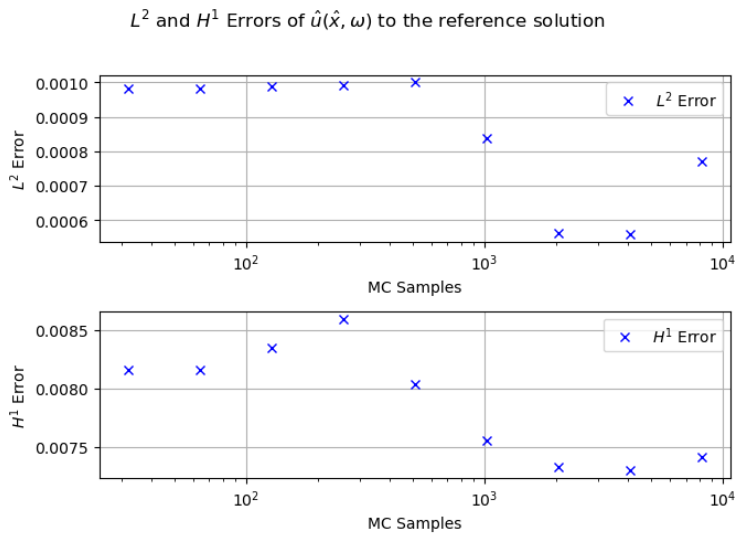


**Figure 4.7** Poisson Model Monte Carlo Error Analysis

The  $L^2$ - and  $H^1$ -errors also do not show any particularly strong convergence. This can also be explained by the different truncation level of the KLE in the reference solution and sparse solution. Accordingly, we can see that this influence cannot be neglected, which is also an interesting result.

The following figure shows the Sobol' single effects and total effects for the first eight KLE random variables. As quantity of interest, the entire functional output of the model  $\hat{u}$  is considered, as described in section 3.3. The efficient algorithm introduced in 3.4.2 was used. As convergence is only visible for a large

number of samples, the mesh resolution KLE and FEM 8 ( $h = 1/12, M = 258$ ) was used to calculate a total of 12000 samples.

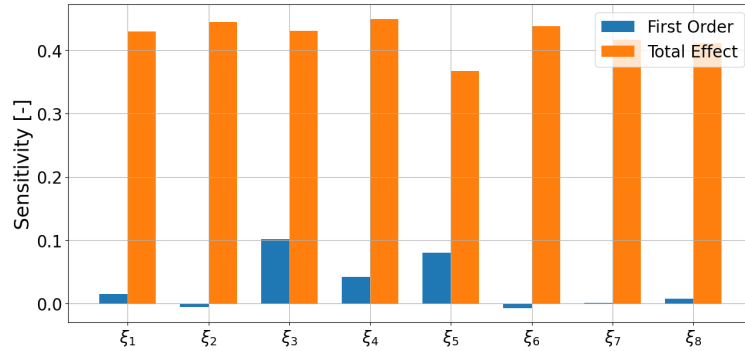


**Figure 4.8** Sobol' Indices for Poisson Model

A possible explanation for the different magnitude of the influences primarily related to the first order effect is the form of the eigenfunctions 4.3. Otherwise, it is surprising at first glance that the 3rd and 5th random variables have the greatest individual impact on the output variance. The slightly negative first order effects must indicate an approximation error, as the true effect must be non-negative.

# 5 Domain Mapping Method for Variants of the Poisson Equation

## 5.1 Random right-hand Side

The following section deals with a variation of the already introduced Poisson model, in which the right-hand side  $f$  is no longer constant but a function with parametric random variables. This change allows us to analyze a first uncertainty quantification of two different uncertainty sources. The geometry of the domain thereby stays the same as before with the reference domain  $D_{ref} = \{x \in \mathbb{R}^2 | \|x\|_2 < 1\}$  and the random field  $V : \overline{D_{ref}} \times \Omega_2 \rightarrow \mathbb{R}^d$  introduced in (4.3). The resulting strong formulation of the partial differential equation with  $u(\cdot, \omega) \in C^2(D(\omega_2), \mathbb{R}^2)$  looks as follows

$$\begin{aligned} -\Delta u(x, \omega) &= f(x, \omega_1) & | & x \in D(\omega_2) \\ u(x, \omega) &= 0 & | & x \in \delta D(\omega_2) \end{aligned}$$

with

$$f : D(\omega_2) \times \Omega_1 \rightarrow \mathbb{R},$$

$$f(x, \omega_1) = \begin{cases} \omega_1^{(1)}, & x_1 \leq 0, x \in D_{ref} \cap D(\omega_2) \\ \omega_1^{(2)}, & x_1 > 0, x \in D_{ref} \cap D(\omega_2) \\ 0 & \text{otherwise} \end{cases}$$

where  $\omega_1^{(1)}, \omega_1^{(2)} \sim U([0, 1])$

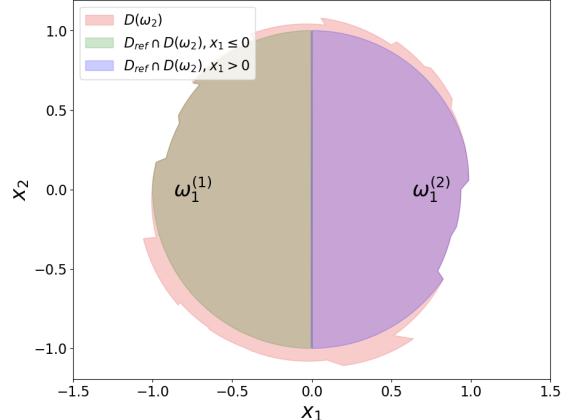


**Figure 5.1** Sample for random right-hand Side

We again use the following notation for the truncated KLE

$$V : \overline{D_{ref}} \times \Omega_2 \rightarrow \mathbb{R}^d$$

$$V(\hat{x}, \omega_2) = \mu(\hat{x}) + \sum_{m=1}^M \sqrt{\gamma_m} \cdot g_m(\hat{x}) \cdot \xi_m(\omega_2) \quad \text{with } \xi_m(\omega_2) \sim U(-\sqrt{3}, \sqrt{3})$$

with the same mean, covariance function, and reference domain as the Poisson model and define  $\omega := \begin{pmatrix} \omega_1 \\ \omega_2 \end{pmatrix}$ .

We once more assume 4.2.1 for the random field  $V$ . The resulting variational formulation of the two related problems for  $u(x, \omega)$  and  $\hat{u}(\hat{x}, \omega)$  is the same as in lemma 4.2.3 and is therefore left out here. For the proof of the pathwise existence of a unique solution, we can as well refer to lemma 4.2.4 with the additional remark that we use the bound  $\forall \omega_1 \in \Omega_1, \omega_2 \in \Omega_2 : 0 \leq f(x, \omega_1) \leq 1 \forall x \in D(\omega_2)$  instead of  $f \equiv 1$ . The pointwise evaluation for the convergence analysis was carried out for  $\hat{P} = (0.2, 0.2)^T$ .

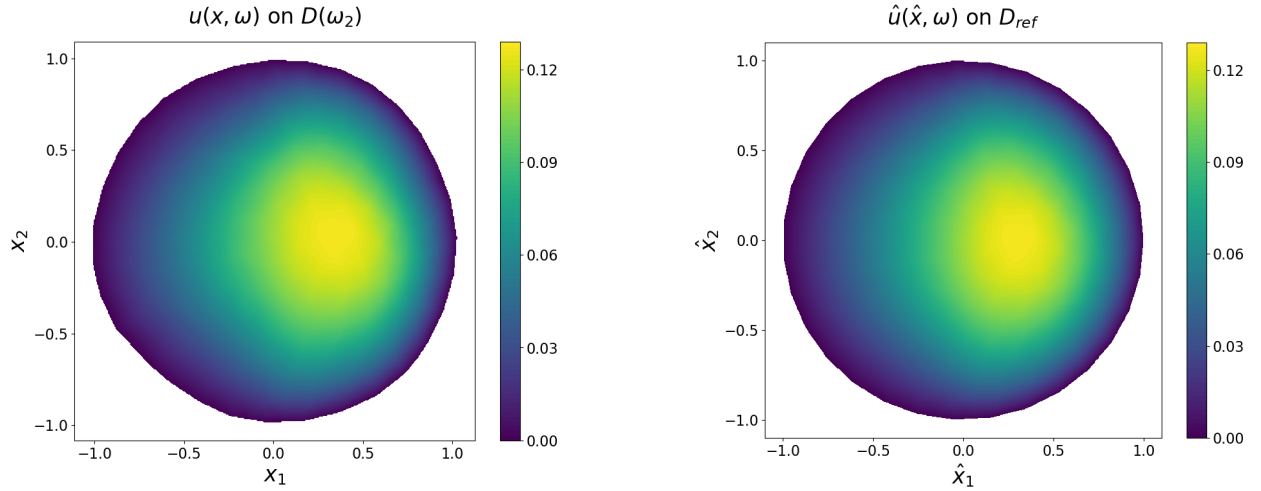


**Figure 5.2** Solution Sample of random right-hand Side Model  $\omega_1 = (0.11, 0.79)^T$

The Monte Carlo analysis for the mean and variance estimation was carried out with the mesh resolution KLE 14 ( $h = 1/24, M = 769$ ) and FEM 10 ( $h = 1/16$ ). 20000 samples were used. At the same time, these are the samples for the reference solution in the convergence analysis. The samples for the convergence analyses on the sparse grid were calculated with a mesh resolution KLE and FEM 10 ( $h = 1/16, M = 386$ ).

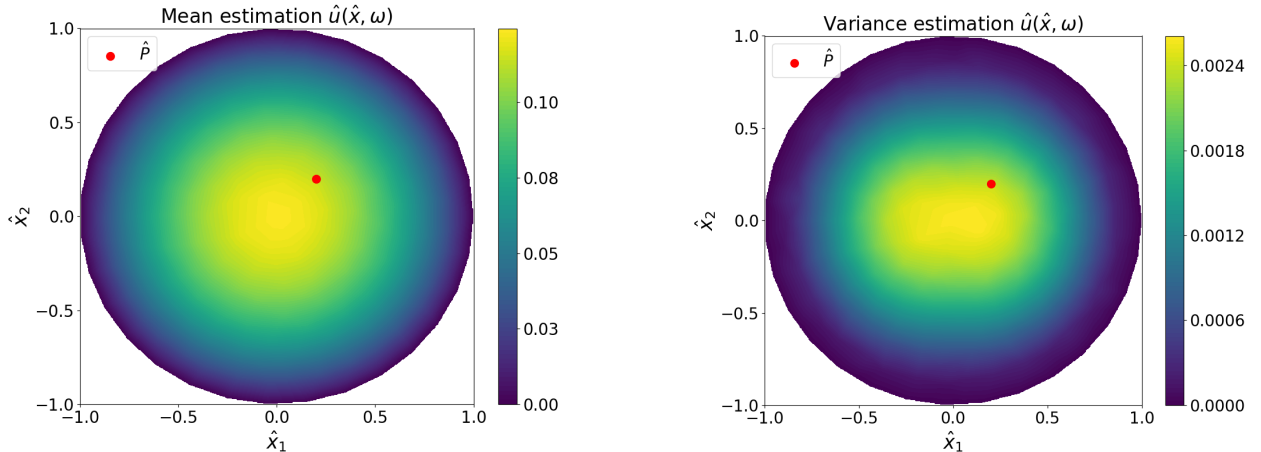


**Figure 5.3** Monte Carlo Estimation of random right-hand Side Model

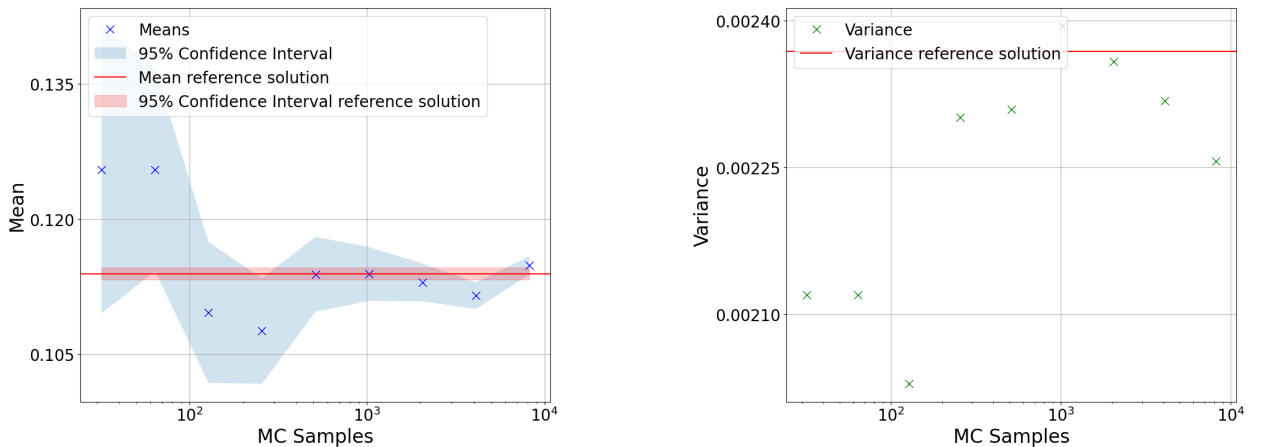


**Figure 5.4** Monte Carlo Convergence Analysis random right-hand Side Model

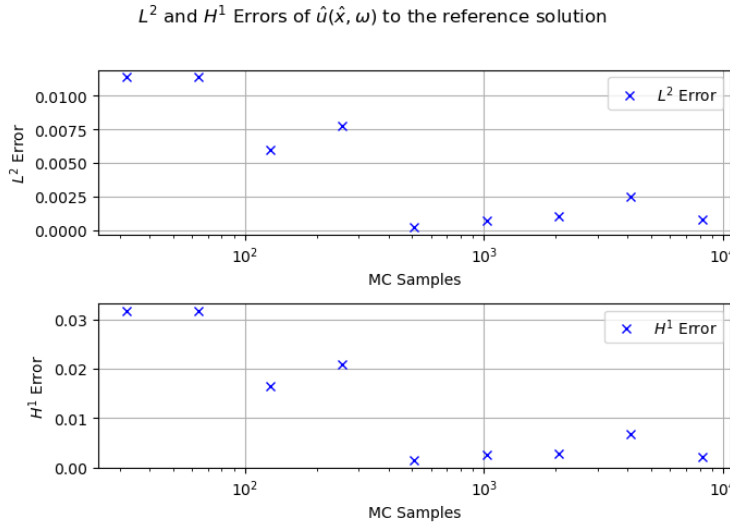


**Figure 5.5** Monte Carlo Error Analysis random right-hand Side Model

Interestingly, the sparse solutions of this model seem to converge better to the reference solution than in the Poisson model with deterministic right-hand side. An approximation to the reference solution can be observed in the pointwise analysis as well as in the global convergence.

As mentioned, in this model, an informative quantification of the two random sources can be done by calculating the Sobol' indices. The samples were calculated with a mesh resolution KLE and FEM 8 ( $h = 1/12$ ), leading to a KLE truncation level of  $M = 258$ . The result suggests that the influence of the two random variables in  $\omega_1$  on the variance of the solution is far more significant than the influence of  $\omega_2$ . Again, the whole functional value was used in the manner of algorithm 3.4.2.

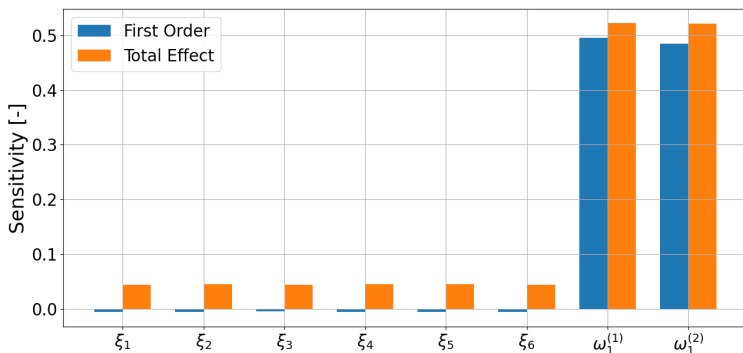


**Figure 5.6** Sobol' Indices for the random right-hand Side Model with 12000 Samples

## 5.2 Diffusion Model

The following variation of the original Poisson model again works with a constant right-hand side  $f \equiv 1$  and  $D_{ref} = \{x \in \mathbb{R}^2 \mid \|x\|_2 < 1\}$ , but an additional random field  $A(x, \omega_1)$  is used as the diffusion coefficient. The strong formulation with  $u(\cdot, \omega) \in C^2(D(\omega_2), \mathbb{R}^2)$  looks as follows

$$\begin{aligned} -\nabla \cdot (A(x, \omega_1) \cdot \nabla u(x, \omega)) &= f(x) & | & \quad x \in D(\omega_2) \\ u(x, \omega) &= 0 & | & \quad x \in \delta D(\omega_2) \end{aligned}$$

where we denote  $\omega = \begin{pmatrix} \omega_1 \\ \omega_2 \end{pmatrix}$ . We define the diffusion coefficient as the following log-normal random field  $A : \mathbb{R}^2 \times \Omega_1 \rightarrow \mathbb{R}$ ,  $A(x, \omega_1) := \exp(Z(x, \omega_1))$  where  $Z(x, \omega_1)$  is a random field using  $\mu(x) = 0$  and the exponential covariance function 2.2.3 with  $l = 0.1$  and  $\sigma = 5$ . Once again the truncated KLE is applied for  $Z(x, \omega_2)$  leading to

$$A(x, \omega_1) = \exp \left( \sum_{m=1}^M \sqrt{\gamma_m} \cdot g_m(x) \cdot \xi_m(\omega_1) \right) \quad \text{where } \xi_m(\omega_1) \sim \mathcal{N}(0, 1), \quad (5.1)$$

where  $(\gamma_m, g_m)$  are the eigenpairs to the corresponding covariance kernel of  $Z$ . In figure 5.7, one such sample of  $A$  and  $Z$  can be seen. To emphasize the global definition, the plot shows a different, bigger domain than the reference domain  $D_{ref}$  or a sample domain  $D(\omega_2)$ . In detail, we are using the KLE domain independence, which is explained in subsection 2.2.2. The random field  $V(\hat{x}, \omega_2)$  is modeled equivalently as in the Poisson model defined in equation (4.3).

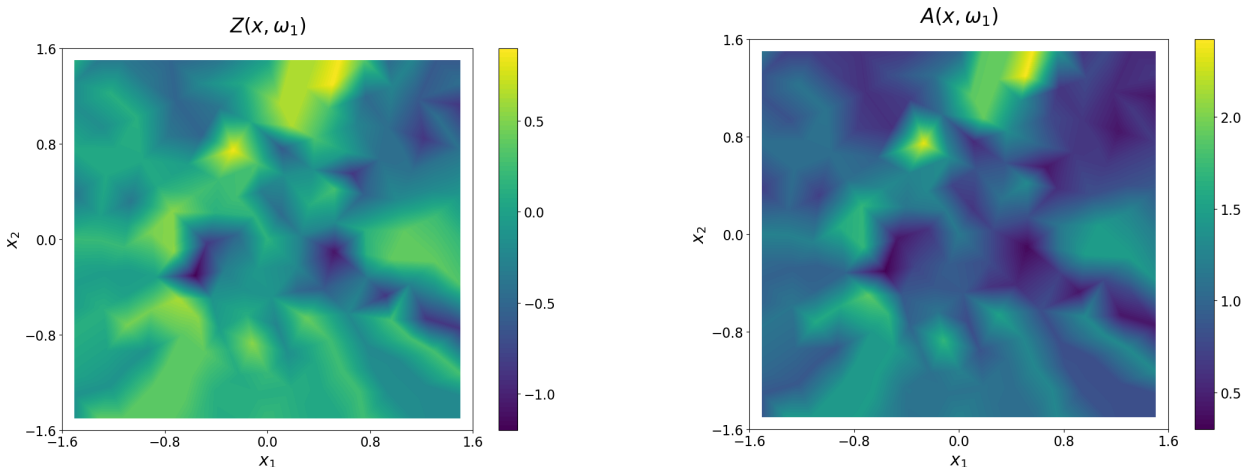


**Figure 5.7** Sample of Diffusion Coefficient

**Lemma 5.2.1.** Let us assume 4.2.1 for the random field  $V$ . For fixed  $\omega_1 \in \Omega_1$  and  $\omega_2 \in \Omega_2$ , the two variational problems:

Find  $u(\cdot, \omega) \in H_0^1(D(\omega_2))$  s.t.

$$\begin{aligned} a(u, v) &= l(v) \quad \forall v \in H_0^1(D(\omega_2)) \\ a(u, v) &:= \int_{D(\omega_2)} \langle A(x, \omega_1) \cdot \nabla u(x, \omega), \nabla v(x, \omega_2) \rangle dx \\ l(v) &:= \int_{D(\omega_2)} f(x) v(x, \omega_2) dx \end{aligned}$$

and:

Find  $\hat{u}(\cdot, \omega) \in H_0^1(D_{ref})$  s.t.

$$\begin{aligned}\hat{a}(\hat{u}, \hat{v}) &= \hat{l}(\hat{v}) \quad \forall \hat{v} \in H_0^1(D_{ref}) \\ \hat{a}(\hat{u}, \hat{v}) &:= \int_{D_{ref}} \left\langle A(V(\hat{x}, \omega_2), \omega_1) \cdot \det(J(\hat{x}, \omega_2)) \cdot \left( J(\hat{x}, \omega_2)^T \cdot J(\hat{x}, \omega_2) \right)^{-1} \cdot \nabla \hat{u}(\hat{x}, \omega), \nabla \hat{v}(\hat{x}) \right\rangle d\hat{x} \\ \hat{l}(\hat{v}) &:= \int_{D_{ref}} \det(J(\hat{x}, \omega_2)) \cdot (f \circ V)(\hat{x}, \omega_2) \cdot \hat{v}(\hat{x}) d\hat{x}\end{aligned}$$

are connected via

$$\hat{u}(\hat{x}, \omega) = u(V(\hat{x}, \omega_2), \omega).$$

*Proof.*

$$\begin{aligned}& \int_{D_{ref}} \det(J(\hat{x}, \omega_2)) \cdot (f \circ V)(\hat{x}, \omega_2) \cdot \hat{v}(\hat{x}) d\hat{x} \\ &= \int_{D(\omega_2)} f(x) \cdot v(x, \omega_2) dx \\ &= \int_{D(\omega_2)} \langle A(x, \omega_1) \cdot \nabla_x u(x, \omega), \nabla_x v(x, \omega_2) \rangle dx \\ &= \int_{D_{ref}} \det(J(\hat{x}, \omega_2)) \cdot \langle A(V(\hat{x}, \omega_2), \omega_1) \cdot J^{-T}(\hat{x}, \omega_2) \cdot \nabla_{\hat{x}} \hat{u}(\hat{x}, \omega), J^{-T}(\hat{x}, \omega_2) \cdot \nabla_{\hat{x}} \hat{v}(\hat{x}) \rangle d\hat{x} \\ &= \int_{D_{ref}} \det(J(\hat{x}, \omega_2)) \cdot A(V(\hat{x}, \omega_2), \omega_1) \cdot \left( J^{-T}(\hat{x}, \omega_2) \cdot \nabla \hat{u}(\hat{x}, \omega) \right)^T J^{-T}(\hat{x}, \omega_2) \cdot \nabla \hat{v}(\hat{x}) d\hat{x} \\ &= \int_{D_{ref}} \det(J(\hat{x}, \omega_2)) \cdot A(V(\hat{x}, \omega_2), \omega_1) \cdot \left( \left( J^{-1}(\hat{x}, \omega_2) \cdot J^{-T}(\hat{x}, \omega_2) \right)^T \cdot \nabla \hat{u}(\hat{x}, \omega) \right)^T \cdot \nabla \hat{v}(\hat{x}) d\hat{x} \\ &= \int_{D_{ref}} \left\langle A(V(\hat{x}, \omega_2), \omega_1) \cdot \det(J(\hat{x}, \omega_2)) \cdot \left( J(\hat{x}, \omega_2)^T \cdot J(\hat{x}, \omega_2) \right)^{-1} \cdot \nabla \hat{u}(\hat{x}, \omega), \nabla \hat{v}(\hat{x}) \right\rangle d\hat{x}\end{aligned}$$

where again the connection  $\hat{u}(\hat{x}, \omega) = u(V(\hat{x}, \omega_2), \omega)$  and  $\hat{v}(\hat{x}) = v(V(\hat{x}, \omega_2), \omega_2)$  follows from lemma 4.2.2.  $\square$

**Lemma 5.2.2.** Under assumption 4.2.1 and the choice  $f \equiv 1$ ,  $D_{ref} = \{x \in \mathbb{R}^2 | \|x\|_2 < 1\}$  and the diffusion coefficient described in equation (5.1) the pathwise formulation of lemma 5.2.1 has a unique solution  $\hat{u}(\cdot, \omega) \in H_0^1(D_{ref})$ . More precisely, for a given realisation  $\omega_1 \in \Omega_1$  and  $\omega_2 \in \Omega_2$ , we wish to find  $\hat{u}(\cdot, \omega) \in H_0^1(D_{ref})$  s.t. for  $\mathbb{P}$ -a.e.  $\omega \in \Omega$  it holds

$$\hat{a}(\hat{u}, \hat{v}) = \hat{l}(\hat{v}) \quad \forall \hat{v} \in H_0^1(D_{ref})$$

as defined in lemma 5.2.1.

*Proof.* We use lemma 2.2.10, which tells us that for the log-normal random field  $A$ , we have pathwise ellipticity and boundedness

$$0 < A_{min}(\omega_1, \omega_2) \leq A(x, \omega_1) \leq A_{max}(\omega_1, \omega_2) < \infty, \quad \text{a.e. in } D(\omega_2).$$

To apply the lemma, we have to show that the exponential covariance function 2.2.3 we are using for  $A$  is Lipschitz continuous. This is not the case globally, as potentially the random field  $V$  can perturb the domain arbitrarily. That's why we state the solution existence pathwise, as on an arbitrary but fixed, bounded domain-sample  $D(\omega_2)$ , the continuous exponential covariance function is Lipschitz. That's why the random variables  $A_{min}$  and  $A_{max}$  also depend on  $\omega_2$ .

With those additional bounds, the proof follows just as in the case of the pure Poisson model derived in lemma 4.2.4, applying the Lax Milgram theorem 2.3.5.  $\square$

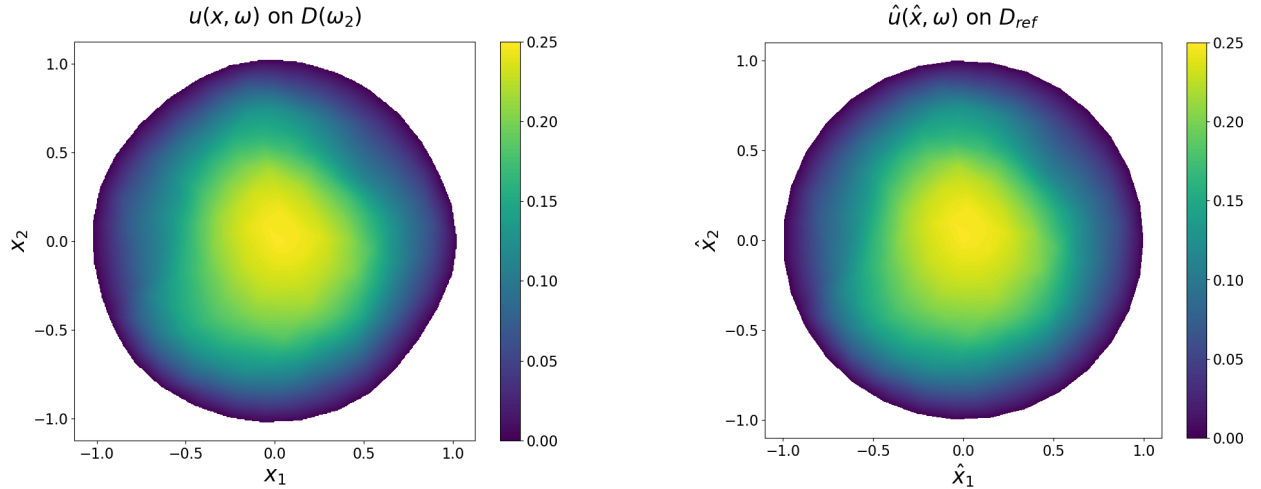


Figure 5.8 Solution Sample of Diffusion Equation

When implementing the variational problem, the question arises about how to obtain the random field  $A$ . Again, the truncated KLE was calculated using the Galerkin method. Compared to calculating  $V$ , we now have a one-dimensional covariance function, which leads to lower computational complexity. Otherwise, the procedure is exactly the same as in subsection 4.3.1. What is special, however, is that we would essentially have to solve the eigenproblem on  $D(\omega_2)$  for  $A(V(\hat{x}, \omega_2), \omega_1)$ . A new calculation of the KLE would be required for each sample, resulting in an extremely high computational effort. The useful domain independence from lemma 2.2.23 becomes significant at this point. Consequently, we can calculate  $A$  w.r.t.  $D_{ref}$  and accept a small shift due to the truncated KLE.

In figure 5.9, we can see the Monte Carlo estimate of the mean and variance using 20000 samples with mesh resolution KLE 14 ( $h = 1/24, M = 769$ ) for both random fields  $A$  and  $V$  and mesh resolution FEM 10 ( $h = 1/16$ ).

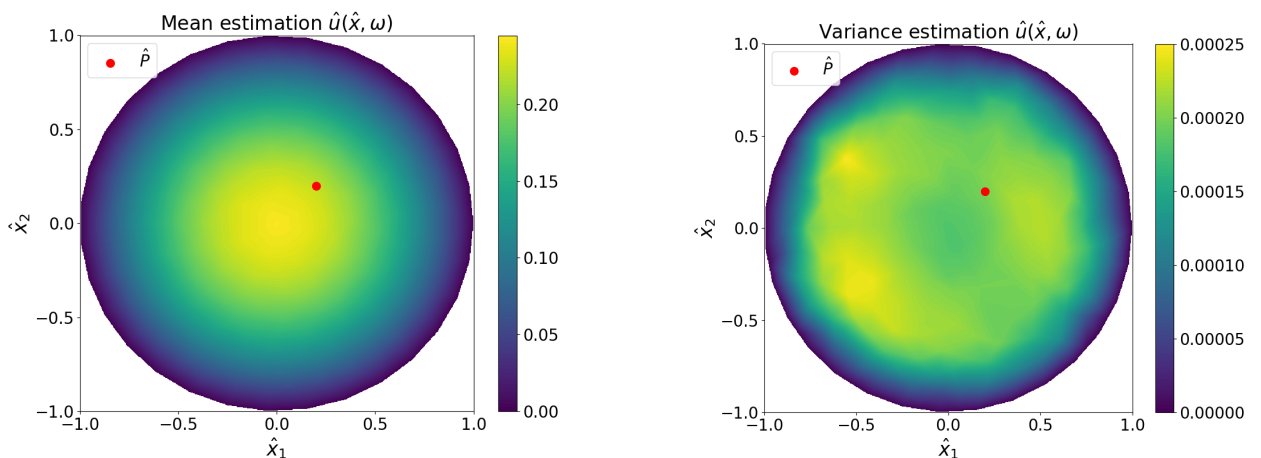
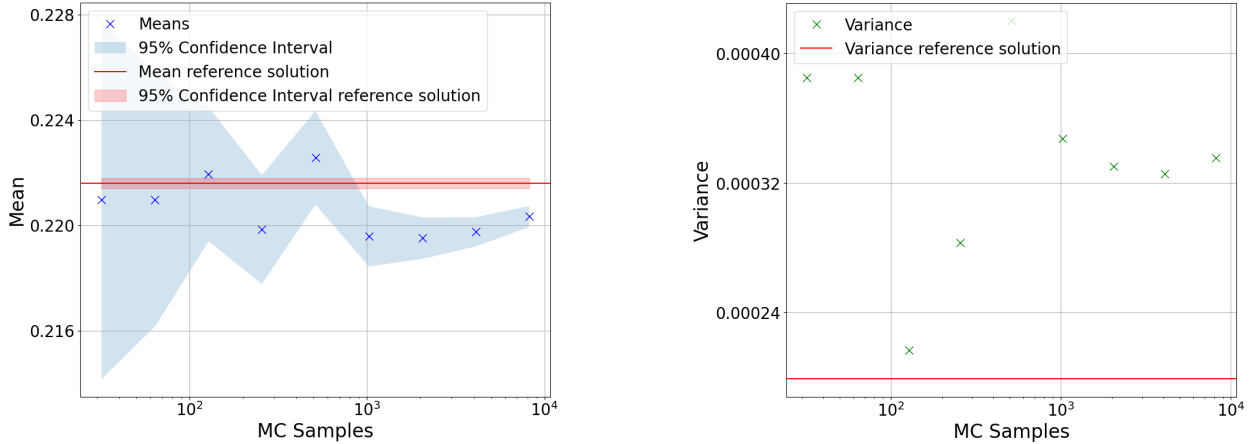


Figure 5.9 Diffusion Model Monte Carlo Estimation

For the Monte Carlo convergence in figure 5.10, pointwise evaluation at  $\hat{P} = (0.2, 0.2)^T$  was chosen as before. The reference solution is the same as in figure 5.9, and the sparse samples work with mesh resolution KLE 10 for both random fields and mesh resolution FEM 10.

## 5 Domain Mapping Method for Variants of the Poisson Equation



**Figure 5.10** Diffusion Model Monte Carlo Convergence Analysis

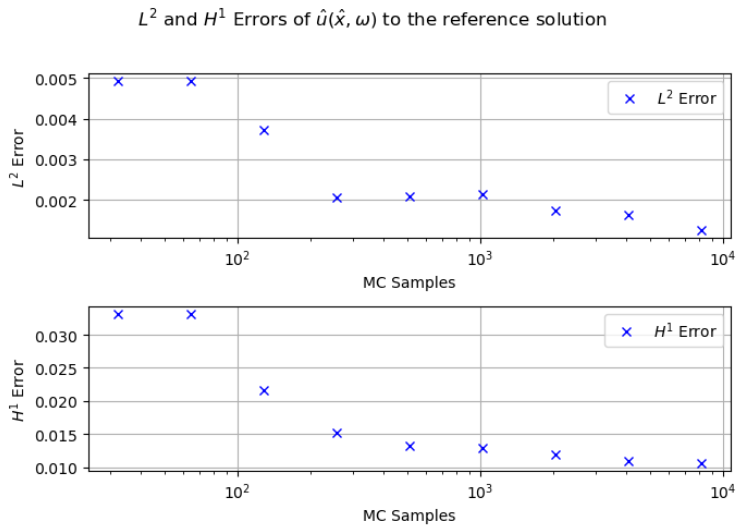


**Figure 5.11** Diffusion Model Monte Carlo Error Analysis

Similar to the Poisson model with deterministic right-hand side, neither the pointwise nor the global Monte Carlo analysis can demonstrate strong convergence. In this case, however, it appears that the sparse solutions approach a solution that is not equal to the reference solution, which is probably due to the different truncation levels  $M$ .

The Sobol' index calculation was carried out as before over the entire solution function  $\hat{u}$  3.4.2. Mesh resolution KLE 8 ( $h = 1/12$ ,  $M = 258$ ) was used for both random fields, and mesh resolution FEM 8 ( $h = 1/12$ ). A total of 12000 samples was used for the calculation. The random variables in the KLE are denoted by  $\xi_m^V$  and by  $\xi_m^Z$  for  $V$  and  $Z$  respectively.

Random Variable of KLE of $V$	Eigenvalue $\gamma_m^V$
$\xi_1^V$	0.087
$\xi_2^V$	0.02741
$\xi_3^V$	0.02739
$\xi_4^V$	0.021

Random Variable of KLE of $Z$	Eigenvalue $\gamma_m^Z$
$\xi_1^Z$	2.45
$\xi_2^Z$	2.18
$\xi_3^Z$	2.15
$\xi_4^Z$	1.9

**Table 5.1** Eigenvalues of KLE of the Random Fields  $V$  and  $Z$

In the results, we can clearly see a dominance of the first random variable of  $Z$ . Of course, the single effect cannot really be greater than the total effect, which suggests an approximation error. In addition,

the single effects of the random variables of  $Z$  generally indicate a significantly larger influence on the variance of the solution.

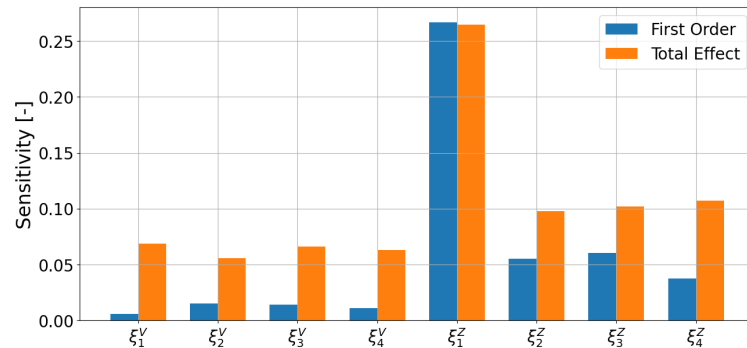


**Figure 5.12** Sobol' Indices for Diffusion Model

# 6 Steel Plate Problem

## 6.1 Model Problem

The model we are looking at in this chapter deals with a thin steel plate with a hole in the middle. One could imagine, for example, an industrial machine that punches this hole in the thin steel plate. An important parameter for the producer is the maximum tensile force that the steel plate can withstand without tearing. If the plate is clamped at the left edge and pulled at the right edge, the most critical points for the potential crack are directly above and below the hole. The stability depends on various fabrication-specific parameters. For example, the Young's modulus of the steel, which is assumed to be non-constant in our model. The question now arises as to what effect a random geometry of the hole has on the stability of the steel plate and to what extent the uncertainty arising from three different sources can be quantified and estimated against each other. The three random sources are the random variables in the modeling of the random field of Young's modulus, the random geometry of the hole, and the tensile force at the right edge. The model with a deterministic fixed hole has already been described in [UC20] and analyzed. Furthermore, for the theoretical foundations of the elasticity equation, the book [Joh12] was used. Another source for analyzing a similar model but with different methods is [Zhe+23].

### 6.1.1 Model on a deterministic Domain

We consider a squared steel plate of length  $0.32m$ , which is assumed to be very thin, and therefore, we don't consider the third dimension. The steel plate has a circular hole of radius  $0.02m$  in its middle and is immovably clamped at the left edge. Here, we denote this domain by  $D_{ref} \subset \mathbb{R}^2$ . The right edge is pulled with a force  $q$ . The resulting partial differential equation for the displacement vector field  $u(\cdot, \omega_1, q) \in C^2(D_{ref}, \mathbb{R}^2)$  is an elasticity equation (Navier-Cauchy equation) of the form:

$$\frac{E(x, \omega_1)}{2(1+\nu)} \cdot \nabla^2 u(x, \omega_1, q) + \frac{E(x, \omega_1)}{2(1-\nu)} \cdot \nabla(\nabla \cdot u(x, \omega_1, q)) + b = 0 \quad | x \in D_{ref} \quad (6.1)$$

$$u(x, \omega_1, q) = 0 \quad | x \in \Gamma_1 \quad (6.2)$$

$$\sigma(x, u, \omega_1) \cdot n(x) = g \quad | x \in \Gamma_2 \quad (6.3)$$

where  $\sigma$  is the stress-tensor defined later in remark 6.2.2. On the other boundaries, a natural boundary condition is applied

$$\sigma(x, u, \omega_1) \cdot n(x) = \begin{pmatrix} 0 \\ 0 \end{pmatrix} \quad | x \in \Gamma \setminus (\Gamma_1 \cup \Gamma_2).$$

In this formulation,  $\nu$  is called the Poisson ratio of the steel,  $b = [0, -\rho g_{\text{grav}}]^T$  is the vector of body forces acting on the plate with  $g_{\text{grav}} = 9.80665 \frac{m}{s^2}$  denoting the standard gravity and  $\rho = 7850 \frac{kg}{m^3}$  the density of the steel. The force  $q$  acting on the right edge is modeled as a random variable  $q \sim \mathcal{N}(60 \cdot 10^6, 12 \cdot 10^6)$ . Thus, the force vector acting on the boundary  $\Gamma_2$  is  $g = (q, 0)^T$ .  $E(x, \omega_1)$  is called Young's modulus, and in this model, it's considered random. We use a log-normal random field with a Whittle-Matérn kernel 2.2.6 with  $q_{\text{mat}} = 1/2$ ,  $l_{\text{mat}} = 0.02$ ,  $\mu_E = 26.011$  and  $\sigma_E = 0.149$  for  $E(x, \omega_1) = \exp(E'(x, \omega_1))$ . A sample can be seen in figure 6.5. The fixed parameter  $\nu = 0.29$  denotes the Poisson ratio of the steel.

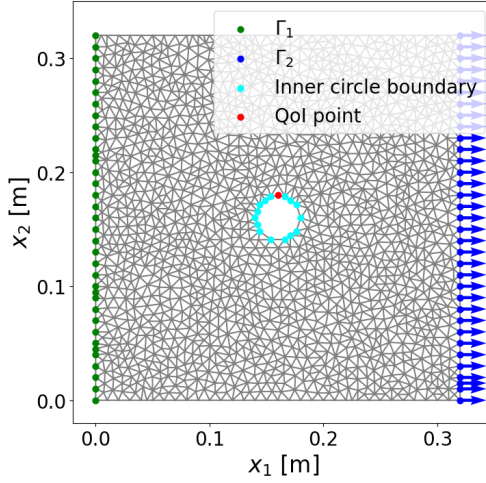


**Figure 6.1** Reference Domain  $D_{ref}$  and Boundaries

### 6.1.2 Perturbation Function and Model on stochastic Domain

In the following, we use a perturbation function in the manner of (4.1) to describe a bijective domain perturbation  $V : \overline{D_{ref}} \rightarrow \mathbb{R}^2$ . In this case, the old circle radius is multiplied by a random factor, and the new circle position is located at  $\bar{x}(\omega_2^{(2)}, \omega_2^{(3)})$  defined as follows:

$$\bar{r}(\omega_2^{(1)}) = 0.02 \cdot \omega_2^{(1)}, \quad \omega_2^{(1)} \sim U([0.5; 2]) \quad (6.4)$$

$$\bar{x}(\omega_2^{(2)}, \omega_2^{(3)}) = \begin{pmatrix} 0.16 + \omega_2^{(2)} \\ 0.16 + \omega_2^{(3)} \end{pmatrix}, \quad \omega_2^{(2)}, \omega_2^{(3)} \sim U([-0.1; 0.1]) \quad (6.5)$$

The points on the circle boundary are perturbed accordingly, and the outer boundary points are fixed. The perturbation in between is calculated via a convex combination between those two points.

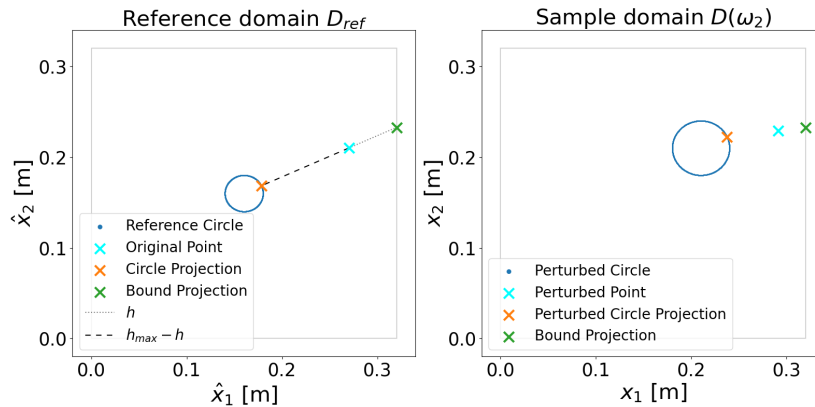


**Figure 6.2** Perturbation Function with Sample  $\omega_2 = (1.5; 0.05; 0.05)^T$

Starting from the original point  $x$  (left plot in figure 6.2 cyan), a line is drawn to the center of the circle, and the projection onto the circle  $x_{circ}$  (orange) and onto the boundary  $x_{bound}$  (green) is calculated on this line. We note the euclidean distance from  $x$  to  $x_{bound}$  with  $h$  and the distance from  $x_{circ}$  to  $x_{bound}$  with  $h_{max}$ , then we get the following convex combination:

$$x = \frac{h}{h_{max}} \cdot x_{bound} + \left(1 - \frac{h}{h_{max}}\right) \cdot x_{circ}$$

We propagate this relation with the perturbation function because we know how the point on the circle moves and that the point on the edge remains the same.

$$V(x, \omega_2) = \frac{h}{h_{max}} \cdot \underbrace{V(x_{bound}, \omega_2)}_{x_{bound}} + \left(1 - \frac{h}{h_{max}}\right) \cdot V(x_{circ}, \omega_2)$$

For the detailed calculation of the projections  $x_{circ}$ ,  $x_{bound}$  and of  $V(x_{circ}, \omega_2)$ , we refer to remark A.1.5. Due to the rather convoluted calculation of the perturbation function  $V$ , the Jacobian  $J$  could not be calculated analytically. Therefore, a numerical approach was chosen in the implementation, which can be calculated directly by FEniCS.

The resulting strong formulation of the elasticity equation on the random domain looks exactly as (6.1) but is defined on  $D(\omega_2)$  instead of  $D_{ref}$ .

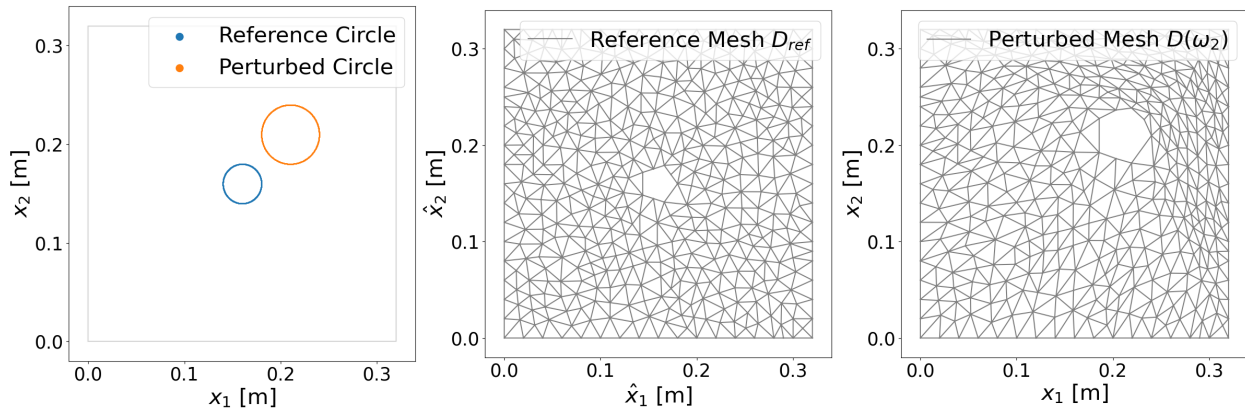


**Figure 6.3** Sample for a perturbed Mesh with  $\omega_2 = (1.5; 0.05; 0.05)^T$

## 6.2 Variational Formulation

**Remark 6.2.1** (Notation). *Various conventions, notations, and abbreviations are used in the following sections, which we would like to record here.*

*The matrix dot product is denoted as follows*

$$(A : B) := \sum_{i=1}^N \sum_{j=1}^M A_{i,j} \cdot B_{i,j} \quad | \quad A, B \in \mathbb{R}^{N \times M}.$$

*We introduce the so-called strain*

$$\varepsilon(u) := \frac{1}{2}(\nabla u + \nabla u^T).$$

*In most of the following proofs, the variable dependency is ignored. The notation remains consistent with chapters 4 and 5, but is still repeated here because the dependencies sometimes look different. The following definitions and dependencies apply.*

$$\begin{aligned} \omega &:= (\omega_1, \omega_2, q)^T \\ \hat{u} &:= \hat{u}(\hat{x}, \omega) = u(V(\hat{x}, \omega_2), \omega) \\ \hat{v} &:= \hat{v}(\hat{x}, \omega_2) = v(V(\hat{x}, \omega_2), \omega_2) \\ \hat{E} &:= \hat{E}(\hat{x}, \omega_1, \omega_2) = E(V(\hat{x}, \omega_2), \omega_1) \end{aligned}$$

$$\begin{pmatrix} J_{11} & J_{12} \\ J_{21} & J_{22} \end{pmatrix} := J(\hat{x}, \omega_2) = \nabla_{\hat{x}} V(\hat{x}, \omega_2)$$

We define the following norm

$$\begin{aligned}\|\hat{u}\|_{H^1(D, \mathbb{R}^2)} &:= \left( \|\hat{u}\|_{L^2(D, \mathbb{R}^2)}^2 + \|\nabla \hat{u}\|_{L^2(D, \mathbb{R}^{2 \times 2})}^2 \right)^{1/2} \\ \|\hat{u}\|_{L^2(D, \mathbb{R}^2)}^2 &:= \int_D \|\hat{u}\|_2^2 d\hat{x} \\ \|\nabla \hat{u}\|_{L^2(D, \mathbb{R}^{2 \times 2})}^2 &:= \int_D \|\nabla \hat{u}\|_F^2 d\hat{x} = \int_D \left( \left( \frac{\partial \hat{u}_1}{\partial \hat{x}_1} \right)^2 + \left( \frac{\partial \hat{u}_1}{\partial \hat{x}_2} \right)^2 + \left( \frac{\partial \hat{u}_2}{\partial \hat{x}_1} \right)^2 + \left( \frac{\partial \hat{u}_2}{\partial \hat{x}_2} \right)^2 \right) d\hat{x}\end{aligned}$$

with  $\|\cdot\|_F$  denoting the Frobenius norm.

The sample spaces for the random variables are denoted as follows

$$\begin{aligned}\omega_1 \in \Omega_1 &:= \{f : \mathbb{R}^2 \rightarrow \mathbb{R}\} \\ \omega_2 \in \Omega_2 &:= [0.5; 2] \times [-0.1; 0.1]^2 \subset \mathbb{R}^3 \\ q \in \Omega_3 &:= \mathbb{R} \\ \Omega &:= \Omega_1 \times \Omega_2 \times \Omega_3\end{aligned}$$

The resulting probability space is  $(\Omega, \mathcal{E}, \mathbb{P})$  where  $\mathcal{E} := \mathcal{B}(\Omega_1) \times \mathcal{B}(\Omega_2) \times \mathcal{B}(\Omega_3)$  and  $\mathbb{P} = \prod_{i=1}^3 \mathbb{P}_i$  ( $\mathbb{P}_i$  being the corresponding probability measures for  $\omega_1, \omega_2, q$ ).

**Remark 6.2.2.** From [UC20], we obtain the following form of the stress tensor

$$\sigma := \sigma(x, u, \omega) = \begin{pmatrix} \frac{E(x, \omega_1)}{1-v^2} \left( \frac{\partial u_1}{\partial x_1} + v \frac{\partial u_2}{\partial x_2} \right) & \frac{E(x, \omega_1)}{2(1+v)} \left( \frac{\partial u_1}{\partial x_2} + \frac{\partial u_2}{\partial x_1} \right) \\ \frac{E(x, \omega_1)}{2(1+v)} \left( \frac{\partial u_1}{\partial x_2} + \frac{\partial u_2}{\partial x_1} \right) & \frac{E(x, \omega_1)}{1-v^2} \left( \frac{\partial u_2}{\partial x_2} + v \frac{\partial u_1}{\partial x_1} \right) \end{pmatrix}$$

which describes to what extent the tensile force on the boundary  $\Gamma_2$  acts on the steel plate.

**Lemma 6.2.3.** Consider a fixed sample  $\omega$ . To match the stress tensor's form in remark 6.2.2, we reformulate the following PDE.

The strong formulated elasticity equation (6.1) defined on the random domain  $D(\omega_2)$  leads to the following variational formulation:

Find  $u(\cdot, \omega) \in W$  s.t.  $a(u, v) = l(v) \forall v(\cdot, \omega_2) \in W$  for

$$\begin{aligned}W &:= \{u \in H^1(D(\omega_2), \mathbb{R}^2), u(x, \omega) = 0 \text{ for } x \in \Gamma_1\} \\ a(u, v) &:= \int_{D(\omega_2)} \text{Tr} \left( \left( \frac{1}{1+v} \varepsilon(u) + \frac{v}{1-v^2} (\nabla \cdot u) \cdot \begin{pmatrix} 1 & 0 \\ 0 & 1 \end{pmatrix} \right) \cdot \nabla (E(x, \omega_1)v(x, \omega_2)) \right) dx \\ l(v) &:= \int_{D(\omega_2)} \langle b, v(x, \omega_2) \rangle dx + \int_{\Gamma_2} \langle g, v(x, \omega_2) \rangle ds.\end{aligned}$$

*Proof.* We will use that

$$\begin{aligned}\nabla^2 u(x, \omega) &= \nabla \cdot (\nabla u(x, \omega)) = \begin{pmatrix} \frac{\partial^2 u_1}{\partial x_1^2} + \frac{\partial^2 u_1}{\partial x_2^2} \\ \frac{\partial^2 u_2}{\partial x_1^2} + \frac{\partial^2 u_2}{\partial x_2^2} \end{pmatrix} \\ \nabla(\nabla \cdot u(x, \omega)) &= \nabla \left( \frac{\partial u_1}{\partial x_1} + \frac{\partial u_2}{\partial x_2} \right) = \begin{pmatrix} \frac{\partial^2 u_1}{\partial x_1^2} + \frac{\partial^2 u_2}{\partial x_1 \partial x_2} \\ \frac{\partial^2 u_1}{\partial x_1 \partial x_2} + \frac{\partial^2 u_2}{\partial x_2^2} \end{pmatrix}\end{aligned}$$

and let  $n(x)$  denote the outward normal vector on the boundary.

$$\begin{aligned}
 & \int_{D(\omega_2)} \left\langle \frac{E(x, \omega_1)}{2(1+\nu)} \cdot \nabla^2 u(x, \omega) + \frac{E(x, \omega_1)}{2(1-\nu)} \nabla(\nabla \cdot u(x, \omega)) + b, v(x, \omega_2) \right\rangle dx = 0 \\
 & \Leftrightarrow \underbrace{\int_{D(\omega_2)} \left\langle \nabla^2 u(x, \omega), \underbrace{\frac{E(x, \omega_1)}{2(1+\nu)} v(x, \omega_2)}_{:=\tilde{v}(x, \omega_1, \omega_2)} \right\rangle dx}_{(I)} + \underbrace{\int_{D(\omega_2)} \left\langle \nabla(\nabla \cdot u(x, \omega)), \underbrace{\frac{E(x, \omega_1)}{2(1-\nu)} v(x, \omega_2)}_{:=\bar{v}(x, \omega_1, \omega_2)} \right\rangle dx}_{(II)} \\
 & = - \int_{D(\omega_2)} \langle b, v(x, \omega_2) \rangle dx
 \end{aligned}$$

$$\begin{aligned}
 (I): \quad \int_{D(\omega_2)} \langle \nabla^2 u, \tilde{v} \rangle dx &= \int_{D(\omega_2)} \left( \left( \frac{\partial^2 u_1}{\partial x_1^2} + \frac{\partial^2 u_1}{\partial x_2^2} \right) \tilde{v}_1 + \left( \frac{\partial^2 u_2}{\partial x_1^2} + \frac{\partial^2 u_2}{\partial x_2^2} \right) \tilde{v}_2 \right) dx \\
 &= \int_{D(\omega_2)} \left( \frac{\partial^2 u_1}{\partial x_1^2} \tilde{v}_1 + \frac{\partial^2 u_2}{\partial x_1^2} \tilde{v}_2 \right) dx + \int_{D(\omega_2)} \left( \frac{\partial^2 u_1}{\partial x_2^2} \tilde{v}_1 + \frac{\partial^2 u_2}{\partial x_2^2} \tilde{v}_2 \right) dx \\
 &= \int_{\Gamma(\omega_2)} \left( \frac{\partial u_1}{\partial x_1} \tilde{v}_1 + \frac{\partial u_2}{\partial x_1} \tilde{v}_2 \right) \cdot n_1 ds - \int_{D(\omega_2)} \left( \frac{\partial u_1}{\partial x_1} \frac{\partial \tilde{v}_1}{\partial x_1} + \frac{\partial u_2}{\partial x_1} \frac{\partial \tilde{v}_2}{\partial x_1} \right) dx \\
 &\quad + \int_{\Gamma(\omega_2)} \left( \frac{\partial u_1}{\partial x_2} \tilde{v}_1 + \frac{\partial u_2}{\partial x_2} \tilde{v}_2 \right) \cdot n_2 ds - \int_{D(\omega_2)} \left( \frac{\partial u_1}{\partial x_2} \frac{\partial \tilde{v}_1}{\partial x_2} + \frac{\partial u_2}{\partial x_2} \frac{\partial \tilde{v}_2}{\partial x_2} \right) dx \\
 &= - \int_{D(\omega_2)} \nabla u : \nabla \tilde{v} dx + \int_{\Gamma(\omega_2)} \left( \frac{\partial u_1}{\partial x_1} \tilde{v}_1 + \frac{\partial u_2}{\partial x_1} \tilde{v}_2, \frac{\partial u_1}{\partial x_2} \tilde{v}_1 + \frac{\partial u_2}{\partial x_2} \tilde{v}_2 \right) \cdot n ds
 \end{aligned}$$

In part (II), a convex combination is needed to match the general formulation of the partial differentials with the coefficients given in remark 6.2.2.

$$\begin{aligned}
 (II): \quad \int_{D(\omega_2)} \langle \nabla(\nabla \cdot u), \bar{v} \rangle dx &= \int_{D(\omega_2)} \left( \left( \frac{\partial^2 u_1}{\partial x_1^2} + \frac{\partial^2 u_2}{\partial x_1 \partial x_2} \right) \bar{v}_1 + \left( \frac{\partial^2 u_1}{\partial x_1 \partial x_2} + \frac{\partial^2 u_2}{\partial x_2^2} \right) \bar{v}_2 \right) dx \\
 &= \int_{D(\omega_2)} \left( \left( \frac{\partial^2 u_1}{\partial x_1^2} + \alpha \frac{\partial^2 u_2}{\partial x_1 \partial x_2} \right) \bar{v}_1 + \beta \frac{\partial^2 u_1}{\partial x_1 \partial x_2} \bar{v}_2 \right) dx \\
 &\quad + \int_{D(\omega_2)} \left( (1-\alpha) \frac{\partial^2 u_2}{\partial x_1 \partial x_2} \bar{v}_1 + \left( (1-\beta) \frac{\partial^2 u_1}{\partial x_1 \partial x_2} + \frac{\partial^2 u_2}{\partial x_2^2} \right) \bar{v}_2 \right) dx \\
 &= \int_{\Gamma(\omega_2)} \left( \left( \frac{\partial u_1}{\partial x_1} + \alpha \frac{\partial u_2}{\partial x_2} \right) \bar{v}_1 + \beta \frac{\partial u_1}{\partial x_2} \bar{v}_2 \right) n_1 ds \\
 &\quad - \int_{D(\omega_2)} \left( \left( \frac{\partial u_1}{\partial x_1} + \alpha \frac{\partial u_2}{\partial x_2} \right) \frac{\partial \bar{v}_1}{\partial x_1} + \beta \frac{\partial u_1}{\partial x_2} \frac{\partial \bar{v}_2}{\partial x_1} \right) dx \\
 &\quad + \int_{\Gamma(\omega_2)} \left( (1-\alpha) \frac{\partial u_2}{\partial x_1} \bar{v}_1 + \left( (1-\beta) \frac{\partial u_1}{\partial x_1} + \frac{\partial u_2}{\partial x_2} \right) \bar{v}_2 \right) n_2 ds \\
 &\quad - \int_{D(\omega_2)} \left( (1-\alpha) \frac{\partial u_2}{\partial x_1} \frac{\partial \bar{v}_1}{\partial x_2} + \left( (1-\beta) \frac{\partial u_1}{\partial x_1} + \frac{\partial u_2}{\partial x_2} \right) \frac{\partial \bar{v}_2}{\partial x_2} \right) dx \\
 &= \int_{\Gamma(\omega_2)} \left\langle \left( \left( \frac{\partial u_1}{\partial x_1} + \alpha \frac{\partial u_2}{\partial x_2} \right) \bar{v}_1 + \beta \frac{\partial u_1}{\partial x_2} \bar{v}_2, (1-\alpha) \frac{\partial u_2}{\partial x_1} \bar{v}_1 + \left( (1-\beta) \frac{\partial u_1}{\partial x_1} + \frac{\partial u_2}{\partial x_2} \right) \bar{v}_2 \right), n \right\rangle ds \\
 &\quad - \int_{D(\omega_2)} \left( \left( \frac{\partial u_1}{\partial x_1} + \alpha \frac{\partial u_2}{\partial x_2} \right) \frac{\partial \bar{v}_1}{\partial x_1} + \beta \frac{\partial u_1}{\partial x_2} \frac{\partial \bar{v}_2}{\partial x_1} + (1-\alpha) \frac{\partial u_2}{\partial x_1} \frac{\partial \bar{v}_1}{\partial x_2} + \left( (1-\beta) \frac{\partial u_1}{\partial x_1} + \frac{\partial u_2}{\partial x_2} \right) \frac{\partial \bar{v}_2}{\partial x_2} \right) dx
 \end{aligned}$$

For now, we investigate both of the  $\Gamma$ -integrals from (I) and (II):

$$\begin{aligned}
& \int_{\Gamma(\omega_2)} \tilde{v}^T \cdot \begin{pmatrix} \frac{\partial u_1}{\partial x_1} + \alpha \frac{\partial u_2}{\partial x_2} & (1-\alpha) \frac{\partial u_2}{\partial x_1} \\ \beta \frac{\partial u_1}{\partial x_2} & (1-\beta) \frac{\partial u_1}{\partial x_1} + \frac{\partial u_2}{\partial x_2} \end{pmatrix} \cdot n \, ds \\
& + \int_{\Gamma(\omega_2)} \tilde{v}^T \cdot \begin{pmatrix} \frac{\partial u_1}{\partial x_1} & \frac{\partial u_1}{\partial x_2} \\ \frac{\partial u_2}{\partial x_1} & \frac{\partial u_2}{\partial x_2} \end{pmatrix} \cdot n \, ds \\
& = \int_{\Gamma(\omega_2)} v(s, \omega_2)^T \cdot \left( \frac{E(s, \omega_1)}{2(1-v)} \begin{pmatrix} \frac{\partial u_1}{\partial x_1} + \alpha \frac{\partial u_2}{\partial x_2} & (1-\alpha) \frac{\partial u_2}{\partial x_1} \\ \beta \frac{\partial u_1}{\partial x_2} & (1-\beta) \frac{\partial u_1}{\partial x_1} + \frac{\partial u_2}{\partial x_2} \end{pmatrix} + \frac{E(s, \omega_1)}{2(1+v)} \begin{pmatrix} \frac{\partial u_1}{\partial x_1} & \frac{\partial u_1}{\partial x_2} \\ \frac{\partial u_2}{\partial x_1} & \frac{\partial u_2}{\partial x_2} \end{pmatrix} \right) \cdot n \, ds \\
& = \int_{\Gamma(\omega_2)} v(s, \omega_2)^T E(s, \omega_1) \begin{pmatrix} \frac{1}{1-v^2} \frac{\partial u_1}{\partial x_1} + \frac{\alpha}{2(1-v)} \frac{\partial u_2}{\partial x_2} & \frac{1-\alpha}{2(1-v)} \frac{\partial u_2}{\partial x_1} + \frac{1}{2(1+v)} \frac{\partial u_1}{\partial x_2} \\ \frac{\beta}{2(1-v)} \frac{\partial u_1}{\partial x_2} + \frac{1}{2(1+v)} \frac{\partial u_2}{\partial x_1} & \frac{1-\beta}{2(1-v)} \frac{\partial u_1}{\partial x_1} + \frac{1}{1-v^2} \frac{\partial u_2}{\partial x_2} \end{pmatrix} \cdot n \, ds \\
& = \int_{\Gamma(\omega_2)} v(s, \omega_2)^T \sigma(s, u, \omega) \cdot n \, ds
\end{aligned}$$

By coefficient comparison to the formulation in remark 6.2.2 we get  $\alpha = \frac{2v}{1+v} = 1 - \beta$  and  $\beta = \frac{1-v}{1+v} = 1 - \alpha$ . Considering the whole equation again leads to the following:

$$\begin{aligned}
& - \int_{D(\omega_2)} \nabla u : \nabla \tilde{v} \, dx \\
& - \int_{D(\omega_2)} \left( \left( \frac{\partial u_1}{\partial x_1} + \frac{2v}{1+v} \frac{\partial u_2}{\partial x_2} \right) \frac{\partial \tilde{v}_1}{\partial x_1} + \frac{1-v}{1+v} \frac{\partial u_1}{\partial x_2} \frac{\partial \tilde{v}_2}{\partial x_1} + \frac{1-v}{1+v} \frac{\partial u_2}{\partial x_1} \frac{\partial \tilde{v}_1}{\partial x_2} + \left( \frac{2v}{1+v} \frac{\partial u_1}{\partial x_1} + \frac{\partial u_2}{\partial x_2} \right) \frac{\partial \tilde{v}_2}{\partial x_2} \right) dx \\
& + \int_{\Gamma(\omega_2)} v^T \sigma(s, u, \omega) \cdot n \, ds \\
& = - \int_{D(\omega_2)} \langle b, v(x) \rangle \, dx \\
& \Leftrightarrow \int_{D(\omega_2)} \nabla u : \nabla \tilde{v} \, dx \\
& + \int_{D(\omega_2)} \left( \left( \frac{\partial u_1}{\partial x_1} + \frac{2v}{1+v} \frac{\partial u_2}{\partial x_2} \right) \frac{\partial \tilde{v}_1}{\partial x_1} + \frac{1-v}{1+v} \frac{\partial u_1}{\partial x_2} \frac{\partial \tilde{v}_2}{\partial x_1} + \frac{1-v}{1+v} \frac{\partial u_2}{\partial x_1} \frac{\partial \tilde{v}_1}{\partial x_2} + \left( \frac{2v}{1+v} \frac{\partial u_1}{\partial x_1} + \frac{\partial u_2}{\partial x_2} \right) \frac{\partial \tilde{v}_2}{\partial x_2} \right) dx \\
& = \int_{D(\omega_2)} \langle b, v(x) \rangle \, dx + \int_{\Gamma_2(\omega_2)} \langle g, v(x) \rangle \, ds
\end{aligned}$$

The left-hand side can now be transformed into a symmetric form again

$$\begin{aligned}
& \int_{D(\omega_2)} \left( \frac{1}{2(1+v)} \nabla u + \frac{1}{2(1-v)} \begin{pmatrix} \frac{\partial u_1}{\partial x_1} + \frac{2v}{1+v} \frac{\partial u_2}{\partial x_2} & \frac{1-v}{1+v} \frac{\partial u_2}{\partial x_1} \\ \frac{1-v}{1+v} \frac{\partial u_1}{\partial x_2} & \frac{2v}{1+v} \frac{\partial u_1}{\partial x_1} + \frac{\partial u_2}{\partial x_2} \end{pmatrix} \right) : (\nabla (E(x, \omega_1)v(x, \omega_2))) \, dx \\
& = \int_{D(\omega_2)} \left( \frac{1}{1-v^2} \frac{\partial u_1}{\partial x_1} + \frac{v}{1-v^2} \frac{\partial u_2}{\partial x_2} \quad \frac{1}{2(1+v)} \left( \frac{\partial u_1}{\partial x_2} + \frac{\partial u_2}{\partial x_1} \right) \right) : (\nabla (E(x, \omega_1)v(x, \omega_2))) \, dx \\
& = \int_{D(\omega_2)} \left( \frac{1}{1+v} \varepsilon(u) + \frac{v}{1-v^2} (\nabla \cdot u) \cdot \begin{pmatrix} 1 & 0 \\ 0 & 1 \end{pmatrix} \right) : (\nabla (E(x, \omega_1)v(x, \omega_2))) \, dx \\
& = \int_{D(\omega_2)} \text{Tr} \left( \left( \frac{1}{1+v} \varepsilon(u) + \frac{v}{1-v^2} (\nabla \cdot u) \cdot \begin{pmatrix} 1 & 0 \\ 0 & 1 \end{pmatrix} \right) \cdot \nabla (E(x, \omega_1)v(x, \omega_2)) \right) \, dx
\end{aligned}$$

□

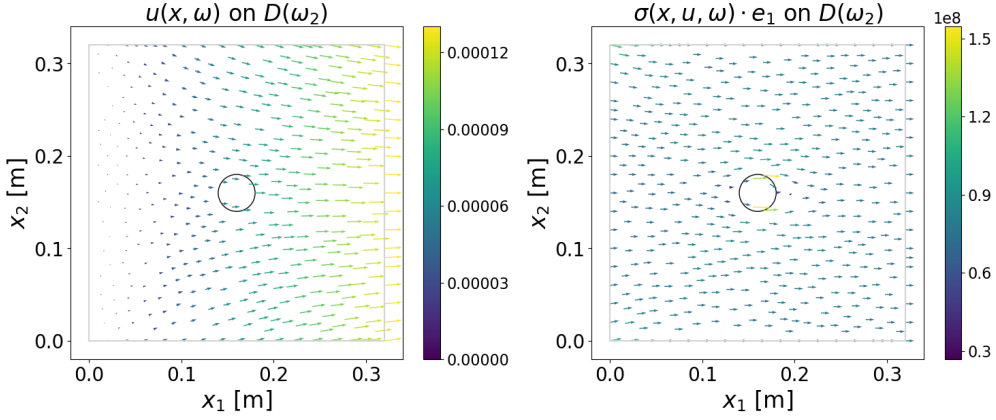


**Figure 6.4** Solution for single Sample without perturbation  $\omega_2 = (1; 0; 0)^T$  leading to  $D(\omega_2) = D_{ref}$

**Lemma 6.2.4.** *The result of applying the Domain Mapping Method on the variational problem in lemma 6.2.3 looks as follows:*

Find  $\hat{u} \in \hat{W}$  s.t.  $\hat{a}(\hat{u}, \hat{v}) = \hat{l}(\hat{v}) \forall \hat{v} \in \hat{W}$  for

$$\begin{aligned}\hat{W} &:= \{\hat{u} \in H^1(D_{ref}, \mathbb{R}^2), \hat{u}(\hat{x}, \omega) = 0 \text{ for } \hat{x} \in \Gamma_1\} \\ \hat{a}(\hat{u}, \hat{v}) &:= \int_{D_{ref}} \det(J) \cdot \text{Tr} \left( \left( \frac{1}{2(1+\nu)} (J^{-T} \cdot \nabla_{\hat{x}} \hat{u} + (J^{-T} \cdot \nabla_{\hat{x}} \hat{u})^T) \right. \right. \\ &\quad \left. \left. + \frac{\nu}{1-\nu^2} \text{Tr}(J^{-T} \cdot \nabla_{\hat{x}} \hat{u}) \cdot \begin{pmatrix} 1 & 0 \\ 0 & 1 \end{pmatrix} \right) \cdot J^{-T} \cdot \nabla_{\hat{x}} (\hat{E} \cdot \hat{v}) \right) d\hat{x} \\ \hat{l}(\hat{v}) &:= \int_{D_{ref}} \det(J(\hat{x}, \omega_2)) \langle b, \hat{v}(\hat{x}, \omega_2) \rangle d\hat{x} + \int_{\Gamma_2} \sqrt{J_{22}^2(\hat{s}, \omega_2) + J_{12}^2(\hat{s}, \omega_2)} \cdot \langle g, \hat{v}(\hat{s}, \omega_2) \rangle d\hat{s}.\end{aligned}$$

*Proof.*

$$\begin{aligned}& \int_{D_{ref}} \det(J(\hat{x}, \omega_2)) \langle b, \hat{v}(\hat{x}, \omega_2) \rangle d\hat{x} + \int_{\Gamma_2} \sqrt{J_{22}^2(\hat{s}, \omega_2) + J_{12}^2(\hat{s}, \omega_2)} \cdot \langle g, \hat{v}(\hat{s}, \omega_2) \rangle d\hat{s} \\ &= \int_{D_{ref}} \det(J(\hat{x}, \omega_2)) \langle b, \hat{v}(\hat{x}, \omega_2) \rangle d\hat{x} + \int_{\Gamma_2} \det(J(\hat{s}, \omega_2)) \cdot \|J^{-T}(\hat{s}, \omega_2) \cdot n\|_2 \cdot \langle g, \hat{v}(\hat{s}, \omega_2) \rangle d\hat{s} \\ &\stackrel{2.1.4}{=} \int_{D(\omega_2)} \langle b, v(x, \omega_2) \rangle dx + \int_{\Gamma_2(\omega_2)} \langle g, v(s, \omega_2) \rangle ds \\ &\stackrel{6.2.3}{=} \int_{D(\omega_2)} \text{Tr} \left( \left( \frac{1}{1+\nu} \varepsilon(u) + \frac{\nu}{1-\nu^2} (\nabla \cdot u) \cdot \begin{pmatrix} 1 & 0 \\ 0 & 1 \end{pmatrix} \right) \cdot \nabla(E(x, \omega_1)v(x, \omega_2)) \right) dx \\ &= \int_{D_{ref}} \det(J) \cdot \text{Tr} \left( \left( \frac{1}{2(1+\nu)} (J^{-T} \cdot \nabla_{\hat{x}} \hat{u} + (J^{-T} \cdot \nabla_{\hat{x}} \hat{u})^T) \right. \right. \\ &\quad \left. \left. + \frac{\nu}{1-\nu^2} \text{Tr}(J^{-T} \cdot \nabla_{\hat{x}} \hat{u}) \cdot \begin{pmatrix} 1 & 0 \\ 0 & 1 \end{pmatrix} \right) \cdot J^{-T} \cdot \nabla_{\hat{x}} (\hat{E} \cdot \hat{v}) \right) d\hat{x}\end{aligned}$$

where we used the connection

$$\nabla_x u(x, \omega) = J^{-T}(\hat{x}, \omega_2) \cdot \nabla_{\hat{x}} \hat{u}(\hat{x}, \omega) = \frac{1}{\det(J(\hat{x}, \omega_2))} \begin{pmatrix} J_{22} & -J_{21} \\ -J_{12} & J_{11} \end{pmatrix} \cdot \begin{pmatrix} \frac{\partial \hat{u}_1}{\partial \hat{x}_1} & \frac{\partial \hat{u}_1}{\partial \hat{x}_2} \\ \frac{\partial \hat{u}_2}{\partial \hat{x}_1} & \frac{\partial \hat{u}_2}{\partial \hat{x}_2} \end{pmatrix}. \quad (6.6)$$

□

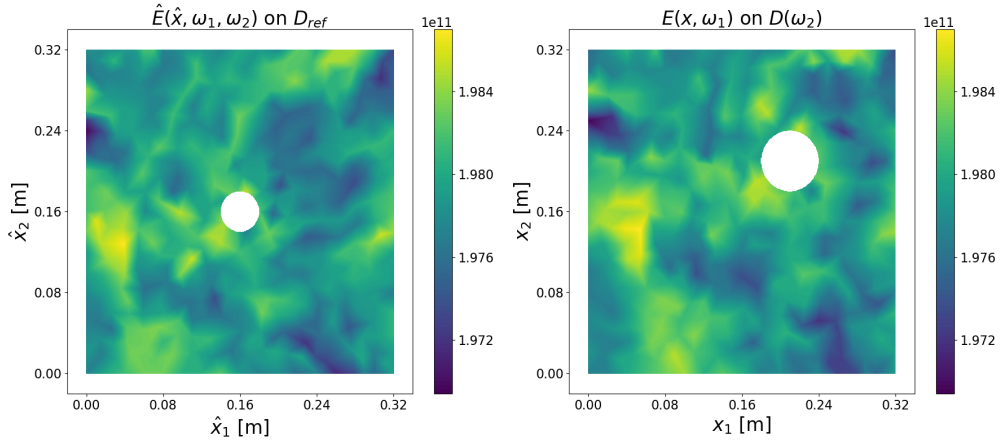


**Figure 6.5** Sample of  $\hat{E}$  and  $E$  for  $\omega_2 = (1.5; 0.05; 0.05)^T$

**Lemma 6.2.5** (Stress tensor defined on  $D_{ref}$ ). *A formulation of the stress tensor using differentials w.r.t.  $\hat{x}$  and defined on  $D_{ref}$  is given as follows:*

$$\hat{\sigma}(\hat{x}, \hat{u}, \omega) := \frac{\hat{E}(\hat{x}, \omega_1, \omega_2)}{\det(J(\hat{x}, \omega_2))} \cdot \begin{pmatrix} \frac{1}{1-\nu^2}(a \cdot \nabla_{\hat{x}} \hat{u}_1) + \nu \cdot b \cdot \nabla_{\hat{x}} \hat{u}_2 & \frac{1}{2(1+\nu)}(a \cdot \nabla_{\hat{x}} \hat{u}_2 + b \cdot \nabla_{\hat{x}} \hat{u}_1) \\ \frac{1}{2(1+\nu)}(a \cdot \nabla_{\hat{x}} \hat{u}_2 + b \cdot \nabla_{\hat{x}} \hat{u}_1) & \frac{1}{1-\nu^2}(b \cdot \nabla_{\hat{x}} \hat{u}_2 + \nu \cdot a \cdot \nabla_{\hat{x}} \hat{u}_1) \end{pmatrix}$$

where  $a := (J_{22}, -J_{21})$  and  $b := (-J_{12}, J_{11})$ .  $\nabla_{\hat{x}} \hat{u}_i$  denotes the  $i$ -th. column of  $\nabla_{\hat{x}} \hat{u}$ .

*Proof.* We use the original formulation

$$\sigma(x, u, \omega) = \begin{pmatrix} \frac{E(x, \omega_1)}{1-\nu^2} \left( \frac{\partial u_1}{\partial x_1} + \nu \frac{\partial u_2}{\partial x_2} \right) & \frac{E(x, \omega_1)}{2(1+\nu)} \left( \frac{\partial u_1}{\partial x_2} + \frac{\partial u_2}{\partial x_1} \right) \\ \frac{E(x, \omega_1)}{2(1+\nu)} \left( \frac{\partial u_1}{\partial x_2} + \frac{\partial u_2}{\partial x_1} \right) & \frac{E(x, \omega_1)}{1-\nu^2} \left( \frac{\partial u_2}{\partial x_2} + \nu \frac{\partial u_1}{\partial x_1} \right) \end{pmatrix}.$$

together with equation (6.6). □

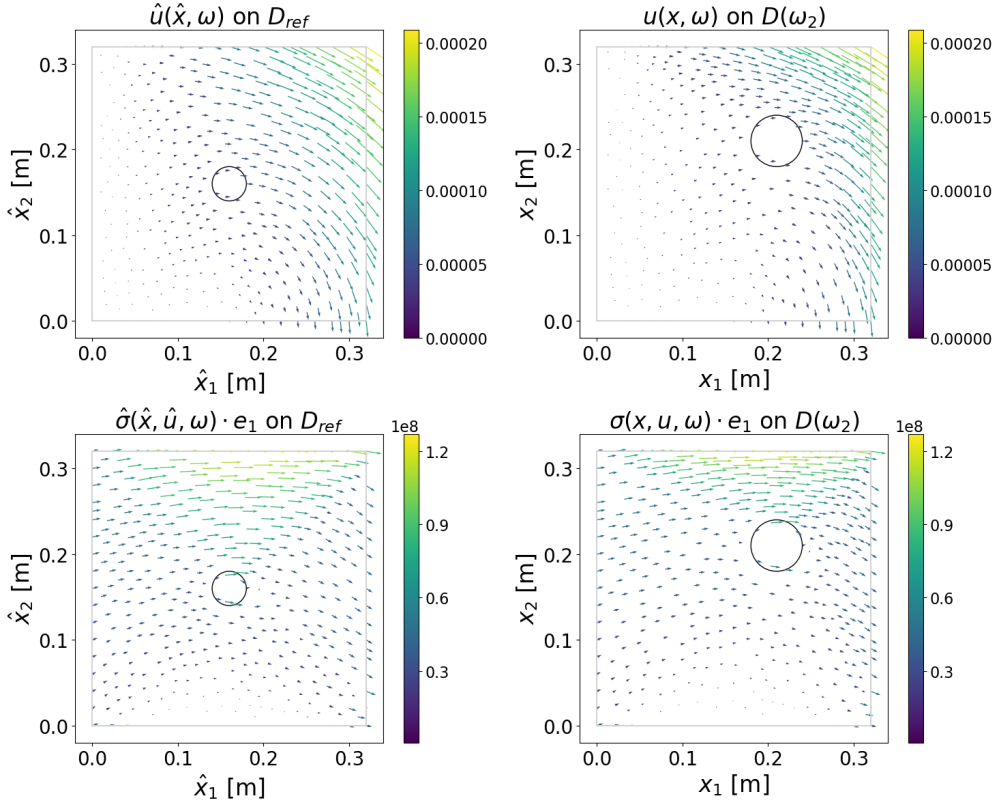


**Figure 6.6** Solution for single Sample with  $\omega_2 = (1.5; 0.05; 0.05)^T$

### 6.2.1 Pathwise Unique Existence

**Lemma 6.2.6.** *Under assumption 4.2.1, the pathwise variational formulation of lemma 6.2.4 has a unique solution  $\hat{u} \in \hat{W}$ . More precisely for a given realisation  $\omega \in \Omega$  we wish to find  $\hat{u}(\cdot, \omega) \in \hat{W}$  s.t. for  $\mathbb{P}$ -a.e.  $\omega \in \Omega$  it holds*

$$\hat{a}(\hat{u}, \hat{v}) = \hat{l}(\hat{v}) \quad \forall \hat{v} \in \hat{W}.$$

*Proof.* For the proof, we use the Lax-Milgram theorem 2.3.5 again. For this, we need some preliminary statements (partly from (4.10)):

$$\sigma_{min}^2 \leq |\det(J)| \leq \sigma_{max}^2 \quad (6.7)$$

$$A : B = \text{Tr}(A^T B) \quad (6.8)$$

$$\text{Tr}(A \cdot B) \leq \|A\|_F \cdot \|B\|_F \quad (6.9)$$

$$\frac{1}{\sigma_{max}} \leq \sigma_i(J^{-1}) \leq \frac{1}{\sigma_{min}} \Rightarrow \|J^{-1}\|_F \leq \frac{1}{\sigma_{min}} \quad (6.10)$$

We use lemma 2.2.10 for  $\hat{E}$

$$0 < \hat{E}_{min}(\omega_1) := \min_{x \in D_{ref}} \hat{E}(\hat{x}, \omega_1, \omega_2) \leq \hat{E}(\hat{x}, \omega_1, \omega_2) \leq \max_{x \in D_{ref}} \hat{E}(\hat{x}, \omega_1, \omega_2) =: \hat{E}_{max}(\omega) < \infty \quad (6.11)$$

Additionally, we use that  $q$  is fixed in the pathwise formulation, and therefore  $g$  is bounded.

1.  $\hat{l}$  bounded:  $\exists C > 0 : |\hat{l}(\hat{v})| \leq C \cdot \|\hat{v}\|_{H^1(D_{ref}, \mathbb{R}^2)}$

$$\begin{aligned}
|\hat{l}(\hat{o})| &= \left| \int_{D_{ref}} \det(J(\hat{x}, \omega_2)) \langle b, \hat{o}(\hat{x}, \omega_2) \rangle d\hat{x} + \int_{\Gamma_2} \sqrt{J_{22}^2(\hat{s}, \omega_2) + J_{12}^2(\hat{s}, \omega_2)} \cdot \langle g, \hat{o}(\hat{s}, \omega_2) \rangle d\hat{s} \right| \\
&\stackrel{(6.7)}{\leq} C_1(\omega) \cdot \left( \int_{D_{ref}} (|\hat{o}_1| + |\hat{o}_2|) d\hat{x} + \int_{\Gamma_2} (|\hat{o}_1| + |\hat{o}_2|) d\hat{x} \right) \\
&\leq C_2(\omega) \cdot \left( \|\hat{v}\|_{L^2(D_{ref}, \mathbb{R}^2)} + \|\hat{v}\|_{L^2(\Gamma_2, \mathbb{R}^2)} \right) \\
&\stackrel{2.3.7}{\leq} C_3(\omega) \cdot \|\hat{v}\|_{H^1(D_{ref}, \mathbb{R}^2)}
\end{aligned}$$

2.  $\hat{a}$  bounded:  $\exists C > 0 : |\hat{a}(\hat{u}, \hat{v})| \leq C \cdot \|\hat{u}\|_{H^1(D_{ref}, \mathbb{R}^2)} \cdot \|\hat{v}\|_{H^1(D_{ref}, \mathbb{R}^2)}$

$$\begin{aligned}
|\hat{a}(\hat{u}, \hat{v})| &= \left| \int_{D_{ref}} \det(J) \cdot \text{Tr} \left( \left( \frac{1}{2(1+\nu)} (J^{-T} \cdot \nabla_{\hat{x}} \hat{u} + (J^{-T} \cdot \nabla_{\hat{x}} \hat{u})^T) \right. \right. \right. \\
&\quad \left. \left. \left. + \frac{\nu}{1-\nu^2} \text{Tr}(J^{-T} \cdot \nabla_{\hat{x}} \hat{u}) \cdot \begin{pmatrix} 1 & 0 \\ 0 & 1 \end{pmatrix} \cdot J^{-T} \cdot \nabla_{\hat{x}} (\hat{E} \cdot \hat{o}) \right) d\hat{x} \right| \\
&\stackrel{(6.7), (6.11)}{\leq} C_1(\omega) \cdot \int_{D_{ref}} \left| \text{Tr} \left( (J^{-T} \cdot \nabla_{\hat{x}} \hat{u} + (\nabla_{\hat{x}} \hat{u})^T \cdot J^{-1}) \cdot J^{-T} \cdot \nabla_{\hat{x}} \hat{v} \right) \right. \\
&\quad \left. + \text{Tr} \left( J^{-T} \cdot \nabla_{\hat{x}} \hat{u} \right) \cdot \text{Tr} \left( J^{-T} \cdot \nabla_{\hat{x}} \hat{v} \right) \right| d\hat{x} \\
&\leq C_1(\omega) \cdot \int_{D_{ref}} \left( \left| \text{Tr} \left( J^{-T} \cdot \nabla_{\hat{x}} \hat{u} \cdot J^{-T} \cdot \nabla_{\hat{x}} \hat{v} \right) \right| + \left| \text{Tr} \left( (\nabla_{\hat{x}} \hat{u})^T \cdot J^{-1} \cdot J^{-T} \cdot \nabla_{\hat{x}} \hat{v} \right) \right| \right. \\
&\quad \left. + \left| \text{Tr} \left( J^{-T} \cdot \nabla_{\hat{x}} \hat{u} \right) \cdot \text{Tr} \left( J^{-T} \cdot \nabla_{\hat{x}} \hat{v} \right) \right| \right) d\hat{x} \\
&\stackrel{(6.9)}{\leq} C_1(\omega) \cdot \int_{D_{ref}} 3 \cdot \|J^{-T} \cdot \nabla_{\hat{x}} \hat{u}\|_F \cdot \|J^{-T} \cdot \nabla_{\hat{x}} \hat{v}\|_F d\hat{x} \\
&\stackrel{(6.10)}{\leq} C_2(\omega) \cdot \int_{D_{ref}} \|\nabla_{\hat{x}} \hat{u}\|_F \cdot \|\nabla_{\hat{x}} \hat{v}\|_F d\hat{x} \\
&\leq C_2(\omega) \cdot \|\nabla_{\hat{x}} \hat{u}\|_{L^2(D_{ref}, \mathbb{R}^{2 \times 2})} \cdot \|\nabla_{\hat{x}} \hat{v}\|_{L^2(D_{ref}, \mathbb{R}^{2 \times 2})} \\
&\leq C_2(\omega) \cdot \|\nabla_{\hat{x}} \hat{u}\|_{H^1(D_{ref}, \mathbb{R}^2)} \cdot \|\nabla_{\hat{x}} \hat{v}\|_{H^1(D_{ref}, \mathbb{R}^2)}
\end{aligned}$$

3.  $\hat{a}$  coercive:  $\exists C > 0 : \hat{a}(\hat{u}, \hat{u}) \geq C \cdot \|\hat{u}\|_{H^1(D_{ref}, \mathbb{R}^2)}^2 \forall \hat{u} \in H^1(D_{ref}, \mathbb{R}^2)$

For this proof we will need

$$\int_{D(\omega_2)} (\varepsilon(u) : \varepsilon(u)) dx \geq C \cdot \|u\|_{H^1(D(\omega), \mathbb{R}^2)}^2 \tag{6.12}$$

for  $u \in H^1(D(\omega), \mathbb{R}^2)$ . The inequality follows from the second Korn's inequality as explained on p. 104 (equation 5.5) of [Joh12]. Since [Joh12] does not make any assumptions about the regularity of the boundary, which seems surprising at first glance, we refer to [Nit81] and [Fic73] for more details. In [Nit81], it is explained how to obtain the inequality for certain non-smooth boundaries, especially proven for two-dimensional polygonal domains. This case can be applied to our domain samples, as the proof works equivalently with the form of our domain samples.

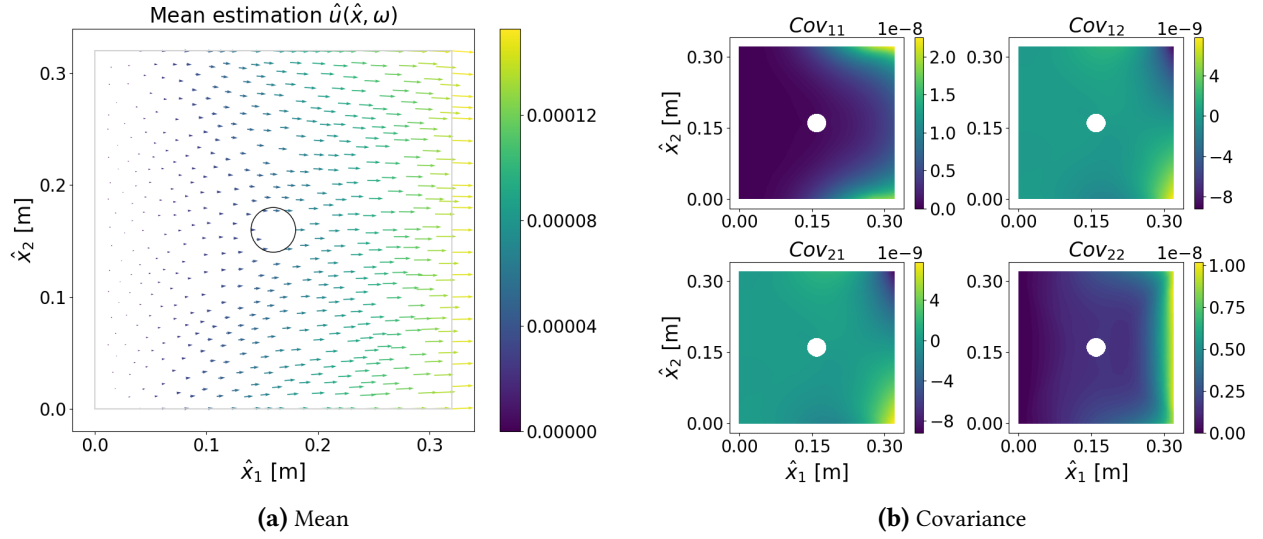
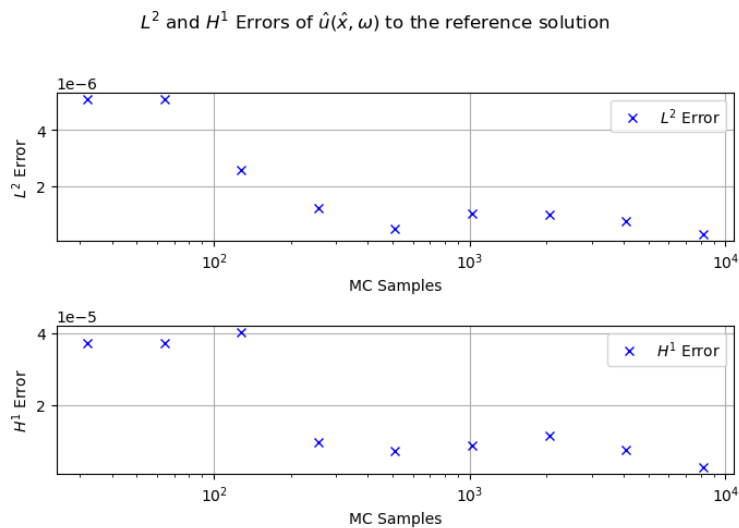
$$\begin{aligned}
& \hat{a}(\hat{u}, \hat{u}) \\
&= \int_{D_{ref}} \det(J) \cdot \text{Tr} \left( \left( \frac{1}{2(1+\nu)} (J^{-T} \cdot \nabla_{\hat{x}} \hat{u} + (J^{-T} \cdot \nabla_{\hat{x}} \hat{u})^T) \right. \right. \\
&\quad \left. \left. + \frac{\nu}{1-\nu^2} \text{Tr} (J^{-T} \cdot \nabla_{\hat{x}} \hat{u}) \cdot \begin{pmatrix} 1 & 0 \\ 0 & 1 \end{pmatrix} \right) \cdot J^{-T} \cdot \nabla_{\hat{x}} (\hat{E} \cdot \hat{u}) \right) d\hat{x} \\
&\stackrel{(6.11)}{\geq} \int_{D_{ref}} \det(J) \cdot \text{Tr} \left( \left( \frac{1}{2(1+\nu)} \left( J^{-T} \cdot \nabla_{\hat{x}} \hat{u} + (J^{-T} \cdot \nabla_{\hat{x}} \hat{u})^T \right) \right. \right. \\
&\quad \left. \left. + \hat{E}_{min}(\omega) \cdot \frac{\nu}{1-\nu^2} \text{Tr} (J^{-T} \cdot \nabla_{\hat{x}} \hat{u}) \cdot \begin{pmatrix} 1 & 0 \\ 0 & 1 \end{pmatrix} \right) \cdot J^{-T} \cdot \nabla_{\hat{x}} \hat{u} \right) d\hat{x} \\
&\geq C_1(\omega) \cdot \int_{D_{ref}} \det(J) \cdot \text{Tr} \left( \left( \frac{1}{2} \left( J^{-T} \cdot \nabla_{\hat{x}} \hat{u} + (J^{-T} \cdot \nabla_{\hat{x}} \hat{u})^T \right) + \text{Tr} (J^{-T} \cdot \nabla_{\hat{x}} \hat{u}) \cdot \begin{pmatrix} 1 & 0 \\ 0 & 1 \end{pmatrix} \right) \cdot J^{-T} \cdot \nabla_{\hat{x}} \hat{u} \right) d\hat{x} \\
&= C_1(\omega) \cdot \int_{D_{ref}} \left( \det(J) \left( \text{Tr} \left( \frac{1}{2} \left( J^{-T} \cdot \nabla_{\hat{x}} \hat{u} + (J^{-T} \cdot \nabla_{\hat{x}} \hat{u})^T \right) \cdot J^{-T} \cdot \nabla_{\hat{x}} \hat{u} \right) + (\text{Tr} (J^{-T} \cdot \nabla_{\hat{x}} \hat{u}))^2 \right) \right) d\hat{x} \\
&= C_1(\omega) \cdot \int_{D(\omega_2)} \left( \text{Tr} \left( \frac{1}{2} (\nabla_x u + \nabla_x u^T) \cdot \nabla_x u \right) + \underbrace{(\text{Tr} (\nabla_x u))^2}_{\geq 0} \right) dx \\
&\geq C_1(\omega) \cdot \int_{D(\omega_2)} (\varepsilon(u) : \varepsilon(u)) dx \\
&\stackrel{(6.12)}{\geq} C_2(\omega) \cdot \int_{D(\omega_2)} \|\nabla u\|_F^2 dx \\
&= C_2(\omega) \cdot \int_{D_{ref}} \det(J) \cdot \|J^{-T} \nabla_{\hat{x}} \hat{u}\|_F^2 d\hat{x} \\
&\stackrel{(6.7)}{\geq} C_3(\omega) \cdot \int_{D_{ref}} \|\nabla_{\hat{x}} \hat{u}\|_F^2 d\hat{x} \\
&\stackrel{2.3.6}{\geq} C_4(\omega) \cdot \|\hat{u}\|_{H^1(D_{ref}, \mathbb{R}^2)}^2
\end{aligned}$$

□

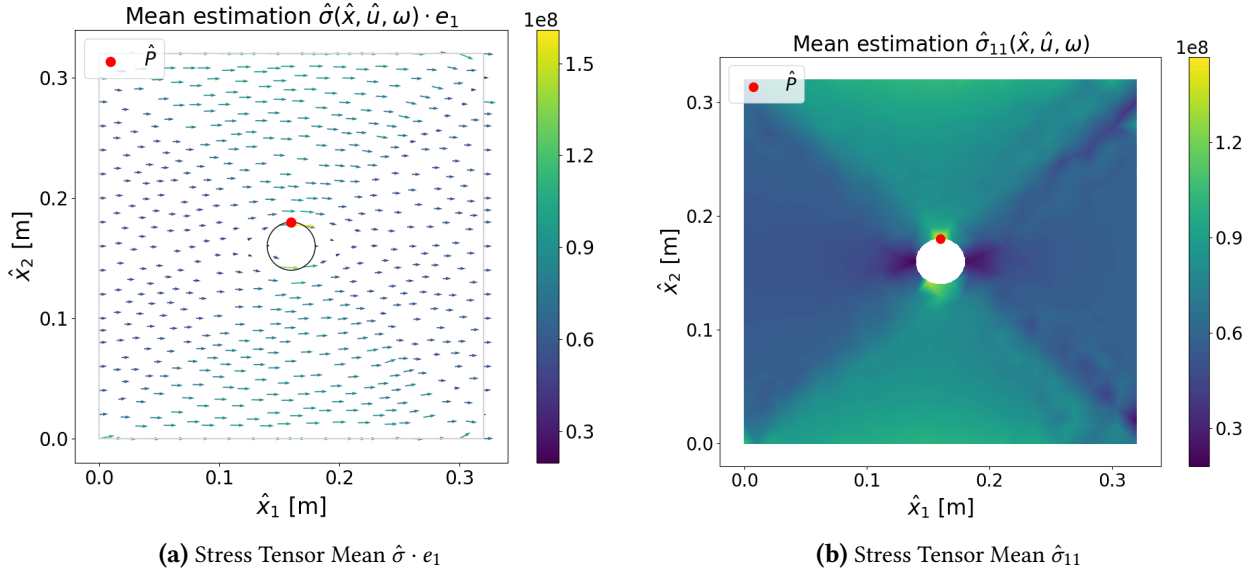
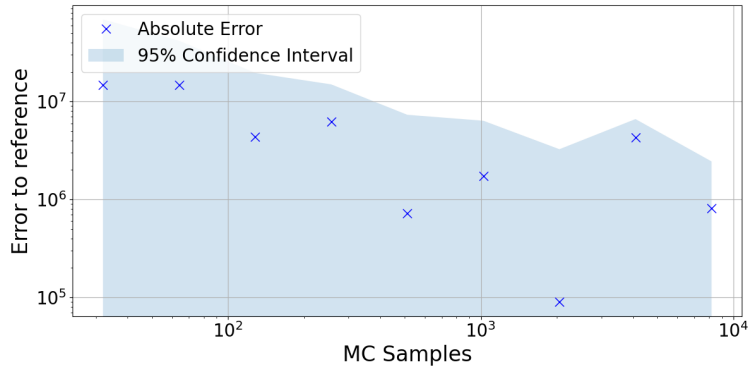
### 6.3 Computational Experiments and Results

The Monte Carlo analysis of the steel plate model was carried out with a FEniCS mesh resolution FEM 18 ( $M = 542$ ,  $h = 1/24$ ), whereby the KLE of the random field E was also discretized with the same mesh resolution. Two parameters are interesting for the evaluation: On the one hand, the entire solution, i.e. the displacement function  $\hat{u}$  on the reference domain  $D_{ref}$  and, on the other hand, the stress tensor's first component  $\hat{\sigma}_{1,1}$  at the point above the circle  $\hat{P} = (0.16, 0.18)^T$ .

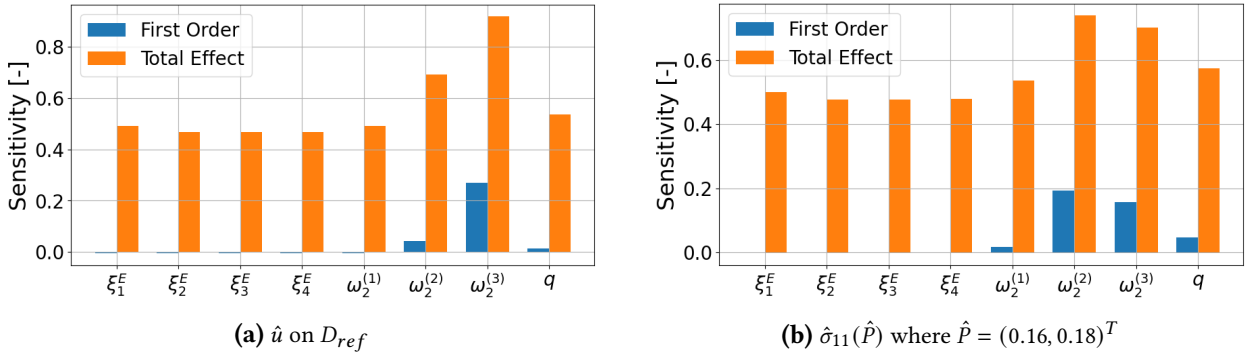
The reference solution uses the same grid parameters in this evaluation and contains  $N = 20000$  samples.

Figure 6.7 MC Analysis of Displacement  $\hat{u}$ Figure 6.8 MC Error Analysis of Displacement  $\hat{u}$ 

As expected, the average displacement  $\hat{u}$  is highest at the right boundary. No anomalies can be seen at the center circle. The covariance shows certain asymmetries, as the functions  $\text{Cov}_{11}$  and  $\text{Cov}_{22}$  differ from each other. In addition, the functions  $\text{Cov}_{12}$  and  $\text{Cov}_{21}$  are each horizontally mirrored and have a negative covariance in the upper right corner and a positive covariance in the lower right corner. Convergence can be derived from the Monte Carlo analysis of the  $L^2$ - and  $H^1$ -error. Nevertheless, the error does not decrease for each Monte Carlo solution with more samples. With the size of the errors around  $10^{-5}$ , however, the approximation is already quite good.

**Figure 6.9** MC Analysis of Stress Tensor Mean  $\hat{\sigma}$ **Figure 6.10** MC Analysis of Stress Tensor  $\hat{\sigma}_{11}$  Convergence in  $\hat{P} = (0.16, 0.18)^T$ 

Looking at the quantity of interest  $\hat{\sigma}_{11}$ , we see the largest values at the points directly above and below the center circle. The stress on the material is therefore highest there, and the steel plate is most likely to crack at that point first in a tensile stress test of the right boundary. The apparent deviations from horizontal symmetry can probably be explained by the discretization of the grid. We can also see the influence of the perturbation function, which depends on the angles of the points from the center, as can be seen in the four differently colored areas. Since the log-log plot shows a roughly linear decrease in the error, we conclude that the Monte Carlo analysis of the quantity of interest  $\hat{\sigma}_{11}(\hat{P})$  converges algebraically. The Sobol' index analysis also addresses the two quantities of interest  $\hat{u}$  and  $\hat{\sigma}_{11}(\hat{P})$ . The samples were calculated with a FEniCS mesh resolution 14 ( $M = 333, h = 1/11$ ). For the analysis,  $N = 12000$  samples were used. For calculating the effects, the algorithm for functional-valued model output with multidimensional range 3.4.3 was used for  $\hat{u}$ , and the single-valued output was used for  $\hat{\sigma}_{11}(\hat{P})$  3.4.1.

**Figure 6.11** Sobol' Indices for the two different Quantities of Interest

The corresponding eigenvalues of the KLE of the random field  $\hat{E}$  for the FEniCS mesh resolution 14 are the following:

Random Variable of KLE of $\hat{E}$	Eigenvalue $\gamma_m^E$
$\xi_1^E$	$5 \cdot 10^{-5}$
$\xi_2^E$	$4.51 \cdot 10^{-5}$
$\xi_3^E$	$4.508 \cdot 10^{-5}$
$\xi_4^E$	$4.01 \cdot 10^{-5}$

**Table 6.1** Eigenvalues of KLE of the Random Field  $\hat{E}$ 

For the interpretation of both results, recall the definition of the perturbation function in (6.4) and (6.5). It becomes clear that the vertical shift of the position of the circle, represented by  $\omega_2^{(3)}$ , has the greatest effect on the displacement function  $\hat{u}$  on the entire reference domain  $D_{ref}$ . Next comes the horizontal shift in the position of the circle  $\omega_2^{(2)}$  and the tensile force  $q$  on the right-hand side of the steel plate with a small, but still visible, direct contribution measured by the first order index. The radius shift and the first four random variables of the KLE of  $\hat{E}$  seem to have almost no direct contribution to the variance of the quantity of interest.

Next, the results using the quantity of interest  $\hat{\sigma}_{11}(\hat{P})$  are analyzed. The point  $\hat{P}$  reflects (together with the horizontally mirrored point directly below the circle) the maximum of the function  $\hat{\sigma}_{11}$  (compare figure 6.9). Physically, it means that the steel plate is most likely to crack at these points. The horizontal shift of the position of the circle  $\omega_2^{(2)}$  has the greatest influence on the variance of this quantity of interest. This is closely followed by the vertical shift of the position of the circle  $\omega_2^{(3)}$ . The tensile force  $q$  has a greater influence on  $\sigma_{11}(\hat{P})$  than on the quantity of interest  $\hat{u}$ . Furthermore, the circle radius and the factors of  $\hat{E}$  have almost no direct contribution.

The total effect, measuring the total contribution including all interactions with other random variables, is always greater than 0.5 in both cases. The rank of contribution stays the same in the first order effect and the total effect.

## 6.4 Model Extension: Random Field Perturbation for the Circle

To extend the steel plate problem, we would now like to include a familiar component from the previous chapters 4 and 5. The reference circle is now perturbed using a random field as in previous sections. In order to achieve a visible, plausible displacement of the circle, which could model a kind of stochastic punching in a steel plate and is adapted to the dimension of the steel plate, the covariance matrix from [HPS16] is equipped with two factors  $\alpha$  and  $\beta$ .

$$\begin{aligned} V(\hat{x}, \omega_2) &= \mu(\hat{x}) + \sum_{m=1}^M \sqrt{\gamma_m} \cdot g_m(\hat{x}) \cdot \xi_m(\omega_2) & \xi_m(\omega_2) &\sim U(-\sqrt{3}, \sqrt{3}) \\ \mathbb{E}[V](\hat{x}) &= \mu(\hat{x}) = \hat{x} \\ \text{Cov}[V](\hat{x}, \hat{y}) &= \alpha \cdot \frac{1}{100} \begin{pmatrix} 5 \cdot \exp(-\beta \cdot 4 \cdot \|\hat{x} - \hat{y}\|_2^2) & \exp(-0.1 \cdot \|2\hat{x} - \hat{y}\|_2^2) \\ \exp(-0.1 \cdot \|\hat{x} - 2\hat{y}\|_2^2) & 5 \cdot \exp(-\beta \cdot \|\hat{x} - \hat{y}\|_2^2) \end{pmatrix} & | & \alpha := 10^3, \beta := 10 \end{aligned}$$

$V$  is defined on the reference disk  $\hat{x} \in \left\{x \in \mathbb{R}^2 \mid \left\|x - \begin{pmatrix} 0.16 \\ 0.16 \end{pmatrix}\right\|_2 \leq 0.02\right\}$ . Equivalently to chapter 4, the random field  $V$  was calculated on the entire reference disk. However, since only values on the inner edge of the steel plate are required, the resulting random field limited to this definition area is denoted with  $\bar{V} := V|_{\Gamma_3}$  where  $\Gamma_3 := \left\{x \in \mathbb{R}^2 \mid \left\|x - \begin{pmatrix} 0.16 \\ 0.16 \end{pmatrix}\right\|_2 = 0.02\right\}$ . This change to the model of random radius and position of the circular hole shows how the Domain Mapping Method can be modeled with a completely arbitrary perturbation function if only the perturbation function can be evaluated on the edge of the circle  $\Gamma_3$ . Furthermore, the points on the outer edge are left fixed, and the perturbation function for the points in between is calculated by a linear combination. The following figure 6.12 shows a sample of a FEM grid shifted in this way.

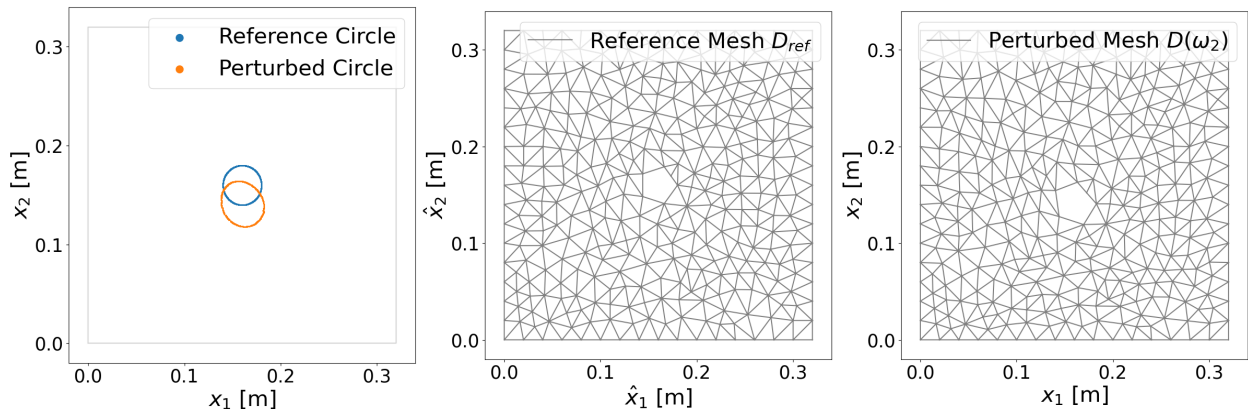
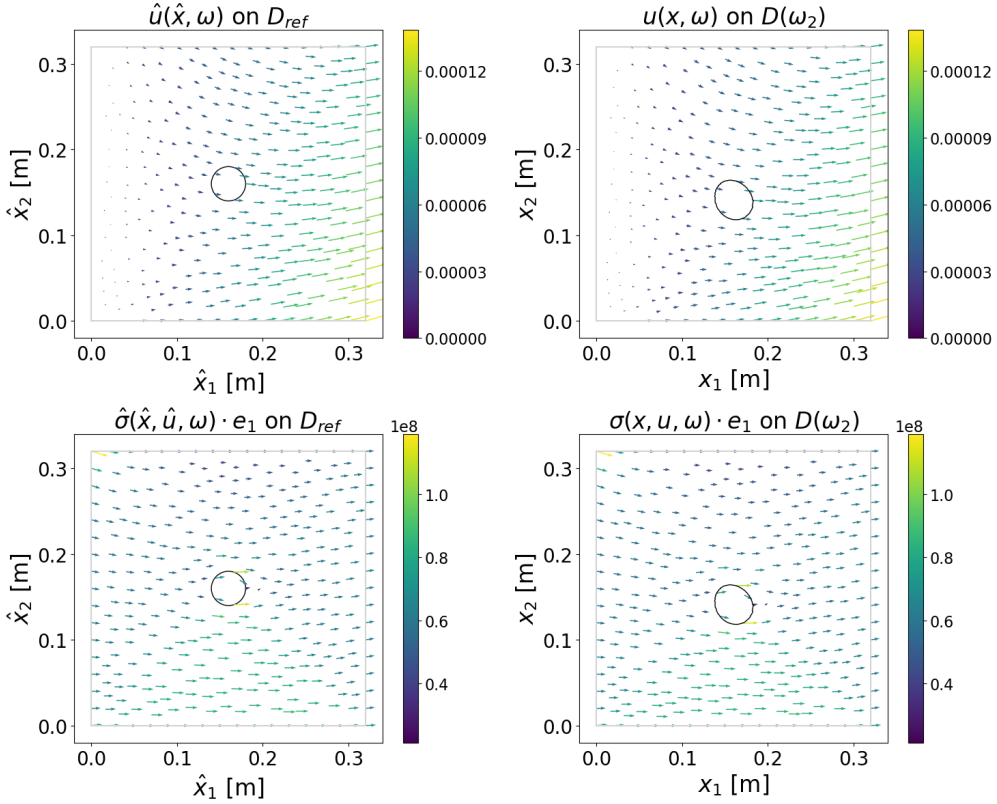


Figure 6.12 Sample for perturbed Mesh with Circle Random Field



**Figure 6.13** Solution Sample with Circle Random Field

Since a Monte Carlo analysis would not provide any new interesting results, the numerical analysis of this model extension is concentrated on the Sobol' index calculation, which can be compared with the model with a random circle radius.

An important property must be checked at this point. The maximum perturbation should not move the circle beyond the outer edge of the steel plate. To do this, we use the form of the truncated KLE and calculate the maximum perturbation for the mesh in the resolution, which we will use for the upcoming Sobol' index calculation.

$$\begin{aligned}
 \|\bar{V}(\hat{x}, \omega_2) - \hat{x}\|_\infty &= \left\| \sum_{m=1}^M \sqrt{\gamma_m} \cdot \left( \frac{\sum_{j=1}^N a_{j,m}^{(1)} \cdot \phi_j(\hat{x})}{\sum_{j=1}^N a_{j,m}^{(2)} \cdot \phi_j(\hat{x})} \right) \cdot \xi_m(\omega_2) \right\|_\infty \\
 &= \max \left\{ \left| \sum_{m=1}^M \sqrt{\gamma_m} \cdot \left( \sum_{j=1}^N a_{j,m}^{(1)} \cdot \phi_j(\hat{x}) \right) \cdot \xi_m(\omega_2) \right|, \left| \sum_{m=1}^M \sqrt{\gamma_m} \cdot \left( \sum_{j=1}^N a_{j,m}^{(2)} \cdot \phi_j(\hat{x}) \right) \cdot \xi_m(\omega_2) \right| \right\} \\
 &\leq \max \left\{ \sqrt{3} \cdot \sum_{m=1}^M \sqrt{\gamma_m} \cdot \max_{j=1,\dots,N} \{|a_{j,m}^{(1)}|\}, \sqrt{3} \cdot \sum_{m=1}^M \sqrt{\gamma_m} \cdot \max_{j=1,\dots,N} \{|a_{j,m}^{(2)}|\} \right\} \\
 &= \sqrt{3} \cdot \sum_{m=1}^M \sqrt{\gamma_m} \cdot \max_{j=1,\dots,N} \{|a_{j,m}^{(1)}|, |a_{j,m}^{(2)}|\}
 \end{aligned}$$

Due to the considerable calculation effort, the following parameters were used for the Sobol' index calculation: for both of the random fields  $E$  and  $V$ , the FEniCS mesh resolution KLE 6 ( $h = 1/8, M = 109$ ) was used and the FEniCS mesh resolution FEM 14 ( $h = 1/24$ ). These led to a maximum perturbation of 0.075, which is smaller than 0.14, which is the distance to the outer edge. Therefore, the truncated KLE can be used without any problems and does not have to be shortened.

The mesh resolution KLE is kept the same for both random fields  $E$  and  $\bar{V}$  so that the influence of the first random variable can be compared with each other, since the total number of random variables in the truncated KLE matches. Another approach that compares the total influence of the set of all random variables

in the respective random fields would also be possible. However, since all previous Sobol' index analyses were concerned with the influence of individual random variables, this variant is chosen.

The Sobol' indices were once again calculated for the entire displacement function  $\hat{u}$  and, on the other hand, for the first entry of the stress tensor  $\hat{\sigma}_{11}(\hat{P})$  at the point  $\hat{P} = (0.16, 0.18)^T$ . For this purpose,  $N = 12000$  samples were calculated.

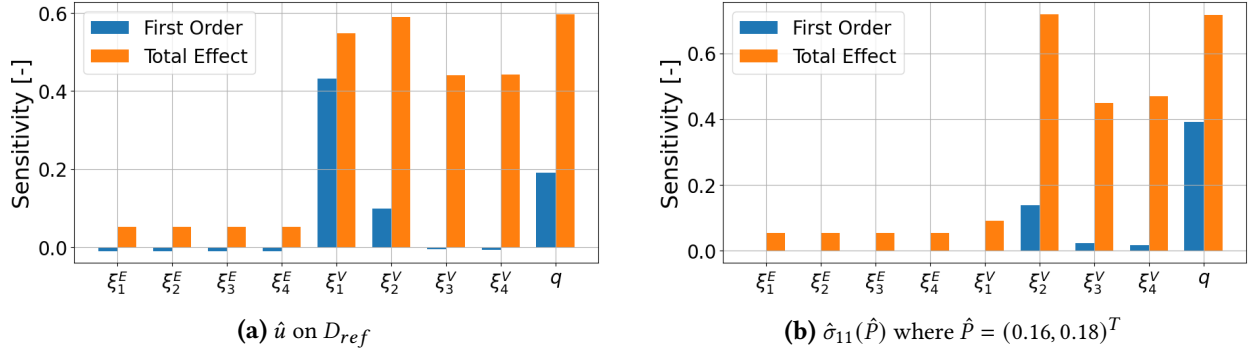


**Figure 6.14** Sobol' Indices for the two different Quantities of Interest

To interpret the result, let's take a look at the associated eigenvalues and eigenfunctions of the random variables in the KLE of  $V$  and  $\hat{E}$ .

Random Variable of KLE of $V$	Eigenvalue $\gamma_m^V$
$\xi_1^V$	0.07344
$\xi_2^V$	0.04875
$\xi_3^V$	0.0004695
$\xi_4^V$	0.0004692

Random Variable of KLE of $\hat{E}$	Eigenvalue $\gamma_m^E$
$\xi_1^E$	$5.03 \cdot 10^{-5}$
$\xi_2^E$	$4.5 \cdot 10^{-5}$
$\xi_3^E$	$4.46 \cdot 10^{-5}$
$\xi_4^E$	$3.93 \cdot 10^{-5}$

**Table 6.2** Eigenvalues of KLE of the Random Fields  $V$  and  $\hat{E}$

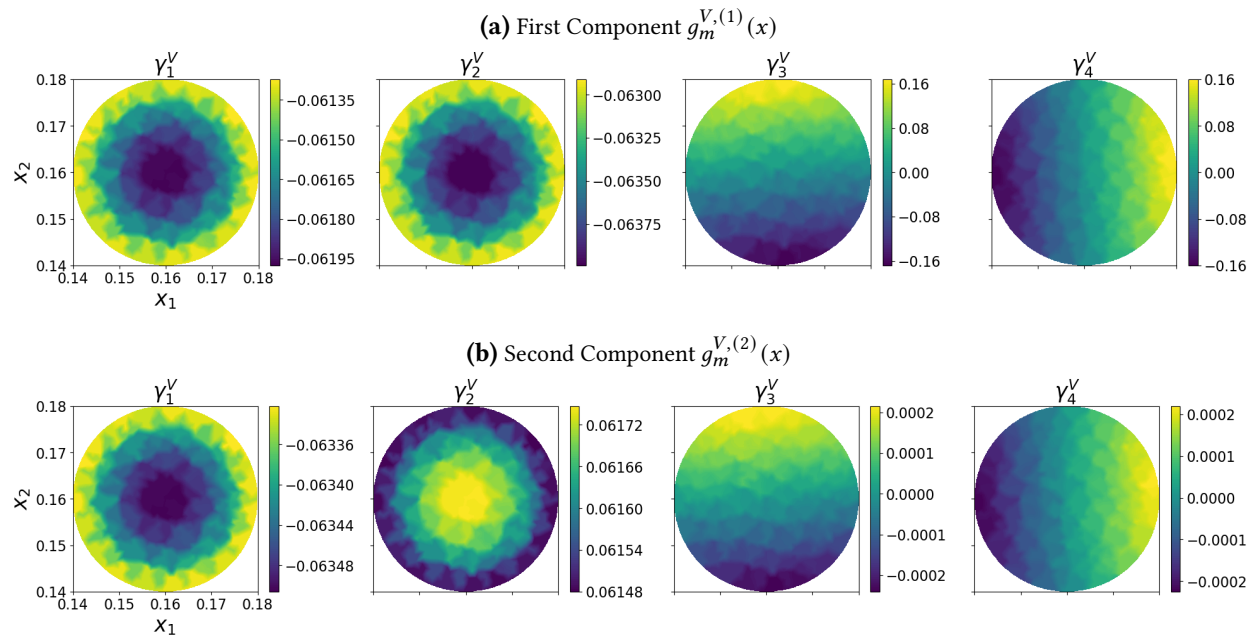


**Figure 6.15** Eigenfunctions  $g_m^V(x)$  of KLE of the Random Field  $V$

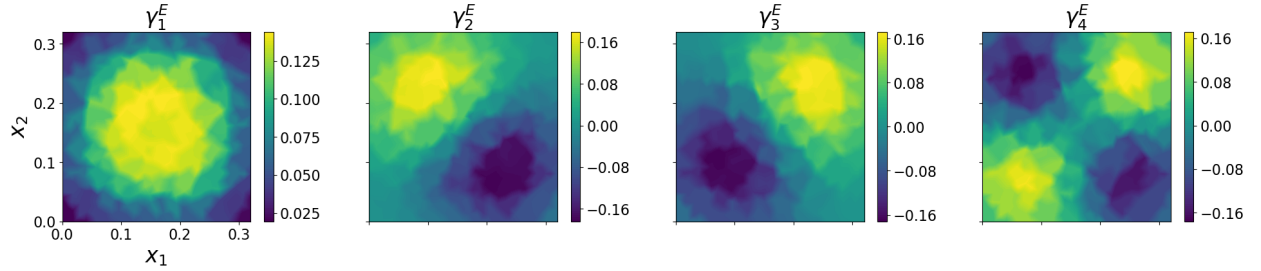


**Figure 6.16** Eigenfunctions  $g_m^E(x)$  of KLE of the Random Field  $\hat{E}$

Interestingly, the results differ with regard to the two different quantities of interest. For the quantity of interest  $\hat{u}$  on the entire definition range  $D_{ref}$ ,  $\xi_1^V$  has the largest first order effect and  $q$  the second largest. However, if we look at the total effect, these two roles switch. This is followed by  $\xi_3^V$ , and all other random variables appear to have virtually no individual contribution. The total effect of the random variables of the Young's modulus  $\hat{E}$  also appears to be very small. Looking at  $\sigma_{11}(\hat{P})$ , the tensile force  $q$  has the largest individual and total effect. In addition,  $\xi_2^V$  has by far the largest effect from the four candidates of the random field  $V$ .  $\xi_1^V$  on the other hand, which belongs to the largest eigenvalue of  $V$  has almost no contribution to the variance of parameter  $\sigma_{11}(\hat{P})$ , which is a big difference to the contribution to the other quantity of interest  $\hat{u}$ . Apparently, the geometry of the eigenfunction  $g_1^V$  leads to a great influence of  $\xi_1^V$  on the overall solution of the PDE  $\hat{u}$ , but almost no influence on the punctual evaluation of  $\hat{\sigma}_{11}$  at the point directly above the circle.

## 7 Conclusion

The work has mainly revolved around the investigation and application of the Domain Mapping Method. This was successfully done using the three examples of the variants of the Poisson equation and the elasticity equation, and typical challenges were highlighted. For example, the difference between Dirichlet boundary conditions and Neumann boundary conditions leads to a substitution on the boundary integral and can also make it more difficult to prove the existence of a unique solution, as it is a different function space. When calculating the variational formulation of the elasticity equation in the steel plate problem, the challenge was to find the correct formulation that matches the form of the stress tensor in the source [UC20]. Since this formulation was not written down in the source, this led to a rather intensive calculation. Together with the application of the Domain Mapping Method, a form of the variational formulation emerges, which at first glance has little to do with the original beautiful and symmetric form of the elasticity equation. In the proof of the existence of the unique pathwise solution of the elasticity problem 6.2.6, the equation could be reduced to a symmetric problem in the decisive part of the coercivity and solved with Korn's inequality.

Furthermore, different methods for modeling the random fields and the geometric perturbation functions were introduced. Approximation tricks were used here, such as in the calculation of the two-dimensional KLE in subsection 4.3.1. On the other hand, however, the limitations of the implementation in Python quickly became apparent, for example, the non-existence of three-dimensional differentiable basis functions in subsection 4.3.2, leading to the approximation of an alternative representation of the Jacobian. With regard to the Sensitivity Analysis, the respective quantities of interest were successfully analyzed using Monte Carlo methods and the Sobol' indices. First, a Sobol' index had to be designed for a model with functional-valued output 3.3.7. An efficient algorithm was selected for the calculation in section 3.4 and implemented. The results allow us to compare the different sources of uncertainty in the models. It is interesting to see what influence the modeling of the geometric mapping, in which one has a lot of freedom in the description of a real inventory, has on the model outcome. For example, in the steel plate model, we see that the two modeling approaches have a significant and different impact on the Sobol' indices. We also see that the choice of the quantity of interest leads to different results, especially in the model describing the perturbation using a random field.

The work was mainly limited by numerical problems in the implementation. On the one hand, the accuracy of the analyses was very limited throughout, as the numerical solution of the differential equations led to computationally expensive model evaluations, but for a Sobol' analysis, many samples are necessary for meaningful results. A reasonable convergence of the Sobol' indices was only seen after many samples, and then very small first order indices were still partly in the negative range, which suggests approximation errors. On the other hand, the correct mathematical description was not always possible in the implementation. For example, the use of constant basis functions is suboptimal, and the simplifications through approximations such as the Galerkin-projection in subsection 4.3.2 were accepted as rough approximations in order to make the code faster. Fortunately, however, I was also able to use computing units from the Leibniz Supercomputing Centre for the numerical simulations, which expanded my possibilities for more accurate results.

Alternatively, implementations in Matlab, Julia, or C might have led to more accurate results, but it can be said that FEniCS support for Python is already well developed, and with other tech stacks, one might have to accept a more error-prone and, therefore slower implementation in order to obtain better results in the end. Especially when considering many different models, the implementation time and the traceability of the code should of course not be neglected.

Now, we come to an outlook on the topics discussed. For selected problems from any application area, the application of the Domain Mapping Method could already provide insightful results about the sources of

uncertainty. However, modeling the perturbation function as realistically as possible (be it through random fields or just individual random variables) is the crucial point. As described in the introduction, the necessary mathematical treatment of the Domain Mapping Method and the calculation of the quantities of interest are currently being investigated for many different differential equations. A direct comparison of different modeling methods would be useful here, and theoretically, a Sensitivity Analysis for the effect of the parameters in the description of the geometric perturbation function on the results of the Sobol' indices could provide interesting results. Of course, this nested Sensitivity Analysis would reach numerical limits extremely quickly with the technical state-of-the-art currently possible. With regard to the numerical effort, an alternative approach would be to analyze other calculation variants for the random field, such as Circular Embedding or the Turning Bands Method [LPS14].

In the case of several random fields, as in the example in the last model extension in the steel plate model, the total influence of all random variables of the associated truncated KLE could be analyzed and not only of the individual random variables in relation to each other. This could also have a manageable computational effort in models with many different random fields as sources and generally would certainly be very exciting to consider on a meta-level if entire random fields were weighed against each other instead of individual random variables.

Future work on similar topics could also include models with dependent random variables. A Sensitivity Analysis could then consist of calculating the Shapley Effects of the various random sources.

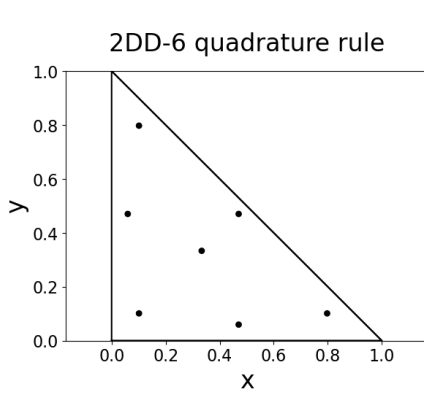
Finally, it is safe to say that the Domain Mapping Method has a wide range of applications and extensions and is well-suited for the description of uncertain geometric perturbations. Together with the steadily growing interest in Uncertainty Quantification of mathematical modeling of real processes, this thesis is located exactly in the interplay between these two relevant and promising fields of research.

# A Appendix

## A.1 Theory

**Lemma A.1.1** (Numerical quadrature for triangles). *A general quadrature rule for triangles can be found on page 313 of [JL01].*

*For approximating polynomials up to order five exactly, the following integration points and weights can be applied for the unit triangle:*



	Coordinates	Weight
2DD-6	$\frac{6-\sqrt{15}}{21}$	$\frac{6-\sqrt{15}}{21} \cdot \frac{155-\sqrt{15}}{2400}$
	$\frac{9+2\sqrt{15}}{21}$	$\frac{6-\sqrt{15}}{21} \cdot \frac{155-\sqrt{15}}{2400}$
	$\frac{6-\sqrt{15}}{21}$	$\frac{9+2\sqrt{15}}{21} \cdot \frac{155-\sqrt{15}}{2400}$
	$\frac{6+\sqrt{15}}{21}$	$\frac{9-2\sqrt{15}}{21} \cdot \frac{155+\sqrt{15}}{2400}$
	$\frac{6+\sqrt{15}}{21}$	$\frac{6+\sqrt{15}}{21} \cdot \frac{155+\sqrt{15}}{2400}$
	$\frac{9-2\sqrt{15}}{21}$	$\frac{6+\sqrt{15}}{21} \cdot \frac{155+\sqrt{15}}{2400}$
	$\frac{1}{3}$	$\frac{1}{3} \cdot \frac{9}{80}$

To apply the numerical quadrature to an arbitrary triangle, one has to look for the affine transformation  $T : U \rightarrow V$  where  $U$  is the unit triangle and  $V$  is the arbitrary triangle with vertices  $(x_1, y_1), (x_2, y_2), (x_3, y_3)$ . It holds:

$$T(x, y) = A \begin{pmatrix} x \\ y \end{pmatrix} + b, \quad A = \begin{pmatrix} x_2 - x_1 & x_3 - x_1 \\ y_2 - y_1 & y_3 - y_1 \end{pmatrix}, \quad b = \begin{pmatrix} x_1 \\ y_1 \end{pmatrix}$$

Now the coordinates of the quadrature rule are transformed, and the weights are fitted to the integration area of the new integral by applying  $\hat{w}_i = w_i \cdot 2 \cdot \text{area}(V)$  for each weight  $w_i$ .

**Theorem A.1.2** (Kolmogorov continuity theorem). *Let  $\{Z(x), x \in D\}$  be a real-valued random field on a bounded domain  $D \subset \mathbb{R}^d$ . Assume that for some  $C, \beta > 0, \alpha \geq 1$  there holds*

$$\mathbb{E}[|Z(x) - Z(y)|^\alpha] \leq C \|x - y\|^{d+\beta}, \quad x, y \in \overline{D}.$$

*Then there exists a continuous version of  $Z$  whose realizations are Hölder continuous on  $\overline{D}$  with exponent  $\gamma$  for any  $\gamma \in (0, \beta/\alpha)$ .*

*Proof.* The proof can be found on page 51 of [SV97]. □

**Lemma A.1.3.** *Let  $\{Z(x), x \in D\}$  be a mean-zero Gaussian random field on a bounded domain  $D \subset \mathbb{R}^d$ . Let  $c$  be the covariance function of  $Z$  and assume that  $c(x, y) = \tilde{c}(x - y)$  where  $\tilde{c}$  is Lipschitz continuous on  $\overline{D}$ . Then,  $Z$  admits a version whose realizations are Hölder continuous on  $\overline{D}$  with coefficient  $\gamma$  for any  $0 < \gamma < 1/2$ .*

*Proof.* Let  $L > 0$  denote the Lipschitz constant of  $\tilde{c}$ , that is

$$|\tilde{c}(z) - \tilde{c}(w)| \leq L \cdot \|z - w\|_2, \quad z, w \in \overline{D}.$$

Then, it holds

$$\begin{aligned} 0 \leq \mathbb{E}[|Z(x) - Z(y)|^2] &= \mathbb{E}[Z(x)^2] - 2 \mathbb{E}[Z(x) \cdot Z(y)] + \mathbb{E}[Z(y)^2] \\ &= 2 \tilde{c}(0) - 2 \tilde{c}(x - y) \\ &\leq 2 L \cdot \|x - y\|_2 \end{aligned}$$

Observe that for  $Z(x) \sim \mathcal{N}(0, \sigma^2)$  it holds  $\mathbb{E}[Z(x)^n] = \sigma^n \mathbb{E}[Y^n]$  where  $Y \sim \mathcal{N}(0, 1)$ , and thus

$$\mathbb{E}[Z(x)^{2p}] = \sigma^{2p} \mathbb{E}[Y^{2p}] = (\mathbb{E}[Z(x)^2])^p \mathbb{E}[Y^{2p}]$$

Since  $Z(x) - Z(y)$  is a mean-zero Gaussian random variable, we have for any  $p \geq 1$

$$\mathbb{E}[|Z(x) - Z(y)|^{2p}] \leq (\mathbb{E}[|Z(x) - Z(y)|^2])^p \leq (2L)^p \|x - y\|^p.$$

By the Kolmogorov Continuity Theorem A.1.2 there exists a version of  $Z$  whose realisations are Hölder continuous on  $\overline{D}$  with exponent  $\gamma$  for any

$$0 < \gamma < \frac{p - d}{2p}$$

Letting  $p \rightarrow \infty$ , we see that there exists a version of  $Z$  with Hölder continuous realizations with any exponent  $0 < \gamma < 1/2$ .  $\square$

**Definition A.1.4.** *The 2-argument arctangent  $\arctan 2 : \mathbb{R}^2 \setminus \{0\} \rightarrow (-\pi, \pi]$  is defined as*

$$\arctan 2(y, x) = \begin{cases} \arctan(y/x) & \text{if } x > 0, \\ \arctan(y/x) + \pi & \text{if } x < 0, \text{ and } y \geq 0, \\ \arctan(y/x) - \pi & \text{if } x < 0, \text{ and } y < 0, \\ \pi/2 & \text{if } x = 0, \text{ and } y > 0, \\ -\pi/2 & \text{if } x = 0, \text{ and } y < 0. \end{cases}$$

**Remark A.1.5** (Calculation of the projections in the steel plate problem's perturbation function in subsection 6.1.2). *For the sake of completeness, the calculation of the projection of a point  $x$  onto the circle  $x_{circ}$  and onto the boundary  $x_{bound}$  in the steel plate problem is explained here. The visual representation can be viewed in the left-hand plot in figure 6.2. In the following algorithmic calculation, the original circle center position  $\begin{pmatrix} 0.16 \\ 0.16 \end{pmatrix}$  and the original radius 0.02 is used. Furthermore the function  $\arctan 2$  denotes the 2-argument arctangent A.1.4.*

---

**Algorithm 1** Calculate perturbation function

---

**Input:** original point  $x$ , sample  $\omega_2$ 

- 1:  $x_c = x - \begin{pmatrix} 0.16 \\ 0.16 \end{pmatrix}$  ▷ Center  $x$
- 2:  $x_{circ,c} = \frac{0.02}{\|x_c\|_2} \cdot x_c$  ▷ Calculate  $x_{circ,c}$
- 3:  $x_{circ} = x_{circ,c} + \begin{pmatrix} 0.16 \\ 0.16 \end{pmatrix}$  ▷ Decenter  $x_{circ,c}$
- 4:  $\theta = \arctan 2(x_c^{(2)}, x_c^{(1)})$  ▷ Calculate angle of  $x_c$
- 5: **if**  $-\pi/4 \leq \theta \leq \pi/4$  **then**
- 6:      $x_{bound} = (0.16; 0.16 \cdot \tan(\theta))^T$
- 7: **else if**  $\pi/4 \leq \theta \leq 3\pi/4$  **then**
- 8:      $x_{bound} = (0.16/\tan(\theta); 0.16)^T$
- 9: **else if**  $-3\pi/4 \leq \theta \leq -\pi/4$  **then**
- 10:      $x_{bound} = (-0.16/\tan(\theta); -0.16)^T$
- 11: **else**
- 12:      $x_{bound} = (-0.16; -0.16 \cdot \tan(\theta))^T$
- 13: **end if**

**Output:**  $x_{circ}, x_{bound}$ 


---

The perturbation function applied to the circle projection looks as follows

$$V(x_{circ}, \omega_2) = \omega_2^{(1)} \cdot \left( x_{circ} + \begin{pmatrix} \omega_2^{(2)} \\ \omega_2^{(3)} \end{pmatrix} \right) + \begin{pmatrix} 0.16 \\ 0.16 \end{pmatrix}$$

## A.2 Code

The entire implementation and creation of the images can be found in the following Github repository <https://github.com/EliasReutelsterz/Masterthesis>. Since the amount of data was too large for the upload (despite large file storage), the notebooks with the outputs were pushed with original data sizes, but the data itself was limited to 100 samples per model. The entire data for reproducing the images used was therefore submitted separately. The documentation can be read in the README.md.

**Remark A.2.1.** In the implementation, a slightly modified formulation of the bilinear form  $a$  in the variational formulation in lemma 6.2.4 was used, which was more suitable for implementation in FEniCS. The following equivalence holds (the first equality was already shown in the derivation in lemma 6.2.3):

$$\begin{aligned} a(u, v) &= \int_{D(\omega_2)} \nabla u : \nabla \tilde{v} \, dx \\ &+ \int_{D(\omega_2)} \left( \left( \frac{\partial u_1}{\partial x_1} + \frac{2v}{1+v} \frac{\partial u_2}{\partial x_2} \right) \frac{\partial \bar{v}_1}{\partial x_1} + \frac{1-v}{1+v} \frac{\partial u_1}{\partial x_2} \frac{\partial \bar{v}_2}{\partial x_1} + \frac{1-v}{1+v} \frac{\partial u_2}{\partial x_1} \frac{\partial \bar{v}_1}{\partial x_2} + \left( \frac{2v}{1+v} \frac{\partial u_1}{\partial x_1} + \frac{\partial u_2}{\partial x_2} \right) \frac{\partial \bar{v}_2}{\partial x_2} \right) dx \\ &= \int_{D(\omega_2)} \nabla u : \nabla \left( \frac{E(x, \omega_1)}{2(1+v)} \cdot v(x, \omega_2) \right) dx \\ &+ \int_{D(\omega_2)} \underbrace{\left( \begin{array}{cc} \frac{\partial u_1}{\partial x_1} + \frac{2v}{1+v} \frac{\partial u_2}{\partial x_2} & \frac{1-v}{1+v} \frac{\partial u_2}{\partial x_1} \\ \frac{1-v}{1+v} \frac{\partial u_1}{\partial x_2} & \frac{2v}{1+v} \frac{\partial u_1}{\partial x_1} + \frac{\partial u_2}{\partial x_2} \end{array} \right)}_{:=G(u)} : \nabla \left( \frac{E(x, \omega_1)}{2(1-v)} \cdot v(x, \omega_2) \right) dx \end{aligned}$$

Now, we can apply the domain mapping again with the help of (6.6).

$$\begin{aligned}\hat{a}(\hat{u}, \hat{v}) &= \int_{D_{ref}} \det(J) \cdot \left( \left( J^{-T} \cdot \nabla_{\hat{x}} \hat{u} \right) : \left( J^{-T} \cdot \nabla_{\hat{x}} \left( \frac{\hat{E}(\hat{x}, \omega_1, \omega_2)}{2(1+\nu)} \cdot \hat{v}(\hat{x}, \omega_2) \right) \right) \right) d\hat{x} \\ &\quad + \int_{D_{ref}} \left( \hat{G}(\hat{u}) \right) : \left( J^{-T} \cdot \nabla_{\hat{x}} \left( \frac{\hat{E}(\hat{x}, \omega_1, \omega_2)}{2(1-\nu)} \cdot \hat{v}(\hat{x}, \omega_2) \right) \right) d\hat{x}\end{aligned}$$

with

$$\hat{G}(\hat{u}) := \begin{pmatrix} a \cdot \nabla_{\hat{x}} \hat{u}_1 + \frac{2\nu}{1+\nu} b \cdot \nabla_{\hat{x}} \hat{u}_2 & \frac{1-\nu}{1+\nu} b \cdot \nabla_{\hat{x}} \hat{u}_1 \\ \frac{1-\nu}{1+\nu} a \cdot \nabla_{\hat{x}} \hat{u}_2 & \frac{2\nu}{1+\nu} a \cdot \nabla_{\hat{x}} \hat{u}_1 + b \cdot \nabla_{\hat{x}} \hat{u}_2 \end{pmatrix}$$

where  $a := (J_{22}, -J_{21})$  and  $b := (-J_{12}, J_{11})$ .  $\nabla_{\hat{x}} \hat{u}_i$  denotes the  $i$ -th. column of  $\nabla_{\hat{x}} \hat{u}$ .

# List of Figures

1.1	Poisson Problem Random Field and Grid Perturbation . . . . .	3
1.2	Steel Plate Problem Random Field and Grid Perturbation . . . . .	4
4.1	Random Field $V$ . . . . .	25
4.2	Solution Sample of Poisson Equation . . . . .	25
4.3	First $N$ Eigenvalues $\gamma_m$ of KLE of the Random Field $V$ . . . . .	31
4.4	First four Eigenfunctions $g_m(\hat{x})$ of KLE of the Random Field $V$ . . . . .	31
4.5	Poisson Model Monte Carlo Estimation . . . . .	33
4.6	Poisson Model Monte Carlo Convergence Analysis . . . . .	34
4.7	Poisson Model Monte Carlo Error Analysis . . . . .	34
4.8	Sobol' Indices for Poisson Model . . . . .	35
5.1	Sample for random right-hand Side . . . . .	36
5.2	Solution Sample of random right-hand Side Model $\omega_1 = (0.11, 0.79)^T$ . . . . .	37
5.3	Monte Carlo Estimation of random right-hand Side Model . . . . .	37
5.4	Monte Carlo Convergence Analysis random right-hand Side Model . . . . .	37
5.5	Monte Carlo Error Analysis random right-hand Side Model . . . . .	38
5.6	Sobol' Indices for the random right-hand Side Model with 12000 Samples . . . . .	38
5.7	Sample of Diffusion Coefficient . . . . .	39
5.8	Solution Sample of Diffusion Equation . . . . .	41
5.9	Diffusion Model Monte Carlo Estimation . . . . .	41
5.10	Diffusion Model Monte Carlo Convergence Analysis . . . . .	42
5.11	Diffusion Model Monte Carlo Error Analysis . . . . .	42
5.12	Sobol' Indices for Diffusion Model . . . . .	43
6.1	Reference Domain $D_{ref}$ and Boundaries . . . . .	45
6.2	Perturbation Function with Sample $\omega_2 = (1.5; 0.05; 0.05)^T$ . . . . .	45
6.3	Sample for a perturbed Mesh with $\omega_2 = (1.5; 0.05; 0.05)^T$ . . . . .	46
6.4	Solution for single Sample without perturbation $\omega_2 = (1; 0; 0)^T$ leading to $D(\omega_2) = D_{ref}$ . . . . .	50
6.5	Sample of $\hat{E}$ and $E$ for $\omega_2 = (1.5; 0.05; 0.05)^T$ . . . . .	51
6.6	Solution for single Sample with $\omega_2 = (1.5; 0.05; 0.05)^T$ . . . . .	52
6.7	MC Analysis of Displacement $\hat{u}$ . . . . .	55
6.8	MC Error Analysis of Displacement $\hat{u}$ . . . . .	55
6.9	MC Analysis of Stress Tensor Mean $\hat{\sigma}$ . . . . .	56
6.10	MC Analysis of Stress Tensor $\hat{\sigma}_{11}$ Convergence in $\hat{P} = (0.16, 0.18)^T$ . . . . .	56
6.11	Sobol' Indices for the two different Quantities of Interest . . . . .	57
6.12	Sample for perturbed Mesh with Circle Random Field . . . . .	58
6.13	Solution Sample with Circle Random Field . . . . .	59
6.14	Sobol' Indices for the two different Quantities of Interest . . . . .	60
6.15	Eigenfunctions $g_m^V(x)$ of KLE of the Random Field $V$ . . . . .	60
6.16	Eigenfunctions $g_m^E(x)$ of KLE of the Random Field $\hat{E}$ . . . . .	61

# Bibliography

- [AGS19] A. Alexanderian, P. A. Gremaud, and R. C. Smith. *Variance-based sensitivity analysis for time-dependent processes*. 2019. arXiv: 1711.08030 [stat.CO].
- [BHP19] S. Badia, J. Hampton, and J. Principe. *Embedded multilevel Monte Carlo for uncertainty quantification in random domains*. 2019. arXiv: 1911.11965 [math.NA].
- [Bar+23] I. A. Baratta et al. *DOLFINx: the next generation FEniCS problem solving environment*. preprint. 2023.
- [BP03] M. Blyth and C. Pozrikidis. “Heat conduction across irregular and fractal-like surfaces”. In: *International Journal of Heat and Mass Transfer* 46 (Apr. 2003), pp. 1329–1339.
- [BEU11] I. Busch, O. G. Ernst, and E. Ullmann. “Expansion of random field gradients using hierarchical matrices”. In: *PAMM* 11.1 (2011), pp. 911–914. eprint: <https://onlinelibrary.wiley.com/doi/pdf/10.1002/pamm.201110437>.
- [CK07] C. Canuto and T. Kozubek. “A fictitious domain approach to the numerical solution of PDEs in stochastic domains”. In: *Numerische Mathematik* 107 (Aug. 2007), pp. 257–293.
- [CDE19] L. Church, A. Djurdjevac, and C. Elliott. “A domain mapping approach for elliptic equations posed on random bulk and surface domains”. In: (Mar. 2019).
- [Cia94] P. Ciarlet. *Three-Dimensional Elasticity*. Mathematical Elasticity Bd. 20. Elsevier Science, 1994. ISBN: 9780444817761.
- [DV+21] S. Da Veiga et al. *Basics and Trends in Sensitivity Analysis*. Philadelphia, PA: Society for Industrial and Applied Mathematics, 2021.
- [Eva10] L. Evans. *Partial Differential Equations*. Graduate studies in mathematics. American Mathematical Society, 2010. ISBN: 9780821849743.
- [FW17] R. Feynman and F. Wilczek. *The Character of Physical Law, with new foreword*. The MIT Press. MIT Press, 2017. ISBN: 9780262341738.
- [Fic73] G. Fichera. “Existence Theorems in Elasticity”. In: *Linear Theories of Elasticity and Thermoelasticity: Linear and Nonlinear Theories of Rods, Plates, and Shells*. Ed. by C. Truesdell. Berlin, Heidelberg: Springer Berlin Heidelberg, 1973, pp. 347–389. ISBN: 978-3-662-39776-3.
- [FP01] M. Fyrillas and C. Pozrikidis. “Conductive heat transport across rough surfaces and interfaces between two conforming media”. In: *International Journal of Heat and Mass Transfer* 44 (May 2001), pp. 1789–1801.
- [Gam+14] F. Gamboa et al. “Sensitivity analysis for multidimensional and functional outputs”. In: *Electronic Journal of Statistics* 8.1 (2014), pp. 575 –603.
- [Hak+23] H. Hakula et al. *Uncertainty quantification for random domains using periodic random variables*. 2023. arXiv: 2210.17329 [math.NA].
- [HPS16] H. Harbrecht, M. Peters, and M. Siebenmorgen. “Analysis of the domain mapping method for elliptic diffusion problems on random domains”. In: *Numerische Mathematik* 134 (Dec. 2016).
- [HKS24] H. Harbrecht, V. Karnaev, and M. Schmidlin. “Quantifying Domain Uncertainty in Linear Elasticity”. In: *SIAM/ASA Journal on Uncertainty Quantification* 12.2 (2024), pp. 503–523. eprint: <https://doi.org/10.1137/23M1578589>.
- [Hip+18] R. Hiptmair et al. “Large deformation shape uncertainty quantification in acoustic scattering”. In: *Advances in Computational Mathematics* 44 (Oct. 2018).

## Bibliography

- [IH90] T. Ishigami and T. Homma. “An importance quantification technique in uncertainty analysis for computer models”. In: *[1990] Proceedings. First International Symposium on Uncertainty Modeling and Analysis* (1990), pp. 398–403.
- [Joh12] C. Johnson. *Numerical Solution of Partial Differential Equations by the Finite Element Method*. Dover Books on Mathematics Series. Dover Publications, Incorporated, 2012. ISBN: 9780486131597.
- [JL01] M. Jung and U. Langer. *Methode der finiten Elemente für Ingenieure*. Springer, 2001.
- [LDM13] C. Lang, A. Doostan, and K. Maute. “Extended stochastic FEM for diffusion problems with uncertain material interfaces”. In: *Comput. Mech.* 51.6 (2013), 1031–1049. ISSN: 0178-7675.
- [LPS14] G. J. Lord, C. E. Powell, and T. Shardlow. *An Introduction to Computational Stochastic PDEs*. Cambridge Texts in Applied Mathematics. Cambridge University Press, 2014.
- [MNK11] P. Mohan, P. Nair, and A. Keane. “Stochastic projection schemes for deterministic linear elliptic partial differential equations on random domains”. In: *International Journal for Numerical Methods in Engineering* 85 (Feb. 2011).
- [Nit81] Nitsche, J. A. “On Korn’s second inequality”. In: *RAIRO. Anal. numér.* 15.3 (1981), pp. 237–248.
- [NCS11] A. Nouy, M. Chevreuil, and E. Safatly. “Fictitious domain method and separated representations for the solution of boundary value problems on uncertain parameterized domains”. In: *Computer Methods in Applied Mechanics and Engineering* 200.45 (2011), pp. 3066–3082. ISSN: 0045-7825.
- [NC10] A. Nouy and A. Clement. “eXtended Stochastic Finite Element Method for the numerical simulation of heterogenous materials with random material interfaces”. In: *International Journal for Numerical Methods in Engineering* 83 (Sept. 2010), pp. 1312 –1344.
- [PG15] S. Pranesh and D. Ghosh. “Faster computation of the Karhunen-Loeve expansion using its domain independence property”. In: *Computer Methods in Applied Mechanics and Engineering* 285 (2015), pp. 125–145.
- [RS78] M. Reed and B. Simon. *Methods of Modern Mathematical Physics. IV Analysis of Operators*. New York: Academic Press, 1978.
- [Sal02] A. Saltelli. “Making best use of model evaluations to compute sensitivity indices”. In: *Computer Physics Communications* 145.2 (2002), pp. 280–297. ISSN: 0010-4655.
- [SM93] K. Sarkar and C. Meneveau. “Gradients of potential fields on rough surfaces: Perturbative calculation of the singularity distribution function  $f(\alpha)$  for small surface dimension”. In: *Phys. Rev. E* 47 (2 1993), pp. 957–966.
- [Smi13] R. C. Smith. *Uncertainty Quantification: Theory, Implementation, and Applications*. Philadelphia, PA: Society for Industrial and Applied Mathematics, 2013. eprint: <https://pubs.siam.org/doi/10.1137/1.9781611973228>.
- [Sob01] I. Sobol’. “Global sensitivity indices for nonlinear mathematical models and their Monte Carlo estimates”. In: *Mathematics and Computers in Simulation* 55.1 (2001). The Second IMACS Seminar on Monte Carlo Methods, pp. 271–280. ISSN: 0378-4754.
- [SV97] D. Stroock and S. Varadhan. *Multidimensional Diffusion Processes*. Grundlehren der mathematischen Wissenschaften. Springer Berlin Heidelberg, 1997. ISBN: 9783540903536.
- [UC20] F. Uribe-Castillo. *Bayesian Analysis and Rare Event Simulation of Random Fields*. Technische Universität München, 2020.
- [XT06] D. Xiu and D. Tartakovsky. “Numerical Methods for Differential Equations in Random Domains”. In: *SIAM J. Scientific Computing* 28 (Jan. 2006), pp. 1167–1185.
- [Zei12] E. Zeidler. *Applied Functional Analysis: Applications to Mathematical Physics*. Springer Publishing Company, Incorporated, 2012. ISBN: 1461269105.

- [Zhe+23] Z. Zheng et al. “A stochastic finite element scheme for solving partial differential equations defined on random domains”. In: *Computer Methods in Applied Mechanics and Engineering* 405 (2023), p. 115860. ISSN: 0045-7825.